
PROJECT TECHNICAL REPORT
TASK E-72B

APOLLO 11 DAP POSTFLIGHT ANALYSIS

NAS 9-8166

17 OCTOBER 1969

Prepared for
NATIONAL AERONAUTICS AND SPACE ADMINISTRATION
MANNED SPACECRAFT CENTER
HOUSTON, TEXAS

Prepared by
Control System Analysis Section

FACILITY FORM 802	N69-40573	
	(ACCESSION NUMBER)	(THRU)
	126	1
	(PAGES)	(CODE)
	CR-101969	31
	(NASA CR OR TMX OR AD NUMBER)	(CATEGORY)

PROJECT TECHNICAL REPORT
TASK E-72B

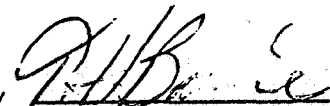
APOLLO 11 DAP POSTFLIGHT ANALYSIS

NAS 9-8166

17 OCTOBER 1969


Prepared for
NATIONAL AERONAUTICS AND SPACE ADMINISTRATION
MANNED SPACECRAFT CENTER
HOUSTON, TEXAS

Approved by



J. E. Alexander, Manager
Guidance and Control
Systems Department

Approved by



R. Lee, Manager
Task E-72B

ABSTRACT

This document presents the final report on the LM and CSM digital autopilot performance during the Apollo 11 mission. The purpose of this subtask is to provide an evaluation of the flight performances of the COLOSSUS 2B and LUMINARY 1A digital autopilots and to compare the flight behavior to preflight simulation results.

ACKNOWLEDGEMENT

This analysis report is the result of work performed by the following members of the TRW Technical Staff:

J. A. Bossart
W. H. Delashmit
W. R. Hamel
R. C. Kropf
R. Lee

TABLE OF CONTENTS

	Page
1.0 INTRODUCTION	1-1
1.1 GENERAL	1-1
2.0 SUMMARY	2-1
3.0 CSM DIGITAL AUTOPILOT	3-1
3.1 TVC DAP PERFORMANCE	3-1
3.1.1 Engine Start Transients and Gimbal Positioning Accuracy	3-2
3.1.2 Propellant Slosh and Spacecraft Body Bending	3-2
3.1.3 Time Histories of Major Burns	3-3
3.2 RCS DAP PERFORMANCE	3-4
3.2.1 Rate Estimator Performance in Acceleration Command Mode	3-4
3.2.2 Transposition and Docking	3-5
3.2.3 Single-Jet Control	3-6
3.2.4 Passive Thermal Control	3-7
4.0 LM DIGITAL AUTOPILOT	4-1
4.1 LM DAP PERFORMANCE DURING POWERED DESCENT	4-1
4.1.1 Program Sequencing	4-2
4.1.2 Ullage and DPS Ignition	4-3
4.1.3 Windows-up Maneuver	4-4
4.1.4 Rotational Hand Controller Activity During Attitude Hold Mode of P64	4-5

TABLE OF CONTENTS (Continued)

	Page
4.1.5 Acceleration Nulling Mode Operation	4-6
4.1.6 Manual Takeover, P66	4-9
4.1.7 Lunar Touchdown	4-10
4.1.8 Spacecraft Response During Powered Descent	4-11
4.1.9 RCS Propellant Consumption	4-14
4.1.10 Single-Jet Control	4-16
4.1.11 Frozen DSKY Displays	4-17
4.1.12 DPS Engine Mount Compliance	4-17
4.2 LM DAP PERFORMANCE DURING POWERED ASCENT	4-19
4.2.1 Lunar Liftoff	4-20
4.2.2 Spacecraft Response During Lunar Orbit Insertion	4-21
4.2.3 C.G. Shifts During Powered Ascent	4-26
4.2.4 Propellant Consumption	4-27
4.2.5 Frozen DSKY Displays	4-27
4.3 RENDEZVOUS SEQUENCE	4-28
REFERENCES	R-1

LIST OF TABLES

	Page
3.1 Apollo 11 SPS Burns	3-8
3.2 Apollo 11 SPS ΔV Performance	3-8
3.3 SPS Startup Transients and Gimbal Positioning Accuracy	3-9
3.4 Fuel Slosh and Body Bending Observed During Apollo 11	3-9
4.1 Events Timeline	4-29
4.2 RCS Propellant Consumption	4-30
4.3 Time Durations of Descent Programs	4-30
4.4 Single-Jet Firings	4-31
4.5 Computed and Theoretical C.G. Locations	4-32
4.6 Rendezvous Data	4-33

LIST OF ILLUSTRATIONS

	Page
3-1 Pitch and Yaw Attitude Errors During LOI 1	3-10
3-2 Pitch Engine Trim Estimate During LOI 1	3-11
3-3 Yaw Engine Trim Estimate During LOI 1	3-12
3-4 Roll Attitude Error During LOI 1	3-13
3-5 LOI 2 Burn Parameters	3-14
3-6 Pitch Attitude Error During TEI	3-15
3-7 Yaw Attitude Error During TEI	3-16
3-8 Pitch and Yaw Engine Trim Estimates During TEI	3-17
3-9 Roll Attitude Error During TEI	3-18
3-10 CMC Automatic Maneuver During Transposition and Docking	3-19
3-11 X-Axis Attitude Hold During RCS Translation	3-20
3-12 Y-Axis Attitude Hold During RCS Translation	3-21
3-13 Z-Axis Attitude Hold During RCS Translation	3-22
3-14 Z-Axis Attitude Hold During Single-Jet Control	3-23
4-1 DPS Ignition Transients	4-34
4-2 Pitch Rate and GDA Position Shortly After DPS Ignition	4-35
4-3 Roll Rate and GDA Position Shortly After DPS Ignition	4-36
4-4 Apollo 10 DPS Phasing Burn - Pitch Rate, Pitch GDA Position, and Pitch Jet Firings	4-37
4-5 Apollo 10 DPS Phasing Burn - Roll Rate, Roll GDA Position, and Roll Jet Firings	4-38
4-6 CDUX (Outer Gimbal Angle) vs Time During X-Axis Override in P63	4-39

LIST OF ILLUSTRATIONS (Continued)

	Page
4-7 X-Axis Override in P63	4-40
4-8 Distance-to-go Downrange vs Time	4-41
4-9A AOSQ, Pitch GDA Drive Time and Drive Direction, Pitch GDA Position	4-42
4-9B AOSR, Roll GDA Drive Time and Drive Direction, Roll GDA Position	4-42
4-10 Offset Acceleration, Pitch GDA Drive Time and Drive Direction, Pitch GDA Position	4-43
4-11 Offset Acceleration, Roll GDA Drive Time and Drive Direction, Roll GDA Position	4-45
4-12 Vertical Velocity (HDOT) vs Time	4-47
4-13 DPS Throttle Command vs Time	4-48
4-14 RHC Pitch Command	4-49
4-15 Altitude vs Time	4-50
4-16 Horizontal Velocity vs Time	4-51
4-17 Altitude Rate vs Time	4-52
4-18 DPS Throttle Command vs Time	4-53
4-19 P-Axis Attitude Error - P63	4-54
4-20 Spacecraft Angular Response - P63/P64	4-55
4-21 Attitude Errors vs Time	4-58
4-22 Pitch Axis Variables	4-59
4-23 Roll Axis Variables	4-60
4-24 Roll Rate vs Time	4-61
4-25 Pitch Rate vs Time	4-62

LIST OF ILLUSTRATIONS (Continued)

	Page
4-26 Pitchover in P64	4-63
4-27 CDUY (Inner Gimbal Angle) vs Time	4-64
4-28 Pitch Compliance vs Throttle Setting	4-65
4-29 Roll Compliance vs Throttle Setting	4-66
4-30 Lunar Liftoff	4-67
4-31 Theoretical APS Thrust Buildup	4-68
4-32 Altitude vs Time During Powered Ascent	4-69
4-33 Altitude Rate vs Time During Powered Ascent	4-70
4-34 Yaw Guidance Commands and Response - Initial Phase of Powered Ascent	4-71
4-35 Pitch Guidance Commands and Response - Initial Phase of Powered Ascent	4-72
4-36 Roll Guidance Commands and Response - Initial Phase of Powered Ascent	4-73
4-37 Lunar Orbit Insertion Response	4-74
4-38 U' Axis Attitude Error and Offset Acceleration For Final Phase of Powered Ascent	4-75
4-39 V' Axis Attitude Error and Offset Acceleration For Final Phase of Powered Ascent	4-76
4-40 Spacecraft Response At APS Cutoff	4-77
4-41 Estimated AOS Acceleration	4-78
4-42 Relationship of Thrust Vectors, Body Centerlines and Center of Gravity on the LM in the X-Z Plane	4-79

1.0 INTRODUCTION

1.1 GENERAL

This report presents the analyses of the inflight performances of the Lunar Module (LM) and Command and Service Module (CSM) digital autopilots (DAP) during the Apollo 11 mission. The analyses were directed primarily toward the powered flight phases of the mission since coasting flight performance of the DAP's was verified in previous flights. No significant modifications in the control logic for coasting flight was implemented for this mission.

Detailed analyses of each Service Module Propulsion System (SPS), Descent Propulsion System (DPS), and Ascent Propulsion System (APS) burn, for which detailed data were available, were performed. Maneuvers and attitude control by the Reaction Control System (RCS) during Passive Thermal Control (PTC), Midcourse Corrections (MCC), and the rendezvous sequence were also examined. The chronology of significant GN & C events is presented below.

SPS Evasive Maneuver	4:40:02 GET
Translunar MCC	26:44:59 GET
Lunar Orbit Insertion 1	75:49:50 GET
Lunar Orbit Insertion 2	80:11:37 GET
Undocking	100:13:38 GET
Descent Orbit Insertion	101:36:14 GET
Powered Descent Initiation	102:33:05 GET
Lunar Touchdown	102:45:40 GET
Lunar Liftoff	124:22:00 GET
Coelliptic Sequence Initiation	125:19:36 GET
Constant Differential Height Maneuver	126:17:47 GET
Terminal Phase Initiation	127:03:32 GET
Terminal Phase Finalize	127:43:08 GET
Docking	128:03:00 GET
Lunar Module Jettison	130:09:00 GET
Transearth Injection	135:23:43 GET
Entry Interface	195:03:07 GET

2.0 SUMMARY

The Thrust Vector Control (TVC) DAP performed nominally during the five SPS burns as indicated by the small residual velocities remaining after each burn. The only significant residuals remained after the Trans-earth Injection (TEI) burn and were attributable to a rapidly moving yaw c.g. location due to SPS propellant expenditure and lightly damped yaw slosh oscillations. Although slosh oscillations were detected during the Lunar Orbit Insertion 1 (LOI1), LOI2, and TEI burns, they presented no stability problems. Body bending was noticeable only during LOI1 and persisted only for four or five cycles. Engine gimbal start transients were less than 0.4 degree for all burns except for the TEI burn when they were approximately 1.2 degrees in magnitude. This response was expected due to a software change which initialized the TVC DAP attitude errors with the attitude errors computed by the Reaction Control System (RCS) DAP.

The CSM RCS DAP performance was generally nominal. One period of RCS DAP control was questioned because the DAP estimates of the spacecraft rates were not consistent with the Inertial Measuring Unit (IMU) gimbal angle changes. However, all RCS jets were disabled and the DAP was operating in a mode equivalent to a complete undetected RCS system failure. The RCS propellant consumption during the transposition and docking maneuver prior to LM withdrawal from the SIVB was higher than predicted. The cause of the higher consumption was an omission in the DSKY entry procedure to achieve proper interface between the automatic turn-around maneuver and manual initiation of the pitch maneuver. The procedure was successfully performed on the third attempt, once the omission was detected. Passive thermal control (PTC) of the spacecraft was performed nominally. A typical time for the PTC activity to exceed the 30 degree deadband was 17 hours.

No significant entry data was available for the Apollo 11 Mission. A circuit breaker was accidentally tripped which deactivated the onboard tape recorder which would have registered the entry data.

The LM DAP performed in accordance with the software design throughout the mission. High-bit-rate downlink data for the Descent Orbit Insertion burn was not available since the burn was performed behind the moon. The residual velocities following the burn were voiced down when communications were regained and indicated satisfactory performance of the DAP.

The bulk of the LM postflight analysis centered on the powered descent phase. The program sequencing through the three powered descent programs was nominal. Transition from the Braking Phase Program (P63) to the Approach or Visibility Phase Program (P64) was accomplished automatically at close to the HI gate target conditions. Astronaut selection of the Rate-of-Descent Program (P66) was performed near the expected 500 foot altitude. The ullage and DPS ignition transients appeared nominal and were quickly damped. Due to an error in the setting of the rate error scaling switch, the "windows-up" maneuver was interrupted to reset the scaling switch. Hence, slightly more RCS propellant was consumed for the maneuver than anticipated. Slosh oscillations were detected approximately 233 seconds into the burn and continued into the P66 phase of the powered descent. These oscillations resulted in slight overshooting of the attitude error deadbands and caused peak-to-peak rate amplitudes as high as 3.0 deg/sec. This response at a frequency of 0.5 to 0.6 Hz agrees with preflight simulation results obtained from the MSC bit-by-bit simulator. There was some concern that the actual descent consumed approximately 88 pounds of RCS propellant compared to a budget of 40 pounds. A determination of propellant usage for each axis of control and for each program phase was made. Also, attempts were made to separate propellant expenditure for manual and automatic control. The actual consumption for automatic control during the P63 and P64 phases of descent agreed well with results from the MSC bit-by-bit simulator. The analysis indicated that approximately 66 pounds of the propellant was consumed by manual control with 51 pounds used during the manual attitude hold phase (P66) of the descent. The budget did not account for the full extent of RCS activity required during the P66 phase. Two periods of no apparent Gimbal Drive Actuator (GDA) activity were observed. Analysis of these periods

indicated that the LGC commanded drive times were sufficiently small that the actual GDA activity could be lost in the granularity of the telemetry data. The downlink indications of RCS jet firings included a multitude of short duration, single-jet firings, some of which are not permissible according to the logic design. Detailed analysis of all of these firings eliminated all "anomalous" firings as noise in the telemetry data and only nineteen single-jet firings were validated. These firings were about the U' or V' axis and were minimum impulse firings, which is permitted by the LGC logic. During the powered descent phase, the DSKY displays were frozen for several short periods of time. Analysis of these events indicated that the behavior was caused by nominal Astronaut/LGC interaction. The GDA responses during the 10% and full throttle portions of the flight were investigated to determine the effects of engine mount compliance. Fair agreement with theoretical estimates of the compliance effect was obtained.

The powered ascent burn from lunar liftoff to lunar orbit insertion appeared nominal. The complete effects of the Fire-in-the-Hole (FITH) sequence could not be investigated because of a short period of data dropout just after APS ignition. The DAP performed the pitchover maneuver nominally and the transients were well damped. In steady-state operation, the spacecraft exhibited the characteristic limit-cycle response. The frequency and amplitudes of this response agreed well with preflight simulation results. An attempt was made to extract c.g. location data during the powered ascent burn for comparison to preflight estimates of c.g. travel during an APS burn. The results had fair correlation to the theoretical values. As in powered descent, some anomalous looking DSKY displays were observed. Again, these proved to be nominal reaction to Astronaut/LGC interaction. An overburn of approximately 2.0 ft/sec was caused by tailoff effects which were greater than expected.

The rendezvous sequence consisted of four RCS translation burns. The burns were performed nominally and the velocity residuals after the burns were nominal and easily nulled by manual translation commands.

3.0 CSM DIGITAL AUTOPILOT

The analysis of the CSM DAP was directed toward evaluation of the TVC DAP for the SPS burns and selected phases of RCS DAP control. The investigation did not attempt to include all periods of DAP control during coasting flight since automatic maneuvers and automatic attitude hold phases had been studied extensively in previous missions. Furthermore, only minor modifications to the CSM DAP had been implemented between the Apollo 10 and Apollo 11 missions. No significant entry data were available for the Apollo 11 mission. The onboard DSE (tape recorder) failed to operate during entry because a circuit breaker was inadvertently tripped.

Periods of DAP control analyzed were:

- a) TVC DAP
 - o SPS Evasive Maneuver
 - o Translunar MCC
 - o Lunar Orbit Insertion 1
 - o Lunar Orbit Insertion 2
 - o Transearth Injection
- b) RCS DAP
 - o Transposition and docking
 - o One period of passive thermal control
 - o Period of single-jet control of the CSM/LM configuration
 - o CMC activity in acceleration command mode

The "Guidance System Operations Plan for Manned CM Earth Orbital and Lunar Missions Using Program COLOSSUS 2A, Section 3" (Reference 1) was used as the standard for CSM DAP logic. The data available for postflight analysis are described in References 2 and 3.

3.1 TVC DAP PERFORMANCE

Only one significant change was made to the TVC DAP between the Apollo 10 and Apollo 11 missions. This modification involved initializing the

pitch and yaw TVC DAP attitude errors, in the CSM-alone configuration, with the RCS DAP attitude errors values at engine ignition. The software change was implemented to improve the short-burn cross-axis-velocity cutoff errors. Consequently, particular emphasis was placed on the Transearth Injection (TEI) burn. The TVC DAP performance during the Apollo 11 mission was generally similar to that experienced in the Apollo 10 mission and was consistent with the DAP design logic and preflight simulation results.

The five SPS burns required during the Apollo 11 mission are summarized in Tables 3.1 and 3.2. The tables present ignition times, burn durations, ullage requirements, and postburn ΔV components displayed on the DSKY.

3.1.1 Engine Start Transients And Gimbal Positioning Accuracy

Table 3.3 summarizes the SPS engine start transients and gimbal positioning accuracies during the LOI1, LOI2, and TEI burns. With one exception, the results were similar to Apollo 10 results. Gimbal positioning was accurate within 0.2 to 0.3 degree. Engine start transients were 0.4 degree or less except during TEI when they were approximately 1.2 degrees in magnitude. The response for the TEI burn was the significant difference from performance of the TVC DAP for the Apollo 10 mission and was a direct result of the TVC DAP modification described above. Preflight simulation results predicted the higher engine transients due to this logic change (Reference 4).

3.1.2 Propellant Slosh And Spacecraft Body Bending

Table 3.4 summarizes propellant slosh and body bending effects during the Apollo 11 mission. These effects were determined by analyzing the Body Mounted Attitude Gyro System (BMAGS) body rates. Bending was evident only during LOI1 and appeared for only four or five cycles. The bending, which could be seen in the pitch response, had a frequency of 16.3 rad/sec. This damped oscillation created no stability problems.

Propellant slosh was detected during the three major SPS burns. As seen previously during the Apollo 10 mission, and as modeled in preflight simulations, the slosh frequencies increased with decreasing vehicle mass. None of the slosh oscillations presented a stability problem, although the yaw slosh oscillations during the TEI burn persisted for the entire burn, damping out slowly.

3.1.3 Time Histories Of Major Burns

Figures 3-1 through 3-4 present TVC DAP pitch and yaw attitude errors, engine trim estimates, and TVC roll attitude errors during LOI1. Figures 3-5 through 3-9 present the same quantities for the LOI2 and TEI burns. These plots are quite similar to those obtained for the Apollo 10 mission (Reference 5). In particular, the peak magnitudes of pitch and yaw attitude errors throughout LOI1 (Figure 3-1) were only 0.1 or 0.2 degree. During the TEI burn (Figures 3-6 and 3-7), the peak pitch and yaw attitude errors were initially less than 0.6 degree and converged to 0.3 degree or less. These small values were results of accurate preburn c.g. estimates, with small initial engine mistrims. For the two short SPS burns, the SPS evasive and the Translunar MCC, the engine gimbal was not changed from the padloaded position. This position was still adequate for the LOI1 burn since the c.g. shift during the two short burns was negligible. LOI2 was initiated with the engine gimbal position existing at the end of LOI1. Since a configuration change was associated with the TEI burn, a new set of engine gimbal angles was required.

The TVC roll DAP performed in accordance with the phase plane design. During LOI1 (Figure 3-4), the roll attitude error was biased toward the negative 5.0 degrees deadband. However, during the entire 358 second burn, the roll attitude error intercepted the deadband only once. Estimates of the roll torque existing at this time were obtained by fitting the roll attitude error with a second-order polynomial and assuming an average roll inertia of 50,000 slug-ft². The estimated roll torque was in the range of -0.4 to -1.4 ft-lbs. Similar behavior was detected during the first LOI burn of the Apollo 10 mission. During TEI (Figure 3-9), the roll attitude

error traversed between the positive and negative deadbands, except for the last 30 seconds of the burn. At this time, the attitude error was biased toward the positive deadband. Again, the magnitude of the roll torque was estimated by curve fitting the roll attitude error. The computed torque was 0.9 to 1.2 ft-lbs for an inertia of 15065 slug-ft².

3.2 RCS DAP PERFORMANCE

The RCS DAP was used extensively during the Apollo 11 mission for maneuvering to and holding attitudes for SPS burns, passive thermal control (PTC) initiation, and navigation sightings. In addition, all PTC periods were implemented under CMC control. The utilization of the RCS DAP during the Apollo 11 mission was quite similar to that during the Apollo 10 mission, which was evaluated in detail and reported in Reference 5. This factor, plus the fact that the RCS DAP was unchanged between flights, allowed a less extensive evaluation of the RCS DAP for the Apollo 11 mission. Instead, periods of particular interest were selected and analyzed.

3.2.1 Rate Estimator Performance In Acceleration Command Mode

Following a period of landmark tracking (approximately 98:47:00 GET), the rate estimates computed by the CMC were not consistent with the rate of change of the IMU gimbal angles. This activity occurred during low-bit rate telemetry transmission and complete analysis was precluded by insufficient data. However, it was observed that all RCS jets were disabled at this time since the Manual Attitude switches for the pitch, yaw, and roll axes were set to the Acceleration Command position. Therefore, the DAP was essentially operating in a mode equivalent to a complete undetected RCS system failure. The CMC estimates the spacecraft angular rates and incorporates accelerations due to commanded jet firings in these estimates. Since the jets are failed off undetected, some rate error is expected. Utilizing the formulation presented in Reference 1 for computing the steady-state rate error in the rate estimator due to an unmodeled acceleration, the rate error due to a two-jet couple was 0.74 deg/sec.

The actual differences between the rate estimates and the body rates based on IMU gimbal angle changes were approximately half this value. Consequently, it can be assumed that the CMC was not commanding jet firings continuously, although this cannot be verified because of lack of data.

3.2.2 Transposition And Docking

During the mission, it was noted that excessive RCS propellant (compared to preflight simulations and budgets) was used to accomplish the transposition and docking maneuver prior to LM withdrawal from the SIVB. The standard procedure used to accomplish this maneuver is to perform the bulk of the required turnaround automatically at 2.0 deg/sec with the pitch rate and pitch direction being initiated manually. This manual initiation is employed to implement the 180 degrees pitch maneuver in the crew's preferred direction rather than in a direction dependent upon the spacecraft location within the attitude error deadbands at the time of initiation of the maneuver. The details of the planned maneuver initiation are listed below:

1. Set up the CMC automatic maneuver routine (R60).
2. Before PROCEEDing on the flashing V50 N18 of the desired final gimbal angles, set the pitch MAN ATT switch to the ACC CMD position, thus disabling the pitch commands from the computer.
3. Key in PROCEED
4. Initiate the pitch motion in the preferred direction via the RHC.
5. Return the MAN ATT switch to its normal position (RATE CMD) and key in a second PROCEED.

The second PROCEED described above is required to maintain the automatic maneuver through completion. When the RHC is returned to the "detent" position, the CMC would attempt to perform an automatic attitude hold if the automatic maneuver routine were not continued via the PROCEED.

Analysis of the flight data indicated that this second PROCEED was omitted the first time the maneuver was attempted and the CMC, after the pitch MAN ATT switch was returned to RATE CMD, damped out the pitch rate that had been input manually. This procedure was attempted three times. On the third try, the PROCEED required by step 5 above was entered and the maneuver continued normally. Figure 3-10 compares the commanded and DAP measured spacecraft rates during the DAP controlled portion of the maneuver. The commanded and actual rates agree well. The initial rate differences are attributable to RHC commands used to initiate the maneuver.

The sequence of building up and damping the spacecraft rates twice before the maneuver was properly initiated caused the vehicles to separate more than expected before the translation maneuver to dock the vehicles was begun. The CMP estimated that the vehicles separation distance after CSM turnaround was approximately 100 feet instead of the 66 feet anticipated from preflight simulations. The RCS propellant consumption above the budget resulted from the two "false starts" prior to the CSM turnaround and the larger amount of RCS propellant required to achieve docking from 100 feet of separation compared to a predicted 66 feet. Figures 3-11 through 3-13 show that the RCS DAP held the post-turnaround attitude in narrow deadband very well. The attitude errors were consistent with the phase-plane logic during this period of high Translational Hand Controller activity.

3.2.3 Single Jet Control

Much attention has been focused on determining the effects, on vehicle state vector accuracy, of unbalanced-couple RCS jet firings in lunar orbit. All data available between LOI1 and CSM/LM separation prior to lunar descent were examined and only one period of single-jet control was found. The interest was not to determine state vector accuracy but to evaluate the DAP performance under single-jet control and to define the frequency of required jet firings during this control mode. This period of

single-jet control was limited to automatic attitude hold with very low spacecraft angular rates. Attitude maneuvers under single-jet control, which would have been more interesting from a controls and a ΔV standpoint, were not performed during this time interval. Figure 3-14 presents the roll-axis phase-plane motion. The attitude error change between 96:34:33 and 96:40:31 GET is consistent with the DAP measured roll rate of 0.014 deg/sec. The positive roll jet firing that occurred when the phase-plane locus reached the -5.0 degrees attitude error deadband caused a $\Delta\omega$ of 0.014 deg/sec, which is consistent with a minimum-impulse single-jet firing. The frequency of single-jet firings during the period analyzed, plus the fact that they were minimum-impulse firings, result in negligible ΔV contributions.

3.2.4 Passive Thermal Control

Passive thermal control presented no problems during the Apollo 11 mission. All spacecraft rates were nulled prior to establishing the PTC mode by performing single-jet attitude hold about the desired PTC initial attitude. Single jet control was attained by disabling two adjacent quads via panel switches (not by loading zeros in DAPDATAR2). After the vehicle rates were nulled the 0.3 deg/sec roll rate was initiated and the attitude error deadbands about the pitch and yaw-axes widened to 30 degrees as in Apollo 10. No extensive analysis was performed on all the PTC periods. A typical CMC controlled PTC period was the interval between 36:01:00 to 52:53:00 GET, a duration of 17 hours. PTC was terminated at the end of this period because the yaw attitude error had diverged to the -30 degrees limit. This PTC period could probably have been extended more than 17 hours if a water dump performed at approximately 48:30:00 GET had not increased the PTC divergence rate.

TABLE 3.1 APOLLO 11 SPS BURNS

Maneuver	Ignition Time (GET)	Burn Duration (Secs)	Ullage
Evasive	4:40:02	2.93	None
T/L MCC	26:44:59	3.13	None
LOI 1	75:49:50	357.53	None
LOI 2	80:11:37	16.78	2 jets 19 sec
TEI	135:23:42	151.41	2 jets 16 sec

TABLE 3.2 APOLLO 11 SPS ΔV PERFORMANCE

Maneuver	ΔV Desired (fps)	N85 ΔV Residuals (fps)					
		Before X	RCS Y	Nulling Z	After X	RCS Y	Nulling Z
Evasive	19.7	-.1	0	-.1	---	---	---
T/L MCC	21.3	.4	0	.5	---	---	---
LOI 1	2925.4	-.1	-.1	+.1	---	---	---
LOI 2	159.1	.4	-.1	-.1	---	---	---
TEI	3283.6	-.7	.9	.2	-.1	.9	.2

--- No Nulling Attempted

TABLE 3.3 SPS STARTUP TRANSIENTS AND GIMBAL POSITIONING ACCURACY

Maneuver	Engine Transient (deg)		Positioning Error (deg)	
	Pitch	Yaw	Pitch	Yaw
LOI 1	.3	.4	.3	.2
LOI 2	Negligible	.3	.3	.3
TEI	1.2	1.3	.3	.3

TABLE 3.4 FUEL SLOSH AND BODY BENDING OBSERVED DURING APOLLO 11

Maneuver	Fuel Slosh (rad/sec)			Body Bending (rad/sec)		
	P	Y	R	P	Y	R
LOI 1	---	---	2.4	16.3	---	---
LOI 2	---	2.7	2.9	---	---	---
TEI	3.8	3.8	5.6	---	---	---

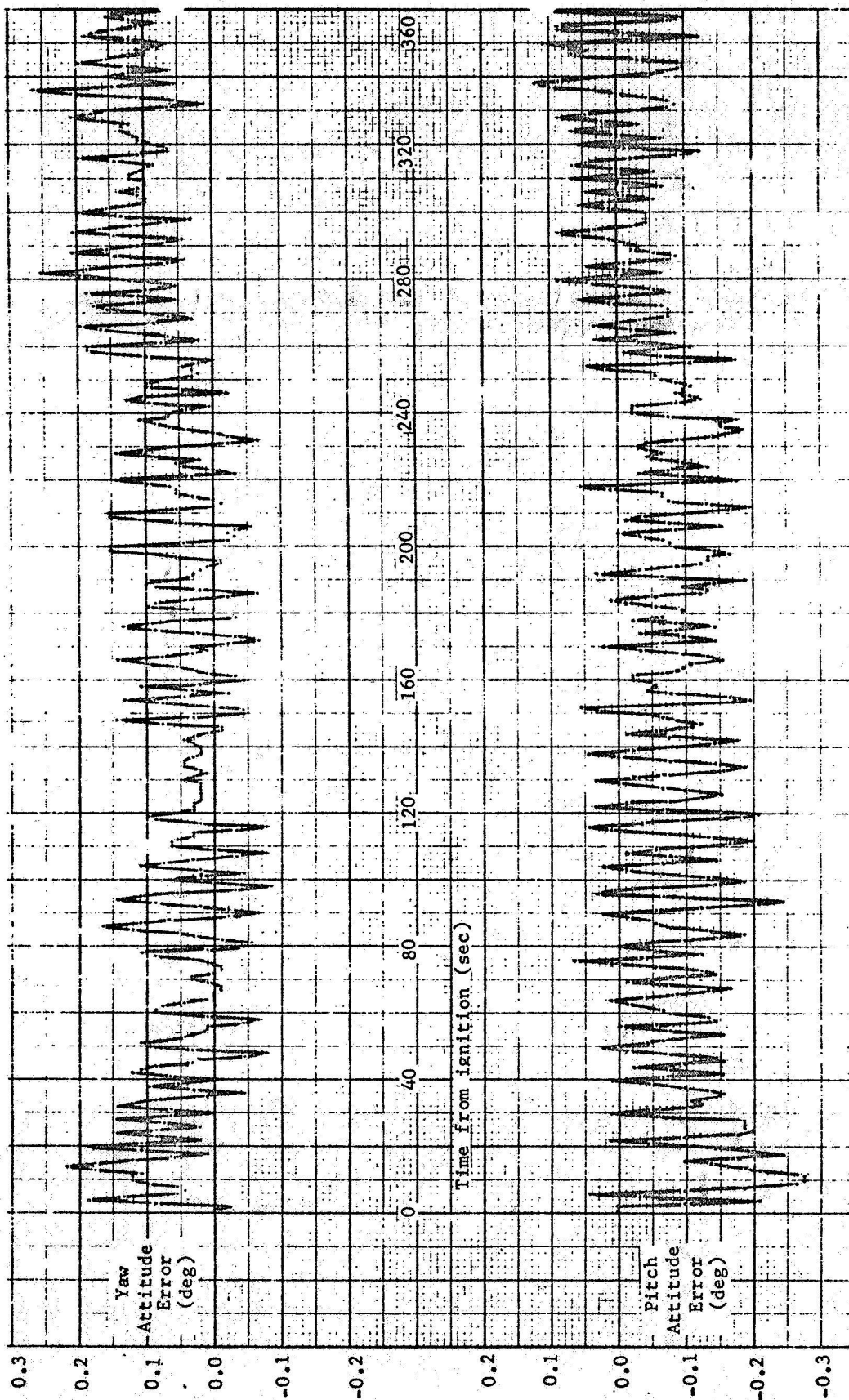


FIGURE 3-1

PITCH AND YAW ATTITUDE ERRORS DURING LOI 1

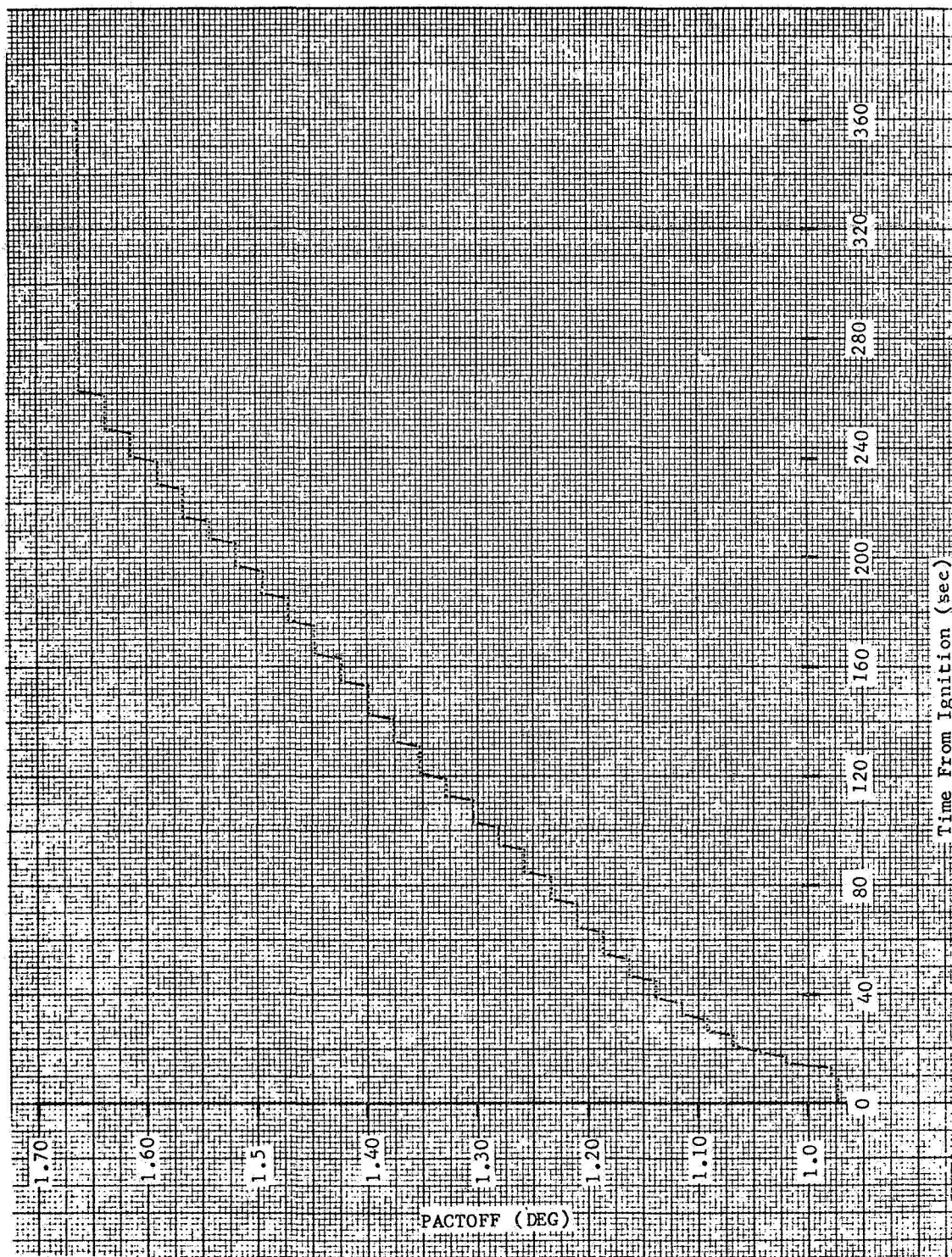


FIGURE 3-2
PITCH ENGINE TRIM ESTIMATE DURING LOI 1

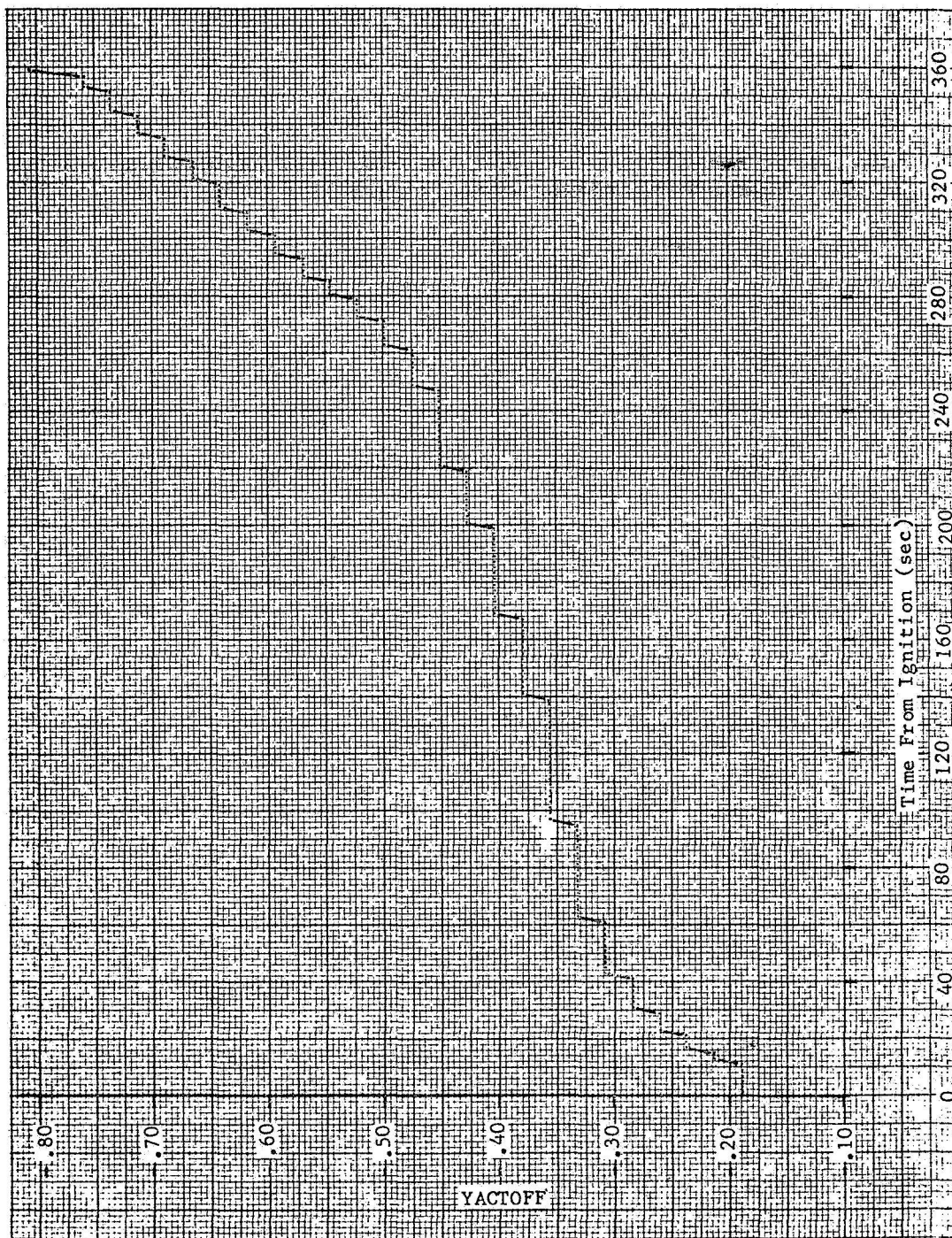


FIGURE 3-3
YAW ENGINE TRIM ESTIMATE DURING LOI 1

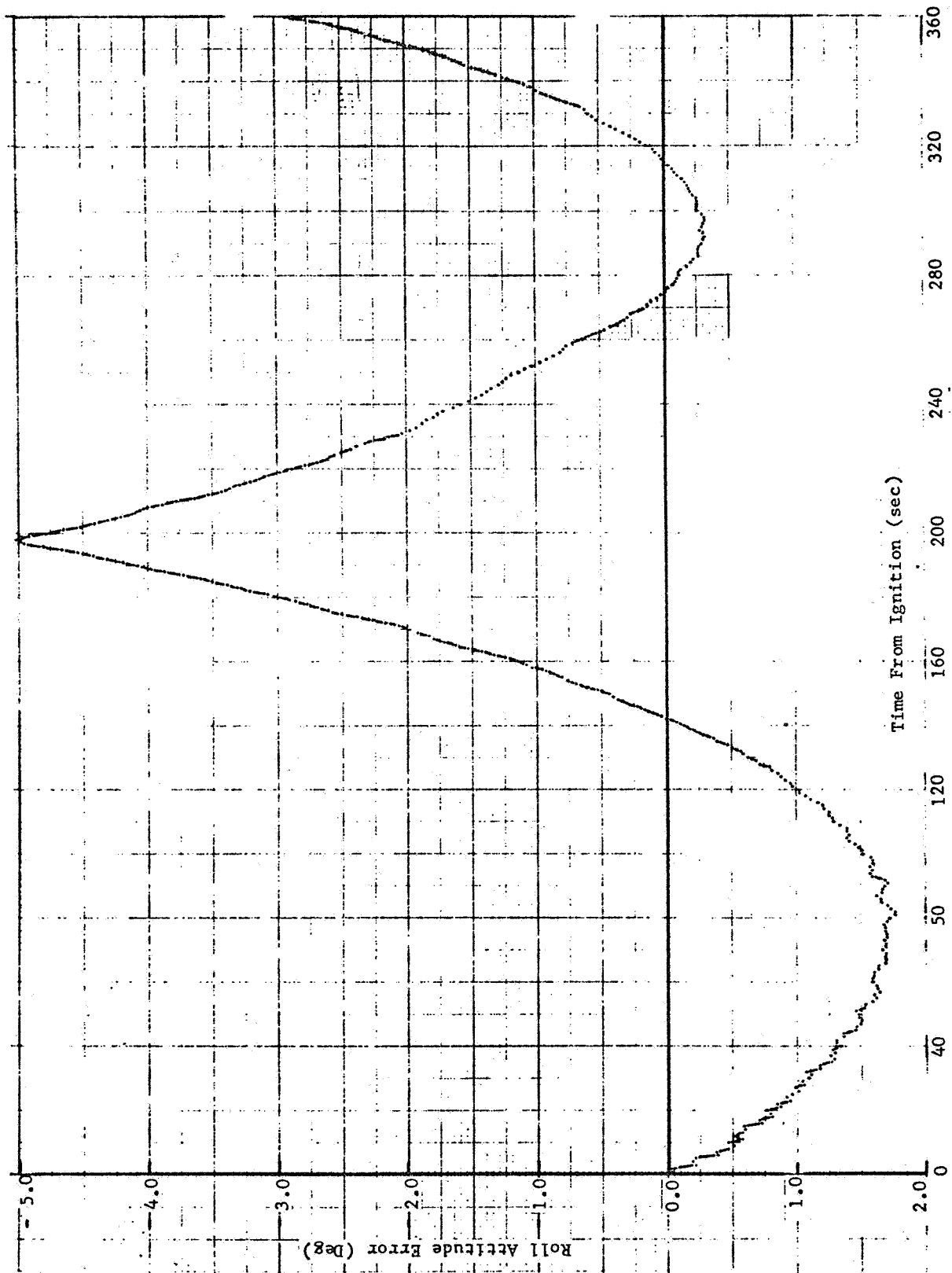


FIGURE 3-4
ROLL ATTITUDE ERROR DURING LOI 1

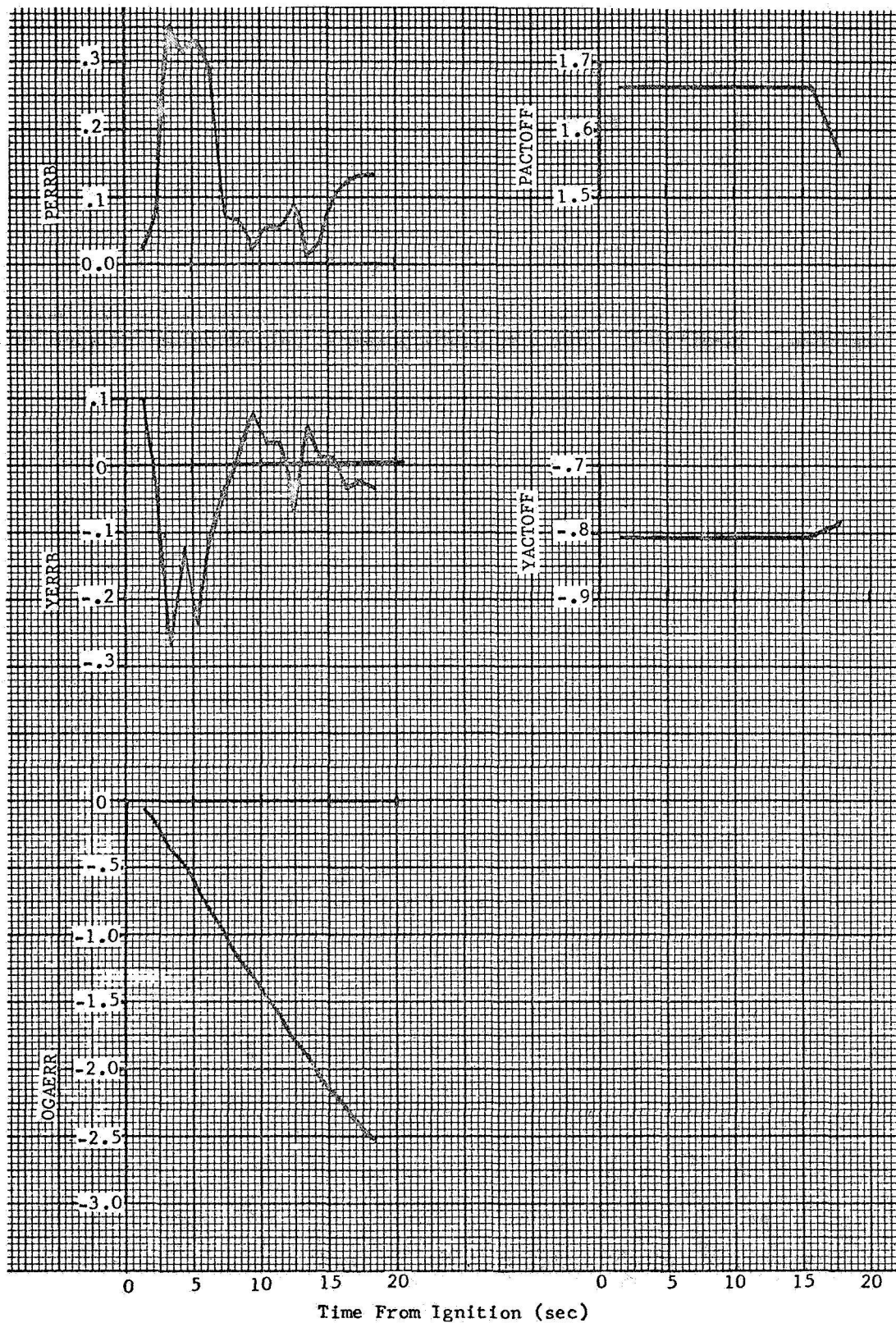


FIGURE 3-5
LOI 2 BURN PARAMETERS

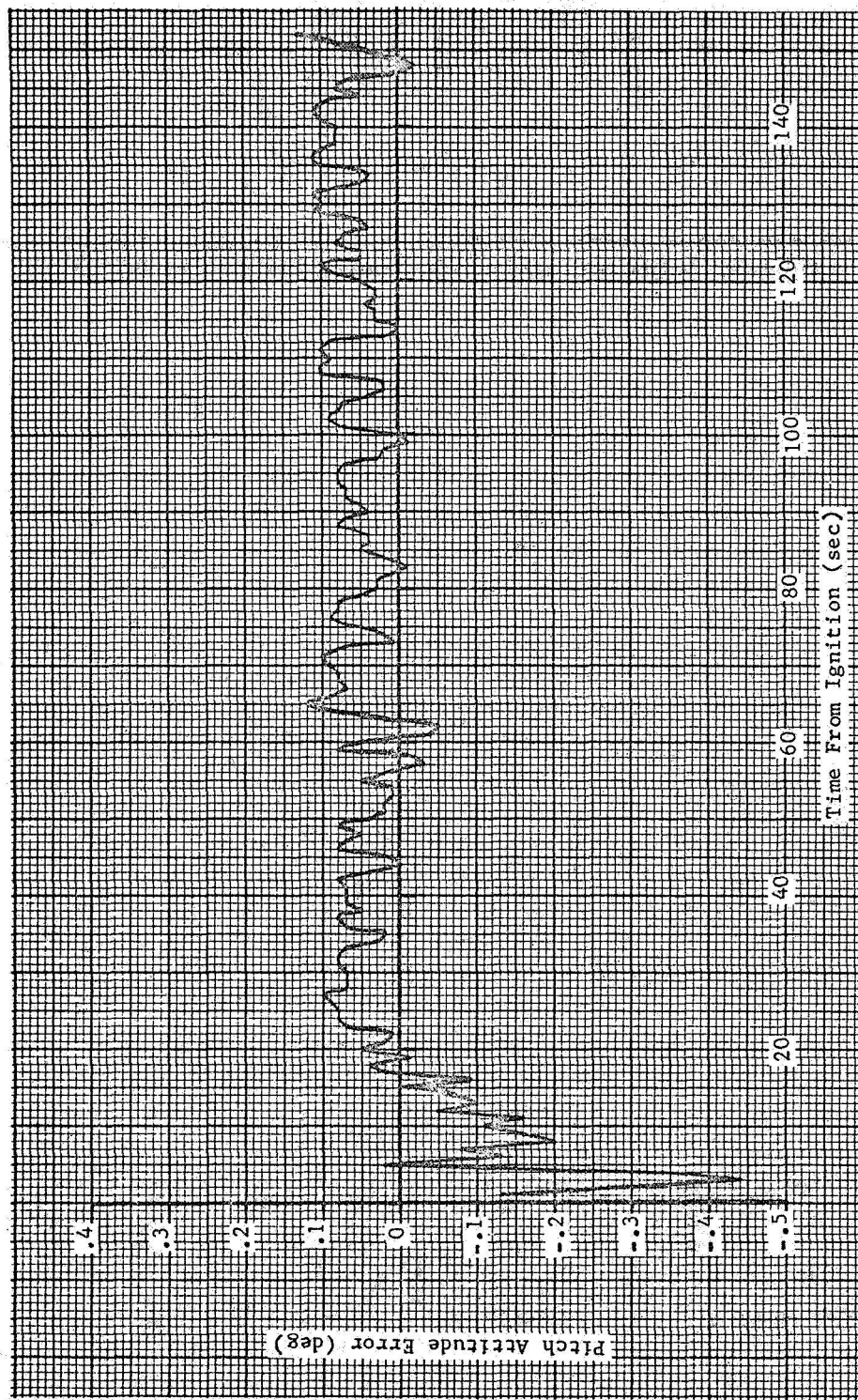


FIGURE 3-6
PITCH ATTITUDE ERROR DURING TEI

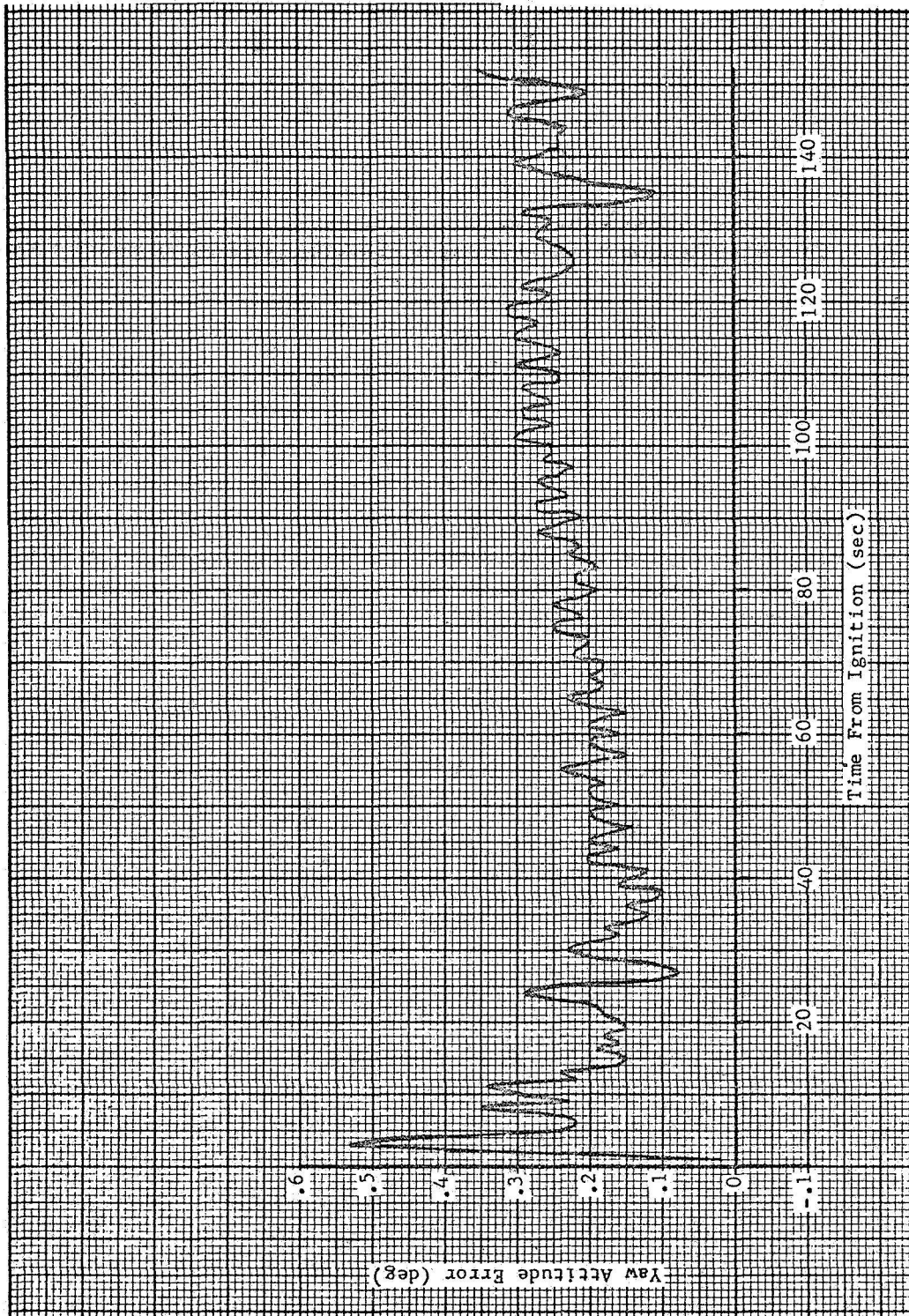


FIGURE 3-7.
YAW ATTITUDE ERROR DURING TEI

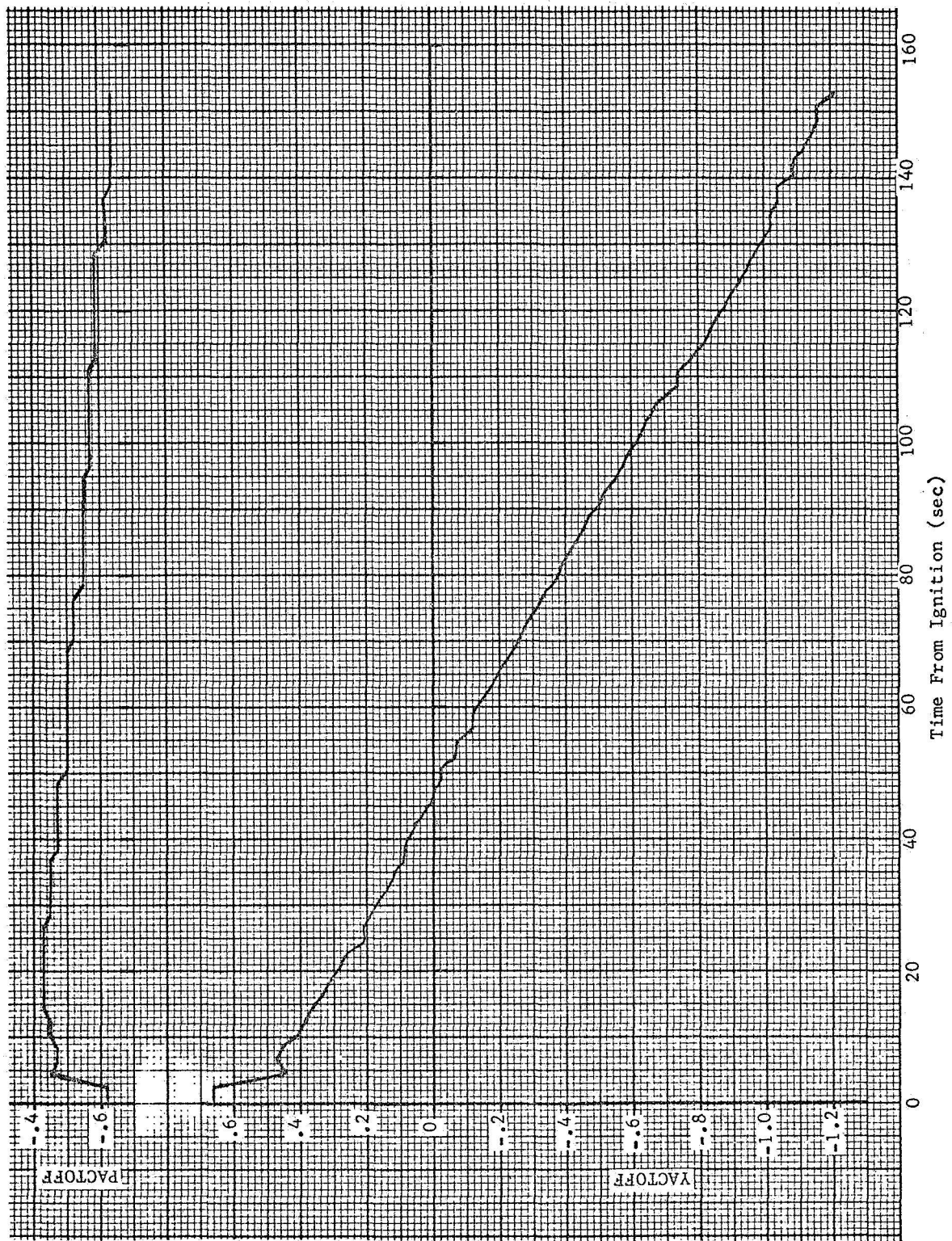


FIGURE 3-8
PITCH AND YAW ENGINE TRIM ESTIMATES DURING TEI

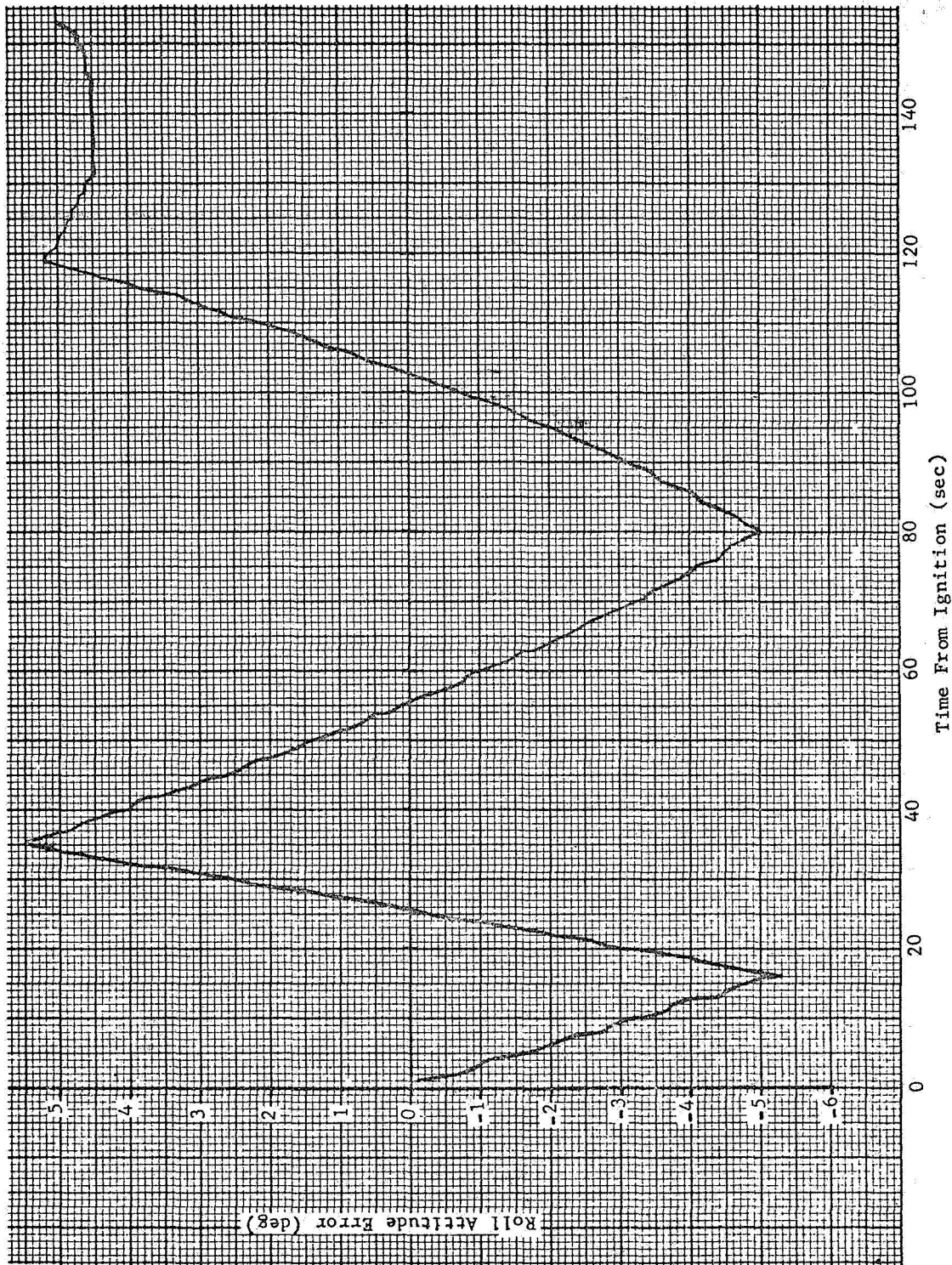


FIGURE 3-9
ROLL ATTITUDE ERROR DURING TEI

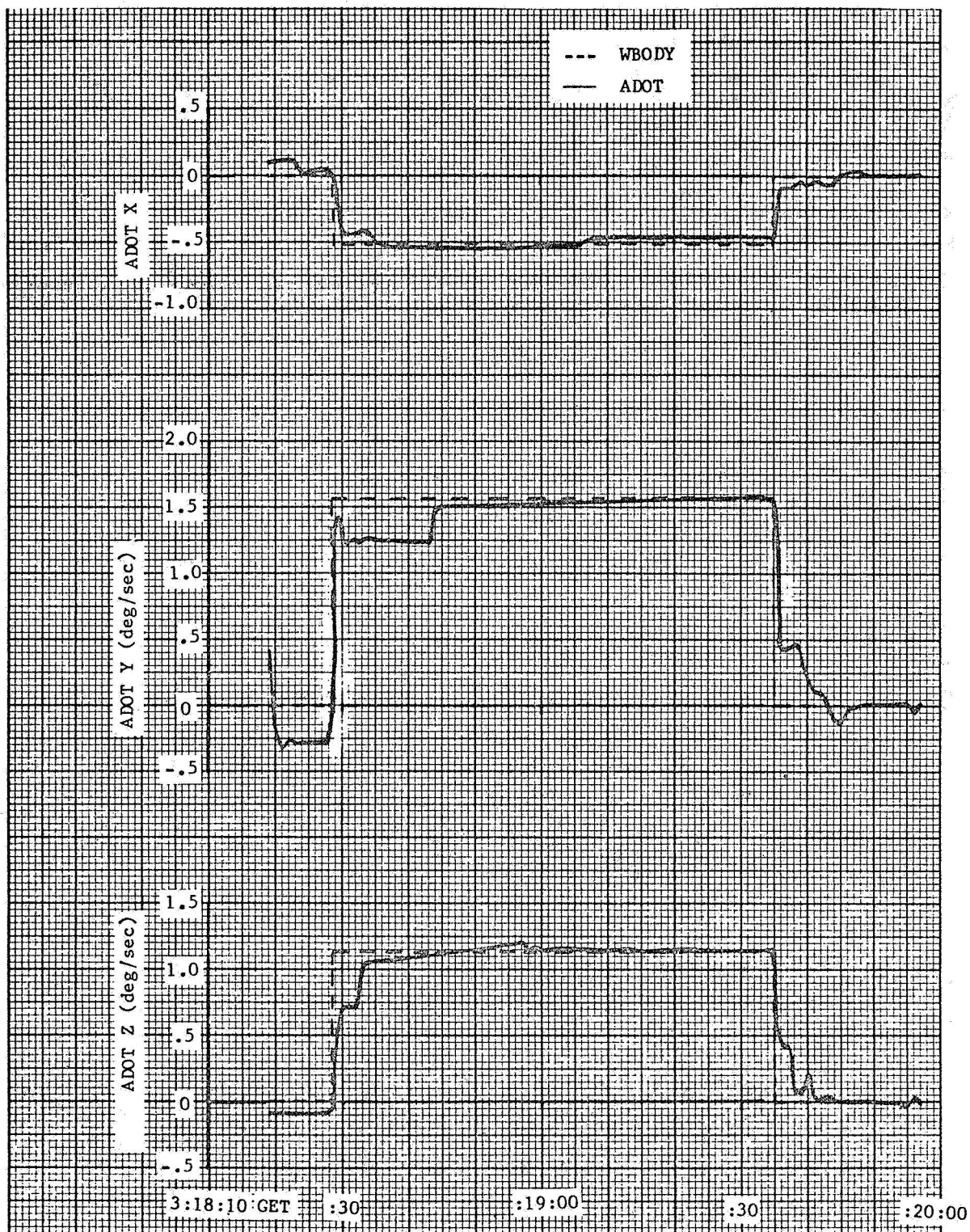


FIGURE 3-10
CMC AUTOMATIC MANEUVER DURING TRANSPOSITION AND DOCKING

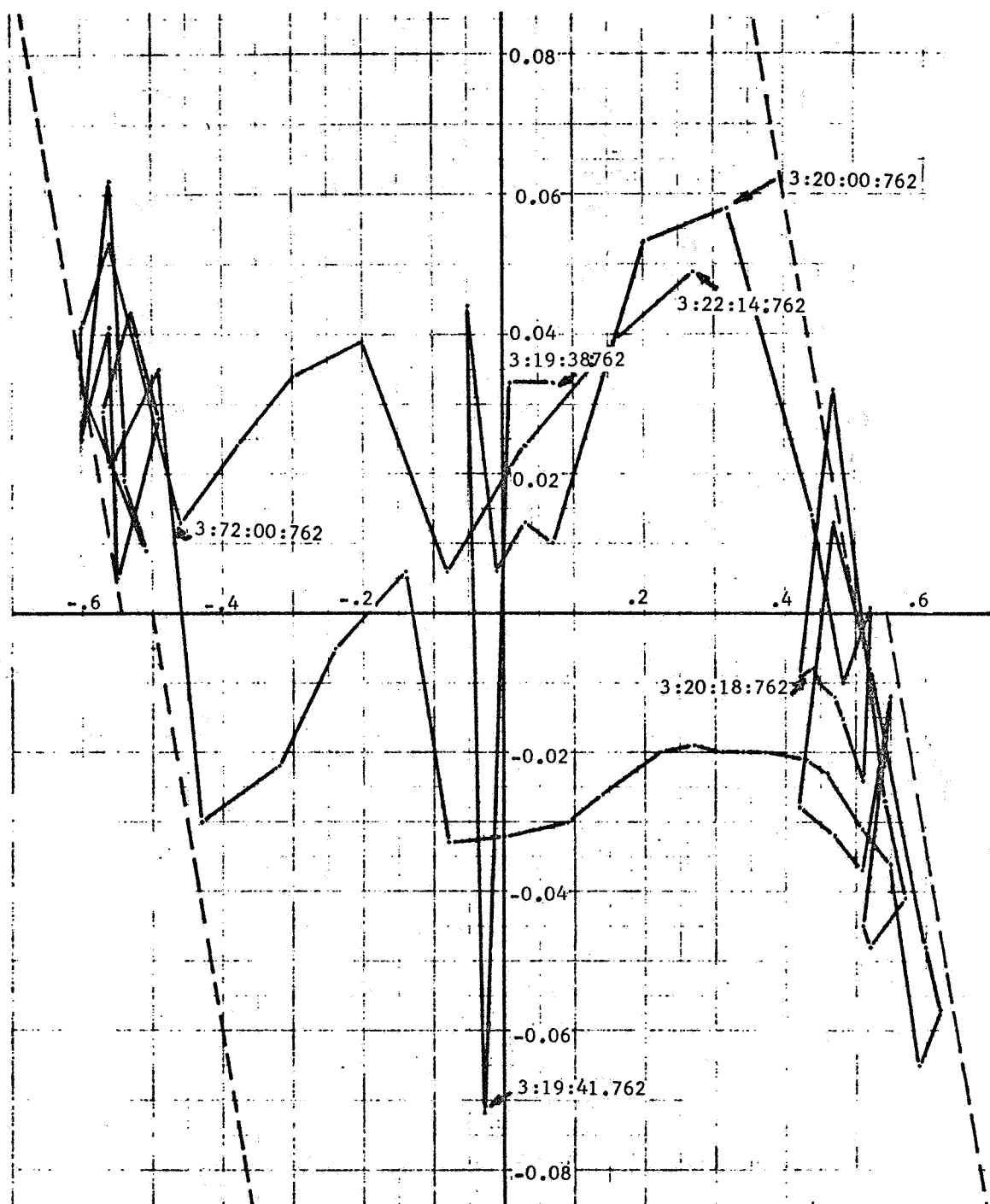


FIGURE 3-11

X-AXIS ATTITUDE HOLD DURING RCS TRANSLATION

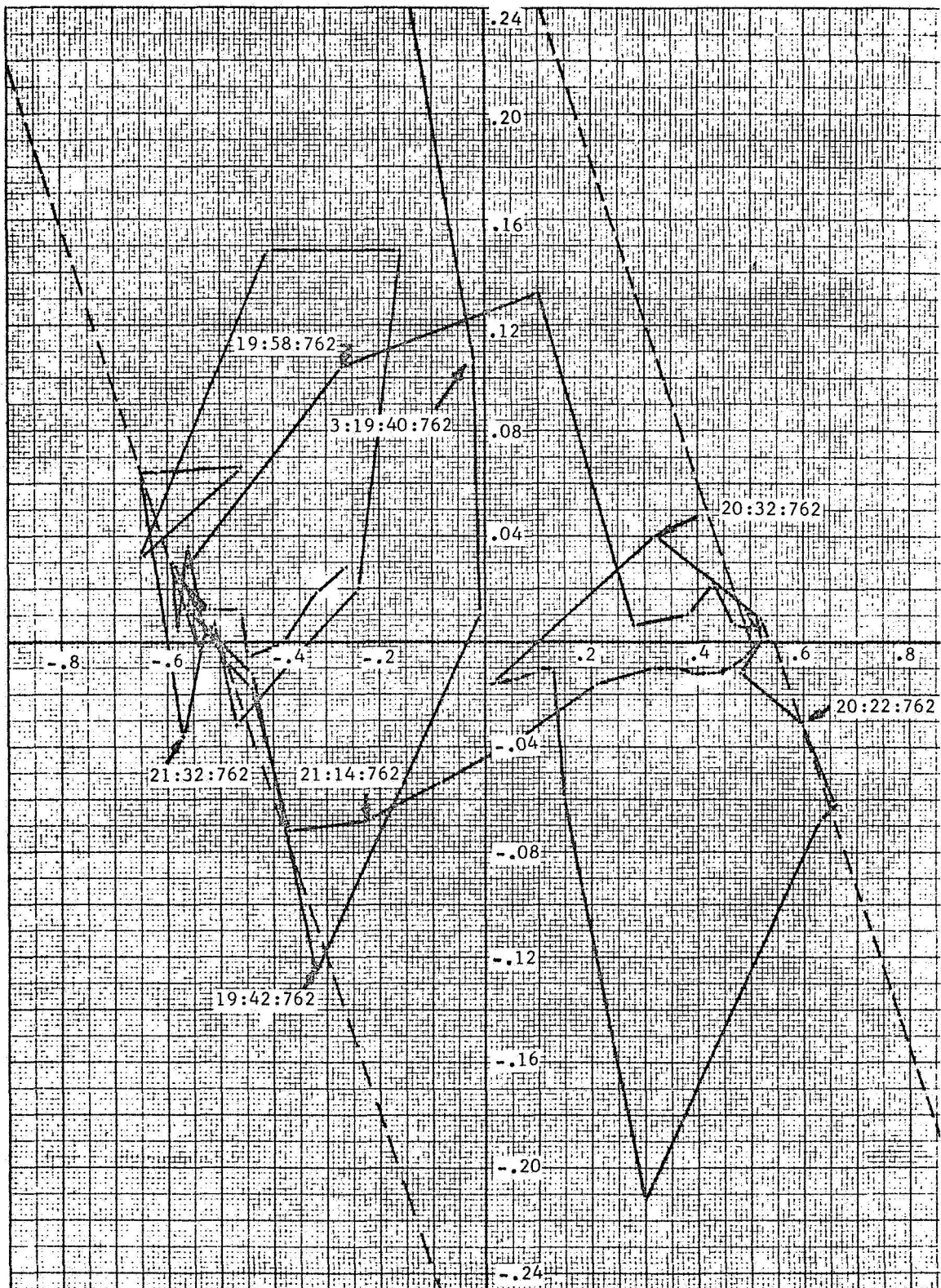


FIGURE 3-12
Y-AXIS ATTITUDE HOLD DURING RCS TRANSLATION

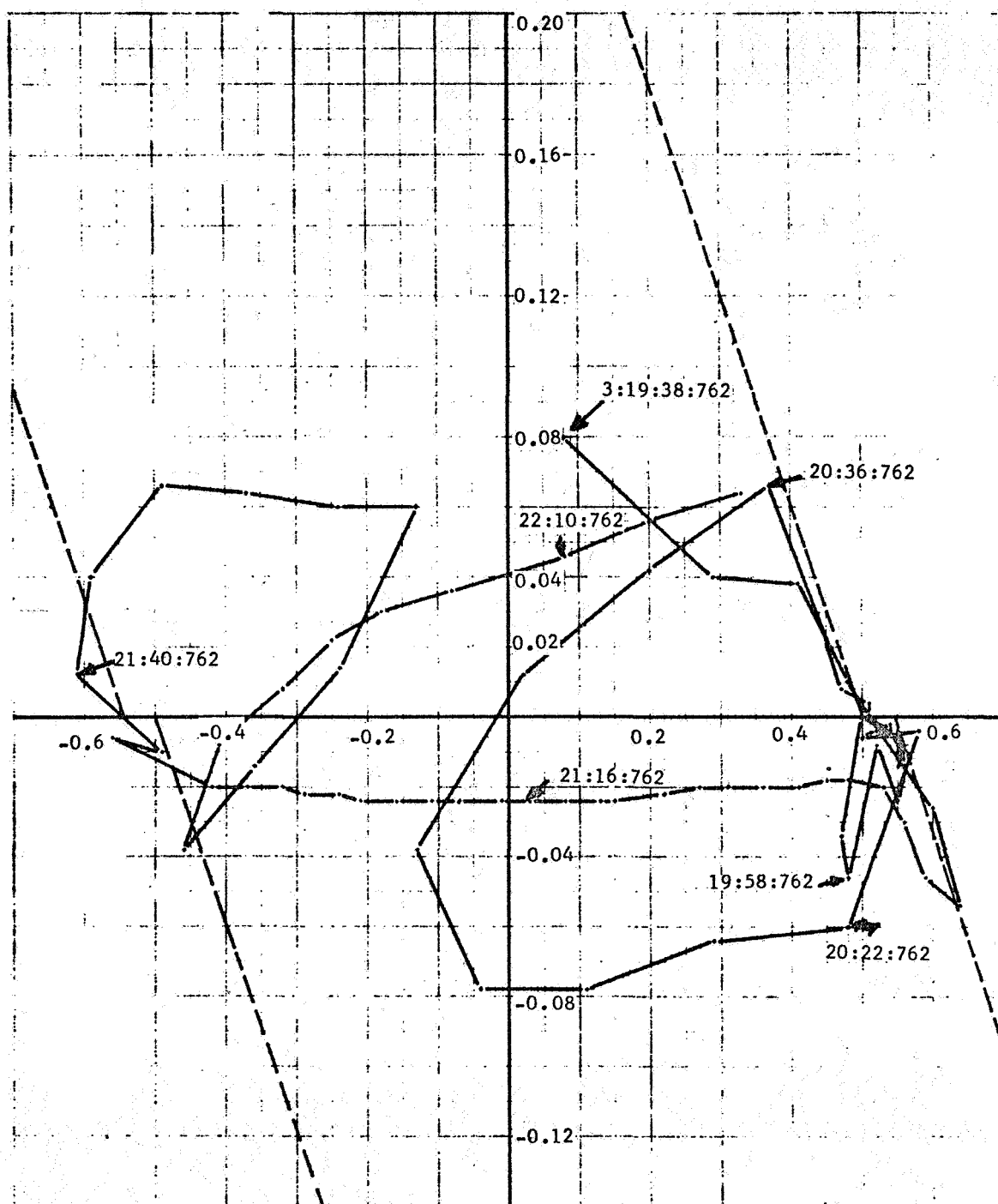


FIGURE 3-13

Z-AXIS ATTITUDE HOLD DURING RCS TRANSLATION

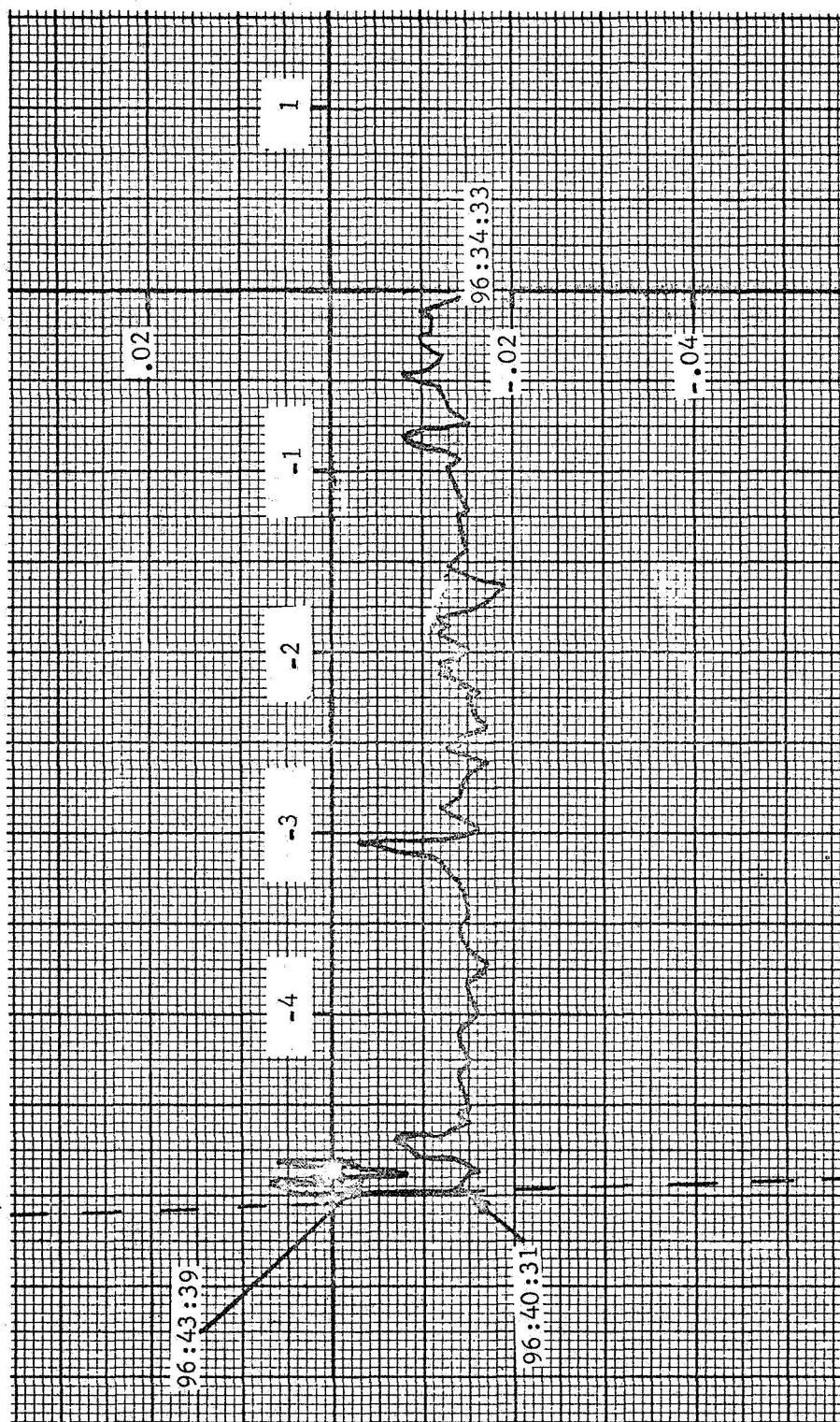


FIGURE 3-14
Z-AXIS ATTITUDE HOLD DURING SINGLE-JET CONTROL

4.0 LM DIGITAL AUTOPILOT

The LM DAP was active in controlling the LM from CSM/LM separation to docking. However, emphasis was placed on evaluating the powered descent and powered ascent phases of the Apollo 11 mission, since these control modes had not been flight tested previously. A brief analysis of the rendezvous sequence was performed. Although significant changes were implemented between the LUMINARY I (Apollo 10) and LUMINARY IA (Apollo 11) flight programs, the modifications primarily affected powered flight performance. This fact coupled with the extensive postflight analysis of the LM DAP performance during automatic attitude hold and automatic maneuvers for the Apollo 10 mission (Reference 5) permitted the omission of coasting flight performance evaluation for the Apollo 11 mission. The Descent Orbit Insertion burn could not be analyzed since it was performed behind the moon, and telemetry data was unavailable.

The periods of LM DAP control analyzed were:

- o Powered Descent
- o Powered Ascent
- o Rendezvous Burns

The "Guidance System Operations Plan for Manned LM Earth Orbital and Lunar Missions Using Program LUMINARY IA (Rev. 099), Section 3 Digital Autopilot (Rev. 1)," (Reference 6) served as the criterion for assessing nominal LGC computations and decisions. The data available for postflight analysis of the LM DAP are described in References 3 and 7. Reference 8 was utilized to track the nominal LGC/Astronaut interaction via the DSKY.

4.1 LM DAP PERFORMANCE DURING POWERED DESCENT

The powered descent of the Apollo 11 mission consisted of three program phases. The initial phase at Powered Descent Initiation (PDI) is P63, the Braking Phase program. This program functions to calculate the required time of DPS ignition and other initial conditions required by the

LGC for a PGNCs - controlled braking phase of the powered landing maneuver, to align the LM to the thrusting ignition attitude, to control the PGNCs during countdown, ignition, and thrusting of the powered landing maneuver until HI gate, and to indicate that HI gate has been reached by automatic selection of the Approach Phase program (P64). The Approach or Visibility Phase program (P64) functions to control the PGNCs between HI gate and LO gate, to control the DPS thrust and attitude during this phase, to provide a capability of redesignating the landing site to which the PGNCs is guiding the LM, and to select P65 automatically when time remaining is less than an internally programmed constant. During the Apollo 11 mission, the crew selected P66, the Rate-of-Descent (ROD) program, instead of the Automatic Landing Phase program (P65). This program provides for automatic control of the DPS thrust level to maintain a constant rate-of-descent as commanded by the crew via the ROD switch. The crew has manual control of the spacecraft inertial attitude via the Rotational Hand Controller (RHC). Table 4.1 presents an events timeline during powered descent and indicates times of program transition.

4.1.1 Program Sequencing

The available telemetry data indicated that, at the time of acquisition of signal from the LM following the DOI burn behind the moon, the LGC was in P63. These first available data were time-tagged at 102:17:17 GET. As indicated above, automatic program sequencing from P63 to P64 should occur when the HI gate targets have been met. For the Apollo 11 mission, the HI gate targets were:

7800 ft	altitude
-148 fps	altitude rate

The values displayed on the DSKY at the time of P63/P64 switchover (102:41:32.070 GET) for the Apollo 11 mission were:

7129 ft	altitude
-124 fps	altitude rate

It should be noted that the conditions at the exact time of switchover cannot be defined since DSKY data are available only once per two seconds

on the downlink data. The differences are considered small and correspond well with the differences between the nominal H1 gate targets and the altitude and altitude rates at P63/P64 switchover obtained from preflight simulations of powered descent (Reference 9).

The scheduled procedure for the Apollo 11 mission was for the crew to select P66 at an expected altitude of 500 ft. The downlink data at the time of entrance to P66 indicated that the altitude was 410 ft and the altitude rate was -10 fps. The 500 ft value was not a rigid constraint and crew discretion was the primary consideration.

4.1.2 Ullage And DPS Ignition

DPS ignition for PDI was preceded by a two-jet RCS ullage using jets 6 and 14. The duration of the ullage was 8.01 seconds. The LM DAP was maintaining the 1.0 degree attitude error deadband about the U'/V' control axes with no toggling of the ullage jets. The Apollo 10 mission, which utilized the same jet pair for ullage preceding the DPS phasing burn indicated some toggling of jet 14 for attitude control. The differences in the RCS jet duty cycles can be attributed to slightly different mass configurations and c.g. locations. One minimum-impulse coupled firing was required for P-axis control during ullage.

The DPS ignition sequence was nominal with the PIPA data, which were available once per two seconds, indicating that the ΔV monitor threshold had been well exceeded in the downlink frame occurring four seconds after ignition. The ignition transients were nominal, indicating good engine trim angles at engine cutoff following the DOI burn. As shown in Figure 4-1, the maximum transient response of the DPS engine was approximately 0.48 and 0.9 degree in pitch and roll, respectively. These values also include any transient effects from engine mount compliance at throttle-up (26 seconds after ignition as specified by ZOOMTIME). The nature of the transients shown in Figure 4-1 is also consistent with performance observed in preflight simulation tests (Reference 9). The maximum body rates obtained during the ignition transient period were:

OMEGAP = -0.4941
OMEGAQ = +0.6917 deg/sec
OMEGAR = -0.6917

and the maximum attitude errors about the control axes were:

PERROR = 1.08
UERROR = -1.022 deg
VERROR = -1.017

The rate and attitude error transients were damped quickly.

To obtain a qualitative comparison between the response of the spacecraft early in the powered descent phase and the behavior obtained for the short (≈ 40 seconds) DPS Phasing burn for the Apollo 10 mission, Figures 4-2 through 4-5 present pitch and roll rates and corresponding Gimbal Drive Actuator (GDA) responses for segments of both burns. Figures 4-2 and 4-3 present the pitch and roll rates and GDA activity for the first 40 seconds of the Apollo 11 powered descent burn. Figures 4-4 and 4-5 illustrate the same variables for the Apollo 10 DPS Phasing burn. Since the mass configurations between the two burns were somewhat different (Apollo 10 had off-loaded APS), the responses should not be identical, but a qualitative comparison indicated general agreement between the responses.

4.1.3 Windows-Up Maneuver

During the initial period of P63, the LM was positioned such that the window was pointed down toward the lunar surface. The crew was required to perform a 180 degree yaw maneuver to the "windows-up" position preparatory to entering P64. The maneuver was performed manually via the X-AXIS OVERRIDE Mode. Figure 4-6 presents the time history of CDUX

(outer gimbal angle) for this maneuver. CDUX will reflect yaw attitude excursions directly. The plot indicates several large periods of data dropout due to loss of communications as the S-Band antenna was repositioned during the maneuver. Despite some loss of data, several facts were observed. The maneuver was initiated via the RHC with the high rate scaling (20 deg/sec maximum on the RHC), as indicated by DAPBOOLS bit 7 (RHC SCALE). During the time period from 102:36:57.0 to 102:37:25.0 GET, the rate scaling switch for the rate error display needles was in the low scaling position (5 deg/sec maximum deflection). The maneuver was initiated with the crew assuming that the rate error scaling was set in the high position (20 deg/sec maximum deflection). Desiring a yaw rate of 5 to 7 deg/sec, the crew deflected the RHC until the yaw rate needle indicated this value, assuming high scaling of the error needles. However, since the scaling switch was in the low scaling position, the commanded rate was actually 1.25 to 1.75 deg/sec instead of the desired 5 to 7 deg/sec rate. The sluggish motion was detected immediately and the RHC was returned to detent as indicated by the flat portion of the CDUX plot. The rate scaling switch was changed to high scaling and the maneuver was completed at rates of -5.5 deg/sec or greater as shown in Figure 4-7. The figure also indicates that the initial phase of the maneuver exhibited rates as high as -3.3 deg/sec instead of the projected -1.25 to -1.75 deg/sec. This overshoot is compatible with the crew familiarization with the responsiveness of the vehicle and probably reflects deflection of the RHC to a point based on past experience with the rate command mode. As shown in Figure 4-6, CDUX approached zero at approximately 102:38:00 GET. At this time, a small + P rate was commanded until CDUX = +4.0 degrees. Hand controller activity to achieve this slight change in attitude was monitored via the RHC discretes in Channel 31.

4.1.4 Rotational Hand Controller Activity During Attitude Hold Mode Of P64

Near the termination of P64, the mode control switch was set from the AUTO position to the ATT HOLD position. With the mode control switch in

this position, the guidance commands are locked out of the DAP control logic and the LM DAP serves to maintain a fixed inertial attitude. This mode allows the crew to exercise the RHC and manually rotate the spacecraft in a rate command mode. The switch was first placed in the ATT HOLD position at 102:41:52.07 GET and reset to the AUTO position at 102:42:02.07 GET. During this time interval several pitch and roll commands were issued.

After the mode control switch was reset to the AUTO position, an accidental downrange redesignation was commanded when the RHC was apparently moved out of detent once at 102:43:08.07 GET issuing a - Q command. In the AUTO mode, this constituted a downrange redesignation. Figure 4-8 shows the effects of this redesignation. The average slope of the time history of the downrange distance-to-go (in stable member coordinates) changed with the redesignation. This accidental redesignation created no difficulties since the mode switch was returned to the ATT HOLD position at 102:43:12.07 GET, preparatory to entrance to P66 at 102:43:22.07 GET. The spacecraft was then under manual attitude control and the automatic redesignation was voided.

While the spacecraft was in attitude hold prior to entrance to P66, more pitch and roll commands were issued. The commands were not sufficiently large to create significant spacecraft transients. The utilization of RCS propellant during the two periods of attitude hold is discussed in a later section of this report.

4.1.5 Acceleration Nulling Mode Operation

As indicated previously, the spacecraft was placed in the attitude hold mode twice during powered descent. Control logic during such modes requires that the trim gimbal system (GTS or time-optimal control law) be rendered inoperative to prevent GTS activity slaved to manual commands. The LM DAP will use the gimbal drives only in the acceleration nulling mode. Drive times for the pitch and roll gimbal drive actuators (GDA's) are computed to trim the thrust direction to null the offset angular accelerations.

The LM DAP was in the attitude hold mode during the two time intervals 102:41:52.07 to 102:42:02.07 GET and 102:43:12.07 to 102:45:46.07 GET. The first time period was during the P64 phase and the second time interval encompassed the last part of P64 and the entire P66 phase. No gimbal drive commands were observed on Channel 12 (bits 9-12) during the time intervals 102:41:54.07 to 102:42:02.07 and 102:43:14.07 to 102:45:38.07 GET. This absence of gimbal drive commands was investigated to evaluate the DAP's performance during this mode of operation which had not previously been exercised in flight. An approximate reconstruction of the LGC computations for this mode was performed. The offset accelerations (AOS) about the Q and R axes, the LGC estimate of LM mass, and the ΔV 's along the X, Y, and Z axes were obtained from the downlink data. These quantities, which were telemetered once per two-second downlink cycle, were used to perform essentially the same computations as the LGC during the acceleration nulling mode. The output of the computations were gimbal drive times and directions. It should be noted that the LGC also performs the computations once every two seconds. However, the reconstructed computations will not give the exact values obtained by the LGC since the time the data are available on downlink does not necessarily correspond to the time at which the LGC performed its computations. Furthermore, since the downlink data are not sampled in "snapshot" form, the various variables are not available at the same instant of time.

The computed drive commands were compared to the downlinked offset accelerations and the GDA positions recorded on oscillograph records to verify the acceleration nulling mode. The computed gimbal drive times also enabled some consideration to be given as to whether the gimbal drive bits of Channel 12 should be set. It should be noted here that the bits of Channel 12 are sampled once every two seconds for transmission. Hence, some setting and resetting of bits could be lost in the time granularity of the data. Figure 4-9A shows the recorded offset acceleration about the pitch axis, the computed pitch GDA drive time and direction (sign of drive time corresponds to direction of gimbal drive), and the actual pitch GDA position for the first period of attitude hold in P64.

For the structural geometry of the GDA's, a negative value of pitch offset acceleration requires the pitch GDA to drive in a positive direction (extend) to null this disturbance acceleration. The computed drive commands were consistent with the polarity of the offset acceleration. The first computed drive time was approximately 18 DAP cycles (1 DAP cycle = 0.1 sec) and the succeeding drive times in the ten second interval were approximately 6, 1, 2, and 3 DAP cycles. Drive times are presented in integral DAP cycles since the LGC truncates its derived drive times to deciseconds or DAP cycles. Figure 4-9A indicates pitch GDA movement for each computed drive time was not detected in the flight. However, since a GDA drive time of one DAP cycle would produce only approximately 0.007 inch displacement of the GDA, the actual movement could have been lost in the granularity of the downlink data. Absence of drive command indications in Channel 12 could be attributed to the once per two second sampling of the channel bits.

Figure 4-9B presents similar plots for the roll axis during the same ten second time period. Due to geometry of the actuators, the roll GDA would be required to extend to counteract a positive roll torque in the acceleration nulling mode. There was an apparent sign inversion on the roll GDA position in the telemetry data. The sign was corrected in the plots. Again, every computed GDA drive command was not accompanied by detectable motion of the GDA but the computed drive times were small.

Figure 4-10 presents the pitch variables for the second period of attitude hold from 102:43:14.07 to 102:45:50.07 GET. Most of the computed drive times were from zero to two DAP cycles. At 102:45:38.07 GET, the pitch GDA drive times showed a significant increase. This activity resulted from large AOS values at touchdown. However, all of the drive times were sufficiently small (less than two seconds) to allow their possible loss due to time granularity of sampling Channel 12. One of the large pitch commands produced by the large AOS values at touchdown was detected in the downlink data. Figure 4-11 shows the response of the roll axis for the same time period with the sign error on the roll GDA position corrected. Again, due to the short commanded drive times, roll

gimbal drive commands do not appear in Channel 12 until the approximate time of touchdown. The large roll commands at this time were detected in the downlink data.

At 102:45:46.07 GET, the mode control switch was changed from ATT HOLD to AUTO. This reinstated the GTS logic which commanded drive times to assist in maintaining the phase-plane deadband. It should be noted that, in the GTS mode, longer drive times for the GDA's may be commanded for the same magnitude of AOS as in the acceleration nulling mode. This results from the GTS attempts to assist in maintaining the attitude error deadbands as well as nulling accelerations in the time-optimal manner.

Another area of interest was the appearance of GDA drive commands in Channel 12 after touchdown with no corresponding GDA movement. Investigations indicated that the DPS engine was disarmed (Channel 30, bit 3) at 102:45:52.07 GET. When the DPS engine is disarmed, the electrical power to the GDA's is removed, preventing the GDA's from responding to any LGC commands. It was quite likely that the LGC was still issuing GDA commands immediately after touchdown since it was still in P66 and in the GTS mode. Some gimbal commands were issued in an apparent attempt to maintain the required attitude error deadband between 102:47:20:07 and 102:47:48.07 GET. Since no power was available, the GDA's did not move. At 102:47:54.07 GET, the LGC entered P68, setting the "engine off" bits even though the engine had actually been off for some time. After P68 was entered, no additional gimbal drive commands were issued.

The operation of the acceleration nulling mode was nominal and the absence of gimbal drive commands on Channel 12 was consistent with the small drive times required and downlink data granularity. The existence of gimbal drive commands at touchdown and approximately two minutes after touchdown also appeared to be in accordance with the design specifications of the gimbal systems.

4.1.6 Manual Takeover, P66

As indicated previously, manual control of the spacecraft was initiated at 102:43:22.07 GET at an altitude of 410 ft and a descent rate of -10 fps.

The DPS engine is throttle controlled at entrance to P66 to yield a descent rate of -3 fps, unless more than one click was entered on the Rate-of-Descent (ROD) switch. Figure 4-12 is a plot of altitude rate versus time in P66. As the figure indicates, the rate-of-descent was reduced to -3.5 fps after entrance to P66. The plot also shows that P66 performed well in maintaining constant altitude rates with commanded discrete variations of 1 fps. Each click of the ROD switch indexes the desired altitude rate by 1 fps. However, downlink data did not provide a means for monitoring the ROD switch activity. The plot in Figure 4-12 does allow a qualitative assessment of the activity since regions of -3.5, -1.4, and -2.5 fps constant altitude rate are apparent. The transients in the altitude rate resulted from a combination of ROD switch activity and the RHC manual activity. Throttle variations could not completely follow the commanded pitch and roll excursions in attempting to maintain a constant altitude rate. Figure 4-13 shows the time history of the throttle command during P66. As would be expected, the throttle command was most stable in regions where the altitude rate approached a steady-state condition. Transition between constant altitude rates resulted in throttle command transients as large as 14% of full throttle.

There was a significant number of pitch and roll commands and a few yaw commands during this phase of powered descent. It was during this period of time that the crew detected the roughness in the vicinity of the intended landing site and took evasive action. The maximum body rates (including commanded rates) during P66 were -1.47, -6.15, and -3.66 deg/sec about the yaw, pitch and roll axes, respectively. These rates were within control capability of the LM DAP. Figure 4-14 illustrates the pitch and roll rates during a typical segment of the manual attitude control.

4.1.7 Lunar Touchdown

The control variables available on downlink telemetry precluded a detailed evaluation of touchdown dynamics. MSC has utilized an integration program using PIPA data to reconstruct the velocity vector prior to touch-

down and based on photographs of the landing pads and surrounding lunar terrain, has determined the time sequence in which the landing pads contacted the lunar surface. The results of these analyses are presented in the "Apollo 11 Mission Report" (Reference 10). The time of touchdown, the altitude rate, and contact sequence determined by these analyses are consistent with the coarse grain control data.

4.1.8 Spacecraft Response During Powered Descent

An overall, three-dimensional view of the descent is provided in Figures 4-15, 4-16, 4-17, and 4-18. The spacecraft altitude history from ignition to touchdown is presented in Figure 4-15. The horizontal velocity of the spacecraft during the final phase of descent (P66) is depicted in Figure 4-16 and the effect of manual attitude control is detectable. The altitude rate history for the entire descent is presented in Figure 4-17. This translational response was consistent with preflight predictions. Figure 4-18 characterizes the DPS throttle profile for powered descent and it appeared nominal compared to preflight simulation results.

The angular response of the spacecraft exhibited some interesting characteristics. As Section 4.1.2 of this report indicated, the angular response during ullage was nominal and the transients congruous with DPS ignition were quickly damped. The response was quiescent for approximately 230 seconds after DPS ignition. The maximum spacecraft rates during this period were 0.10, 0.30, and 0.30 deg/sec about the yaw, pitch, and roll axes, respectively, as determined from the rate gyro data. The attitude errors about the U'/V' control axes were constrained well within the 1 degree deadband. The yaw-axis attitude error during this period of time exhibited an X-axis torque effect. Figure 4-19 illustrates the effect of this disturbance torque. Second-order polynomials were fitted to the curve segments to obtain estimates of the disturbing torque. The torque ranged from -4.22 to -1.69 ft-lbs. The cause of this torque has not been determined although exhaust gas swirl has been suggested as a candidate. As the section on TVC DAP performance indicated, some torque effects were

apparent for the LOI1 and TEI SPS burns. Furthermore, previous flights exhibited such effects during some DPS and SPS burns with roughly the same magnitude of torque.

At the time of the "windows-up" maneuver ($\approx 102:36:57$ GET), slosh oscillations were apparent. Figure 4-20 presents the pitch, roll, and yaw rate gyro response during the P63/P64 phase of descent and discrete events such as incorporation of landing radar data, alarms, throttle down, and changes of control modes are annotated in the figure. Although the appearance of oscillations were concurrent with the "windows-up" maneuver, it cannot be concluded that this maneuver was the primary or sole cause of initiation of the oscillations. Preflight tests performed on the MSC bit-by-bit simulator (Reference 9) indicated a similar appearance of oscillations for runs with and without the X-axis maneuver. The maneuver does contribute to excitation of fuel slosh, but its absence apparently would not preclude oscillatory behavior at a later time. During the "windows-up" maneuver, the pitch and roll axes exhibited oscillations with a frequency of 0.53 Hz and peak-to-peak amplitudes of approximately 0.6 deg/sec. Figure 4-20 illustrates the growth in the oscillations to a maximum of 3.0 and 2.2 deg/sec, peak-to-peak amplitude, for the pitch and roll axes, respectively. Figure 4-21 presents a plot of attitude errors for a 40 second time interval during this time period. The attitude error deadband was maintained, but RCS jet firings were required to assist the GTS in maintaining attitude control. Figures 4-22 and 4-23 present the pitch and roll rates and GDA activity during this time period. The rates exhibit a combination of the slosh oscillations at a frequency of 0.5 to 0.6 Hz and a lower frequency oscillation of 0.1 to 0.09 Hz. The GDA's reacted well to the low frequency signal, but due to their limited drive rates, did not follow the higher slosh frequencies.

Higher resolution plots of the pitch and roll rates are presented in Figures 4-24 and 4-25. These plots are the pitch and roll rate gyro outputs for the same period of time. The low frequency curves were generated by connecting midpoints of the higher frequency oscillations. As the figures indicate, the roll rate exhibited a distinct low frequency characteristic

while the pitch rate had a more erratic steady-state behavior. Further investigations indicated an apparent energy transfer between the pitch and roll axes. In general, the periods where the roll rate displayed distinct low frequency effects, the pitch rate had no definite low frequency characteristics. Conversely, after some transition period, the reverse situation existed. The superposition of oscillations of two frequencies were also noted during preflight simulations on the MSC bit-by-bit simulator (Reference 9). The frequencies and amplitudes of the oscillations from the simulations are comparable to the flight results. The maximum body rates, not including RHC commanded rates, during P63 were -2.4, -2.1, and -1.5 deg/sec about the yaw, pitch and roll axes, respectively. The maximum attitude errors in control axes were -1.79, +1.14, and 1.21 degrees about the yaw, U' and V' axes, respectively.

Some reduction in oscillations occurred at throttle-down (102:39:30.65 GET). The automatic pitchover occurring at the beginning of P64 (\approx 102:41:31.45 GET) was performed by the LGC. Figure 4-26 shows the pitch and roll body rates for this event. The maximum pitch rate commanded for this maneuver was approximately -3.8 deg/sec. As shown in Figure 4-27, the pitchover maneuver resulted in -8.5 degrees change in pitch attitude which is consistent with preflight estimates of the maneuver. Figure 4-26 also shows a slight increase in oscillations after the maneuver. As indicated earlier in this report, the mode control switch was in the ATT HOLD position during two time periods of the P64 phase and the RHC was exercised during these periods. Due to granularity of the data, no detailed evaluation of performance of the rate command mode could be performed. The maximum body rates observed during P64, exclusive of manual commands, were 0.48, -2.4, and -1.5 deg/sec about the yaw, pitch and roll axes, respectively. The maximum attitude errors in control axes were +1.10, -1.39, and -1.86 degrees about the yaw, U', and V' axes, respectively.

Due to the extent of manual attitude control activity during P66, sloss oscillation effects could not be extracted. As previously reported,

maximum body rates during P66 were -1.47, -6.15, and -3.66 deg/sec about the yaw, pitch, and roll axes, respectively.

4.1.9 RCS Propellant Consumption

An investigation of the details of RCS propellant consumption was performed since the actual expenditure was approximately 88 pounds compared to a budgeted value of 40 pounds. Based on individual RCS jet activity defined in the "Bilevel Events Tabulations," the accumulated jet on-times were calculated and RCS propellant consumption on a per axis and per program basis was computed. Since manual RHC commands were issued, those jet firings consistent with the RHC commands, as derived from bit settings of Channel 31, were segregated from RCS activity for automatic control. Table 4.2 shows the predicted propellant consumption based on preflight simulation tests performed on the MSC bit-by-bit simulator and the actual propellant consumption. The propellant usage is divided into expenditures for control about the U'/V' axes and P-axis for each program phase. The simulator performed a program sequence of P63/P64/P65 to effect an automatic landing. The actual flight had a sequence of P63/P64/P66. Hence, direct comparisons for P63 and P64 were available. Also, consumption for manual maneuvers was separated from expenditures for automatic control.

As Table 4.2 indicates, the propellant consumption for control about the U'/V' axes during the P63 phase of the Apollo 11 mission agreed closely with the preflight simulation results. No manual commands were issued about the U'/V' axes during P63. The slightly higher value of RCS propellant consumption required during Apollo 11 was primarily due to the longer duration of P63 for the mission compared to simulation results (Table 4.3). Significantly more propellant was required for P-axis control than was predicted. However, a manual X-axis "windows-up" maneuver was not simulated for the comparison run. Other simulation runs indicated approximately 5 pounds were required for the maneuver. The actual maneuver required considerably more propellant than the simulation since an extra start/stop maneuver sequence was involved in completing the yaw maneuver

(See Section 4.1.3). The amount of propellant expenditure attributed to automatic control about the P-axis appeared extremely high compared to preflight predictions. The cause of this discrepancy is the fact that the criterion used for segregating RCS firings due to manual commands from those for automatic control was quite stringent. The once per two second sampling of the discretes in Channel 3 precluded detection of every RHC command. Furthermore, the number of jet firings attributed to nulling rates once the command was removed was subject to large errors. Hence, a more heuristic evaluation of the consumption would have attributed much more of the total expenditure to manual control requirements.

The propellant required for U-V axes control during the Approach Phase Program (P64) agreed well with the preflight results. Approximately 12.80 pounds of RCS propellant was required, of which 6.00 pounds was probably due to manual control. The propellant required for manual control was determined by accumulating jet on-times during periods of long duration jet firings when Channel 31 showed that the mode switch was in Attitude Hold and that Q and R rotations were commanded. The remaining 6.80 pounds of RCS propellant used for automatic control was slightly less than predicted by the preflight simulation. Some of this difference is probably due to the simulation having a 50 second longer duration in P64 than the actual flight (Table 4.3). Very little propellant was required for P-axis control in both the simulation and the Apollo 11 mission.

The Landing Phase (ROD) Program (P66) required 50.00 pounds of RCS propellant for U-V control and 1.045 pounds of RCS propellant for P-axis control. The bit-by-bit simulator runs did not simulate the P66 mode, since man-in-the-loop capabilities were required to produce meaningful results for comparison. It should be noted that the budget figure was based on results from other simulators which did attempt to simulate the manual control mode. However, none of the runs exercised the RHC to a degree consistent with the activity required during the mission.

4.1.10 Single Jet Control

Investigations of the RCS jet activity presented in the "Bilevel Events Tabulations" uncovered many indications of single-RCS-jet firings, including unbalanced couple firings about the P-axis which is not permitted by the control logic (Reference 6). Single-jet firings are permissible for control about the U'/V' axes if the commanded trim-gimbal nulling drive times are less than two seconds and the jets firings are minimum impulses (14 milliseconds). Past experience has shown that the jet firing data are quite subject to telemetry noise, which can appear in the data as indications of short jet firings. To validate the multitude of indicated single-jet firings, each such firing was correlated with data from the thrust chamber pressure (TCP) sensors. Unfortunately, these data are also subject to noise and during the course of the investigation, various combinations of RCS jet solenoid driver activity and TCP readings were observed. It was necessary to define a criterion for a valid RCS jet firing based on solenoid driver data and TCP data.

The TCP channels will give an "on" indication when the thrust chamber pressure reaches a value of 7 pounds per square inch. Due to this physical limitation, a finite amount of time will be required for the pressure to increase and decrease sufficiently to produce an on-off sequence for an actual jet firing. Therefore, the criterion chosen for validating single jet firings was for the jet driver outputs to indicate a 10 or 20 millisecond jet firing (data has granularity of 10 milliseconds) with TCP indications 5 to 15 milliseconds after the driver on signals. The TCP indications were also constrained to be "on" for approximately 45 to 70 milliseconds after the jet driver signal was removed to account for pressure tailoff effects. The 10 or 20 millisecond indicated firings are actually 14 millisecond firings depending on the time synchronization between the electrical on signal to the solenoid driver and the time the channel is interrogated.

With this criterion as the basis for validation, all of the indicated single-jet P-axis firings were proven to be invalid. Nineteen single-jet

firings about the U'/V' axes were accepted as valid. Table 4-4 lists the validated firings, which were all minimum impulse firings.

4.1.11 Frozen DSKY Displays

Downlink data provides monitoring of DSKY data on a once per two second basis. Perusal of the DSKY data during powered descent indicated twenty-three occurrences of the data in the DSKY registers being frozen for 2 to 20 seconds. Initial investigation of these events indicated that the majority were nominal sequences caused by LGC/Astronaut interfaces. Specifically, some of the incidents corresponded to a flashing verb/noun display by the LGC requesting astronaut decisions, while other incidents were caused by key activity initiated by the crew for interrogation of the computer for information not automatically displayed in the course of the powered descent programs. Still other events were associated with the 1201 and 1202 alarms. After this initial study, four periods remained unexplained. The verb/noun combination was a normal display for the program mode and no alteration of the combination was detected nor was the computer waiting for an astronaut response. Resolution of the question was received from other personnel investigating the problem. The frozen displays were crew-initiated since the crew was interested in monitoring the data in all three registers at certain times during descent. Since the data in the registers were changing rapidly, the displays were frozen for brief periods by striking the ENTER key. This action was not easily detected postflight. Normal displays were restored by striking the KEY RELEASE key. Hence, no period of frozen DSKY displays was left unexplained.

4.1.12 DPS Engine Mount Compliance

Compliance effects for the DPS gimbal system used on Apollo 11 were studied and compared to the compliance effects for the DPS gimbal systems used on Apollo 9 and Apollo 10. The theoretical gimbal trim angles are documented in the SODB (Reference 12). The actual gimbal trim angles were obtained by converting the estimated steady-state GDA positions to a

corresponding DPS engine bell pitch and roll angular position. A linear relationship of 3 degrees/inch was used to convert inches of GDA extend/retract to angular displacement of the engine bell. The signs of the angles were assigned to conform with the geometry associated with extension or retraction of the GDA's away from the null position (engine bell center-line aligned to X-axis). Compliance was defined as:

$$\text{Compliance} \triangleq \text{Actual Trim} - \text{Theoretical Trim}$$

No data were available for the DOI burn. The powered descent burn was used to obtain compliance data for throttle settings of 10.9% and 92.5%. A numerical average of the actual pitch and roll GDA positions was obtained using data sampled at one second intervals between 102:33:09.45 and 102:33:14.45 GET. The throttle setting at this time was 10.9% (minimum throttle). The averaging procedure yielded approximate steady-state GDA position values of 0.4585 and -0.1449 inch for the pitch and roll GDA's, respectively. Before converting the linear position data to angular position of the engine bell, it was necessary to change the sign on the roll GDA position, since, as previously noted, a sign error in the roll GDA telemetry data was found. The estimated engine bell position was -1.3755 and 0.4377 degree in pitch and roll, respectively, compared to theoretical trim values of -1.232 degrees (pitch) and 0.329 degree (roll). The compliance values of 0.14 and 0.11 degree about the pitch and roll axes, respectively, agree well with the theoretical compliance values obtained from the linear, thrust-dependent model. Figure 4-28 and 4-29 are plots of the pitch and roll compliance values obtained for the Apollo 9, 10, and 11 missions as well as the theoretical compliance values.

The large amount of time requiring a throttle setting of 92.5% during the Apollo 11 mission corresponded to large c.g. location shifts due to mass change. The c.g. shift resulted in significant changes in the theoretical trim values during the burn. Hence, a variety of time segments and time increments were used to obtain steady-state GDA position values. This procedure yielded a range of values for the compliance values. The computed pitch compliance varied from -0.49 to -0.13 degree and the roll compliance

ranged between 0.54 and 0.34 degree. The time segments used for these computations were 102:34:06.45 to 102:35:48.45 GET, 102:36:04.45 to 102:36:12.45 GET, and 102:36:54.45 to 102:36:58.45 GET.

Although the computed roll compliance ranged from 0.34 to 0.54 degree, the value was generally greater than 0.45 degree with exception of the isolated 0.34 degree computation. The 0.45 degree value correlates well with the theoretical value for roll compliance. Although the upper limit on the range of computed pitch compliance effects correlates with the theoretical value, the majority of computed values fell toward the smaller magnitude value, which does not agree well with the theoretical value. Further investigation indicated that pitch compliance values of -0.49 to -0.41 degree were obtained from 102:34:06.45 to 102:34:16.45 GET. However, computations of compliance values further into the burn led to progressively decreasing compliance values. This may have been caused by the slosh effects reported in Section 4.1.8, which were more dominant in the pitch axis than the roll axis.

No attempt was made to obtain values of compliance during the throttle down phase of the burn. The slosh effects were large in this phase of the burn and the throttle setting was not constant enough to allow an accurate determination of compliance versus throttle setting.

4.2 LM DAP PERFORMANCE DURING POWERED ASCENT

The Ascent Propulsion System (APS) was utilized from lunar liftoff to lunar orbit insertion. The LM DAP utilized the Powered Ascent program (P12) during this phase. This program functions (1) to display to the crew (prior to ascent engine ignition) certain LGC-stored parameters for possible modification by the crew, (2) to display to the crew (prior to ascent engine ignition) certain FDAI ball readings associated with the early phases of the ascent maneuver, and (3) to control the PGNCs during countdown, ignition, thrusting, and thrust termination of the APS powered ascent from the lunar surface. No additional APS burns were required. The significant events and corresponding times for the Apollo 11 powered ascent burn are tabulated below:

<u>EVENT</u>	<u>TIME (GET)</u>
Enter P12	123:54:04.17
Astronaut Enabled	
Ignition (V99 N74)	124:21:55.085
APS Ignition	124:22:00.78
Engine Off	124:29:15.669
Exit P12	124:32:03.13

4.2.1 Lunar Liftoff

Ullage was not utilized for the lunar ascent phase of the Apollo 11 mission since the LM was not in a zero-g environment. The ignition signal to the APS engine occurred at 124:22:00.78 GET. From Figure 4-30, a short period of low amplitude transients in the spacecraft angular rates can be detected after this "on" signal. Then, significant rate changes were evident until a data dropout shortly after ignition precluded further study of initial transients. In an attempt to correlate this small, initial transient with the APS thrust buildup, the theoretical engine-start thrust profile (Figure 4-31) was studied. An estimate of the thrust level sufficient to offset lunar gravity was computed using the LGC estimate of the vehicle weight at liftoff (10,839.8 pounds) and a lunar gravity of 5.3346 ft/sec^2 . This computed value of thrust was 1795.8 pounds which corresponds to 0.3236 second after the engine "on" signal. The time at which large angular accelerations were first detected was approximately 0.325 second after ignition. Hence, good correlation existed between thrust buildup and angular dynamics at liftoff.

The angular rates at the time of the data dropout were -1.48, 4.45, and 1.68 deg/sec about the yaw, pitch, and roll axes, respectively. The values obtained from preflight simulations were -0.3, 3.5, and 10.9 deg/sec. Apparently, the actual dynamics had higher pitch effects and lower roll effects than were modeled. However, as Figure 4-30 indicates, the actual rates probably had not peaked at the time of the data dropout. Estimates of the angular accelerations at liftoff were obtained by determining the

average slopes of the rate data presented in Figure 4-30. The maximum estimated accelerations for the available data were -12.0, 25.0, and 12.0 deg/sec² about the yaw, pitch, and roll axes, respectively. The yaw and roll accelerations are less than the values obtained from the MSC bit-by-bit simulator. The staging or Fire-in-the-Hold (FITH) forces modeled in the simulator are defined in Reference 13. The measured pitch acceleration appears to be twice the value expected from preflight simulations. Indeed, the model of FITH moments predicts roll torques an order of magnitude greater than the pitch torques. The converse appears to be true from the flight data. It should be emphasized that the comparisons could be made only for the short segment of data available prior to the data dropout.

An attempt was made to obtain a gross estimate of the position of the ascent stage relative to the descent stage at the time of data dropout. Assuming a constant thrust of 3500 pounds and a constant mass of 10,839.8 pounds from the time the thrust offset lunar gravity effects until the loss of data, a vertical displacement of approximately 2.5 inches was obtained. The LGC-computed altitude at the time the telemetry signal was regained (5.7 seconds later) was 118 feet. Hence, at the time the signal was lost, the ascent stage was not fully extracted from the descent stage and no complete assessment of FITH dynamics was possible.

A significant DAP modification in the LUMINARY IA program was the initialization of the LGC AOS estimates at the time of APS ignition in P12 via padloaded erasable quantities (IGNAOSQ and IGNAOSR). This initialization of AOS aids the state estimator in tracking the offset accelerations without the large initial time lags which occur when the LGC estimates are initially zero. The padloaded quantities of 6.25 and 0.63 deg/sec² about the pitch and roll axes, respectively, compare well with the flight-recorded values of 6.62 and 0.375 deg/sec² immediately after ignition.

4.2.2 Spacecraft Response During Lunar Orbit Insertion

The changes in altitude and altitude rate during a portion of the powered ascent burn are shown in Figures 4-32 and 4-33. The plots begin at

124:22:13.085 GET and show the variation of altitude and altitude rate for 380 seconds of the powered ascent burn. Data were not available for all of this time interval due to regions of frozen DSKY readings.

Figures 4-34, 4-35, and 4-36 show the yaw, pitch, and roll guidance commands (CDUD's) and the actual CDU responses to these commands during the first 40 seconds of the burn. The guidance commands were issued in the first 20 seconds of the burn to put the LM in proper orientation for lunar orbit insertion. A data dropout occurred shortly after ignition causing loss of some data. The total changes in CDUD were -16 degrees yaw, -4.1 degrees initial pitch due to the position of the LM on the lunar surface, -52.5 degrees pitchover, and 1.5 degrees roll. All attitude errors and rates due to the guidance commands were nulled within 4 seconds.

Figure 4-37 presents the spacecraft rates during the first 40 seconds of the burn. Following a short transient period the pitch and yaw rates exhibit the nominal limit-cycle characteristics. The frequencies annotated in the plots were computed on a half-cycle basis. Averaging over several oscillation cycles at various times in the burn gave a frequency range of 0.30 to 0.36 Hz for the limit-cycle frequency which agrees very well with preflight estimates of 0.32 to 0.36 Hz. The peak-to-peak amplitudes for the pitch and roll rates were 12.6 and 4.6 deg/sec, respectively. Again, these compare well with preflight results of 12.0 and 6.3 deg/sec for the pitch and roll axes, respectively. A low frequency modulation of the pitch and roll rates can be seen. Data were not available on the pitch and roll attitude errors. Preflight simulations (Reference 9) indicate the presence of the modulation in the pitch and yaw attitude errors and rates, but the attitude errors and rates about the U'/V' control axes do not have this modulation. Flight data at a sufficient frequency were unavailable for detailed definition of the spacecraft response about the control axes.

During the period in which the pitch and roll rates exhibited the nominal limit-cycle "sawtooth" behavior (Figure 4-37), slopes were fitted to the curves to obtain estimates of the offset accelerations due to the APS engine cant and cg. offset and of the accelerations to the two-jet torques required

for control. Examination of the "Bilevel Events Tabulation" indicated that two-jet, -U and +V firings were occurring during this phase of the burn. The estimated acceleration due to the jets, derived from the slopes of the curves agrees well with the theoretical value.

Yaw rate: 2.0751 deg/sec	OMEGAP: 1.8402 deg/sec
Pitch rate: -16.3043 deg/sec	OMEGAQ: -15.2930 deg/sec
Roll rate: 3.4585 deg/sec	OMEGAR: 3.2822 deg/sec

These values were less than predicted by the preflight simulation of powered ascent (Reference 9). The accuracy of the comparison between the preflight simulation and the actual flight is limited by the granularity of the downlink data. Some differences in the actual flight and the simulation results should be expected due to the differences in guidance commands. The maximum attitude errors and rate errors obtained during the response to the guidance commands were:

PERROR: 1.16 deg	OMEGAP ERROR: 1.80 deg/sec
U'ERROR: 2.89 deg	OMEGAU' ERROR: 4.64 deg/sec
V'ERROR: -2.39 deg	OMEGAV' ERROR: -4.33 deg/sec

The simulation results predicted larger maximum attitude errors for the P and V' axes. The maximum attitude error for the U' axis was of opposite sign and larger magnitude for the actual flight than the simulation. The V' axis rate error was significantly less than was expected based on the preflight testing and the U' axis rate error was approximately equal to the expected rate error magnitude.

After completion of the pitchover maneuver, the remainder of the powered ascent burn was considered to be the steady-state burn. The maximum attitude errors and rate errors were:

PERROR: -1.10 deg	OMEGAP ERROR: -0.98 deg/sec
U'ERROR: -2.17 deg	OMEGAU' ERROR: 3.79 deg/sec
V'ERROR: 2.32 deg	OMEGAV' ERROR: -4.00 deg/sec

The magnitudes of the maximum estimated rates and the rate gyro signals were:

OMEGAP:	0.9805 deg/sec	Yaw Rate:	1.0870 deg/sec
OMEGAQ:	4.7131 deg/sec	Pitch rate:	6.8182 deg/sec
OMEGAR:	4.3616 deg/sec	Roll rate:	5.8300 deg/sec

The attitude errors recorded are comparable to the values obtained from the simulation and the U' and V' rate errors were slightly higher than the predicted values.

During powered ascent, the attitude error deadbands associated with the phase-plane logic are functions of the estimated offset accelerations. Preflight simulations indicated that the attitude error response undergoes a change as the offset angular accelerations pass through zero. The change of sign of the AOS's is caused by the c.g. shifting, as a result of the APS propellant depletion, through the fixed APS thrust vector. According to Reference 14, for $|AOS| < 0.7 \text{ deg/sec}^2$, the phase-plane deadbands are set such that the U'/V' attitude errors oscillate almost between the positive and negative deadbands. As $|AOS|$ diminishes, and enters the zone, $0.3 \text{ deg/sec}^2 < |AOS| < 0.7 \text{ deg/sec}^2$, the phase-plane attitude error deadbands are set such that a tight limit cycle at one of the deadbands is held. For a positive AOS, the limit cycle holds about +1.0 degree with small rate and attitude error amplitudes. For a negative AOS, the limit cycle centers about -1.0 degree. As the c.g. shifts closer to being in line with the APS thrust vector and $|AOS| < 0.3 \text{ deg/sec}^2$, the attitude error tends to drift across the phase plane in a manner similar to coasting flight effects.

In an attempt to verify this behavior, computations were performed on Apollo 11 LGC downlink data to obtain the U' and V' offset accelerations (AOSU' and AOSV') and attitude errors (U'ERROR and V'ERROR). Figures 4-38 and 4-39 show the U' and V' attitude errors and offset accelerations from 124:26:43.085 GET until completion of the burn. As the figures indicate, the attitude errors exhibited a tendency to be biased on a deadband when the magnitude of the AOS's were approximately equal to 1.4 deg/sec^2 or less. However, the amplitudes of the limit cycles were quite large with a few

instances in which the attitude error traveled almost to the opposite deadband. In general, a tendency to "hang" at one deadband was detected. When $|AOS|$ was less than approximately 0.7 deg/sec^2 , the Apollo 11 data displayed small limit-cycle amplitudes about the deadbands. The V' axis attitude errors exhibited a smaller amplitude limit cycle than did the U' axis limit cycle. These results correlated well with the preflight simulation results.

When the AOS's changed signs, the corresponding attitude error exhibited a sharp transition to holding a tight limit cycle about the deadband having the same sign as the AOS. This agreed with the preflight simulation results. The only area in which good correlation was not obtained was for the region in which $|AOS| < 0.3 \text{ deg/sec}^2$. The attitude error did not exhibit the "drifting flight" characteristics. However, the existence or nonexistence of such behavior could not be completely verified in postflight analysis due to the small amount of time the magnitude of AOS was less than 0.3 deg/sec^2 .

Figure 4-40 shows the rate response just before APS cutoff. The reversals in sign of the pitch AOS from that noted at the beginning of the burn is apparent. The amplitudes of the rates were significantly reduced from those detected early in the burn (Figure 4-37) since the c.g. was much closer to the APS thrust vector. At this time, only single-RCS-jet firings created +U or -V torques were required for control. Slopes were fitted to the rate data in Figure 4-40 to obtain estimates of the AOS's and the accelerations due to the one-jet firings. A short time before engine cutoff, the pitch AOS, as determined by slope fitting, appeared to increase sharply. The LGC estimate of the AOS did not indicate any such behavior. It is apparent from the plots that the rates, just prior to APS cutoff, deviated from their nominal "sawtooth" behavior and slope fitting data in this area may not be meaningful.

The burn ΔV was 6060.9 ft/sec with a burn time of 434.88 seconds. The orbit achieved had an apolune of 47.3 n.m. and a perilune of 9.5 n.m. The burn residuals were -2.1 , -0.1 , and $+1.8 \text{ ft/sec}$ for ΔV_X , ΔV_Y , ΔV_Z ; respectively. This overburn of approximately 2 ft/sec was a result of higher tailoff effects

than were estimated and incorporated into the LGC guidance computation. Manual nulling was performed to reduce the residuals to +0.4 ΔV_X , -1.0 ΔV_Y , and +1.4 ΔV_Z .

4.2.3 C.G. Shifts During Ascent Burn

Figure 4-41 shows the pitch and roll angular accelerations estimated by the LGC for use in the DAP. The figure indicates that the average pitch acceleration during the period of time covered by Figure 4-37 is 6.8 deg/sec^2 , which agrees with the value obtained by determining the slope of the rate data (Figure 4-37) in this time interval. These data plus the estimated accelerations due to two or one-jet firings were used to determine the c.g. location for comparison to those listed in the "Spacecraft Operational Data Book" (Reference 12).

For the early portion of the flight, RCS jets 6 and 10 were firing to provide the restoring torques. As Figure 4-42 indicates, both of these thrusters lie on one side of the estimated c.g. location. Therefore, referring to Figure 4-42, the two equations can be written:

$$T z \cos \alpha = I_{yy} \ddot{\theta}_1$$

$$T_2 (66.1 + \bar{Z}) - T z = I_{yy} \ddot{\theta}_2$$

where

T = APS thrust (3470 pounds)

T_2 = RCS thrust from two jets (200 pounds)

I_{yy} = Spacecraft inertia about Y-axis (3530 slug-ft²)

$\ddot{\theta}_1$ = Pitch acceleration when no jets are firing (6.80 deg/sec^2)

$\ddot{\theta}_2$ = Pitch acceleration when two jets are firing (11.80 deg/sec^2).

The equations can be solved for z and \bar{Z} , which then allows a determination of \bar{X} via the geometry of the system. A similar approach was used to determine \bar{Y} by considering torques about the Z-axis. However, since the AOS about the roll axis was quite small (Figure 4-41) some estimation of an average roll AOS was required, which introduces some error into the computations. The

process was repeated for a period late in the burn.

Table 4.5 presents the computed c.g. locations with the corresponding SODB values. Good correlation was obtained during the early phases of the burn. Less correlation is seen at the end of the APS burn. The computed y-axis c.g. location is opposite in sign to the theoretical value. This appears to be a valid calculation since Figure 4-41 shows that the roll offset acceleration does pass through zero instead of increasing monotonically, as predicted. Hence, it would appear that APS propellant depletion moved the \bar{Y} c.g. location negatively instead of positively as predicted.

4.2.4 Propellant Consumption

The ascent burn was performed with the APS interconnect open such that the RCS jets utilized APS propellant. The total APS propellant used was approximately 4,893 pounds, resulting in approximately 284 pounds of usable APS propellant remaining after completion of the burn. Approximately 73.2 pounds of the APS fuel was used by the RCS jets for attitude control. More APS propellant and less RCS activity was required than was predicted by preflight simulations on the MSC bit-by-bit simulator. The Apollo 11 ascent burn consumed more APS propellant than was predicted by the preflight simulation because the actual burn was 17 seconds longer than the simulated burn time. Some of the additional RCS propellant expended in the preflight run resulted from different guidance commands between the flight and simulation.

4.2.5 Frozen DSKY Displays

During powered ascent, thirteen periods of frozen DSKY displays were detected. As was the case of such activity during powered descent (Section 4.1.11) the DSKY activity was explainable. Six of the events corresponded to Astronaut/LGC interaction which could be detected by verb/noun changes. The other seven occurrences were results of intentional freezing of the displays via depression of the ENTER button.

4.3 RENDEZVOUS SEQUENCE

The rendezvous sequence following the APS lunar orbit insertion burn consisted of four RCS burns. The timeline of the rendezvous events was:

Coelliptic Sequence Initiation (CSI)	125:19:36 GET
Constant Differential Height Maneuver (CDH)	126:17:49.6 GET
Terminal Phase Initiation Maneuver (TPI)	127:03:51.8 GET
Terminal Phase Finalize Maneuver (TPF)	127:43:08 GET

No detailed analysis of DAP control during the RCS translation burns was performed but a cursory analysis of the data indicated that the attitude error deadband was maintained during the burn. The residual velocities remaining after the burn serve as the standard for performance of the burns. Table 4.6 presents the burn times and residual velocities both before and after manual nulling. The residual velocities prior to nulling were available on downlink telemetry for the CDH and TPI burns and were nominal. Based on these data, the RCS burns appeared to be nominal when compared to past performance of the LM DAP for RCS burns on Apollo 9 and Apollo 10.

TABLE 4.1

EVENTS TIMELINE

EVENT	TIME	SEC. FROM IGN.
ULLAGE STARTED	102:32:56.97	-7.57
DESCENT PROPULSION SYSTEM IGNITION	102:33:04.54	0.0
ULLAGE COMPLETED	102:33:04.985	0.445
MANUAL "WINDOWS-UP" MANEUVER	102:36:57.00	232.46
"DATA GOOD" PRESENT (LRV LRH)	102:37:50.07	285.53
Δ H DATA AVAILABLE (DOWNLINK)	102:37:54.07	289.53
1202 ALARM (P63)	102:38:28.07	323.53
FIRST Δ H INCORPORATED (V57)	102:38:44.07	339.53
FIRST VEL. INCORPORATED (FW11, BIT 5)	102:38:50.07	345.53
1202 ALARM (P63)	102:39:10.07	365.53
AUTOMATIC THROTTLE DOWN IN P63	102:39:30.65	386.11
ENTER P64	102:41:32.07	507.53
1201 ALARM (P64)	102:42:20.07	555.53
1202 ALARM (P64)	102:42:48.07	583.53
ENTER P65 (AUTO LANDING PROGRAM)		
ENTER P66 (ROD PROGRAM)	102:43:22.07	617.53
LUNAR TOUCHDOWN	102:45:39.8	755.26

TABLE 4.2
RCS PROPELLANT CONSUMPTION

Program	Preflight Run 2.0.7 Data			Apollo Data		
	U-V	P	U-V		P	
			Automatic Control	Manual Control	Automatic Control	Manual Control
P63	10.18 pounds	0.044 pounds	11.00 pounds	N/A	3.69 pounds	8.76 pounds
P64	7.27 pounds	0.57 pounds	6.80 pounds	6.00 pounds	0.389 pounds	0
P66	N/A	N/A	N/A	50.00 pounds	N/A	1.045 pounds

TABLE 4.3

TIME DURATIONS OF DESCENT PROGRAMS

	Preflight Run 2.0.7	Apollo 11
DPS Ignition to End of P63	498.5118 seconds	507.530 seconds
P64	160.2166 seconds	110.000 seconds

TABLE 4-4
SINGLE-JET FIRINGS

	NUMBER OF SINGLE-JET FIRINGS
PROGRAM PHASE	
P63	6
P64	7
P66	6
JET NUMBER	
1	2
2	5
5	0
6	2
9	3
10	4
13	2
14	1

TABLE 4.5
COMPUTED AND THEORETICAL C.G. LOCATIONS

	C.G. Location Early in Burn (inches)			C.G. Location Late in Burn (inches)		
	X	Y	Z	X	Y	Z
Computed SODB	+246.40	+0.03	+2.65	264.97	-0.10	+4.77
	+243.67	+0.14	+2.82	256.5	+0.28	+5.00

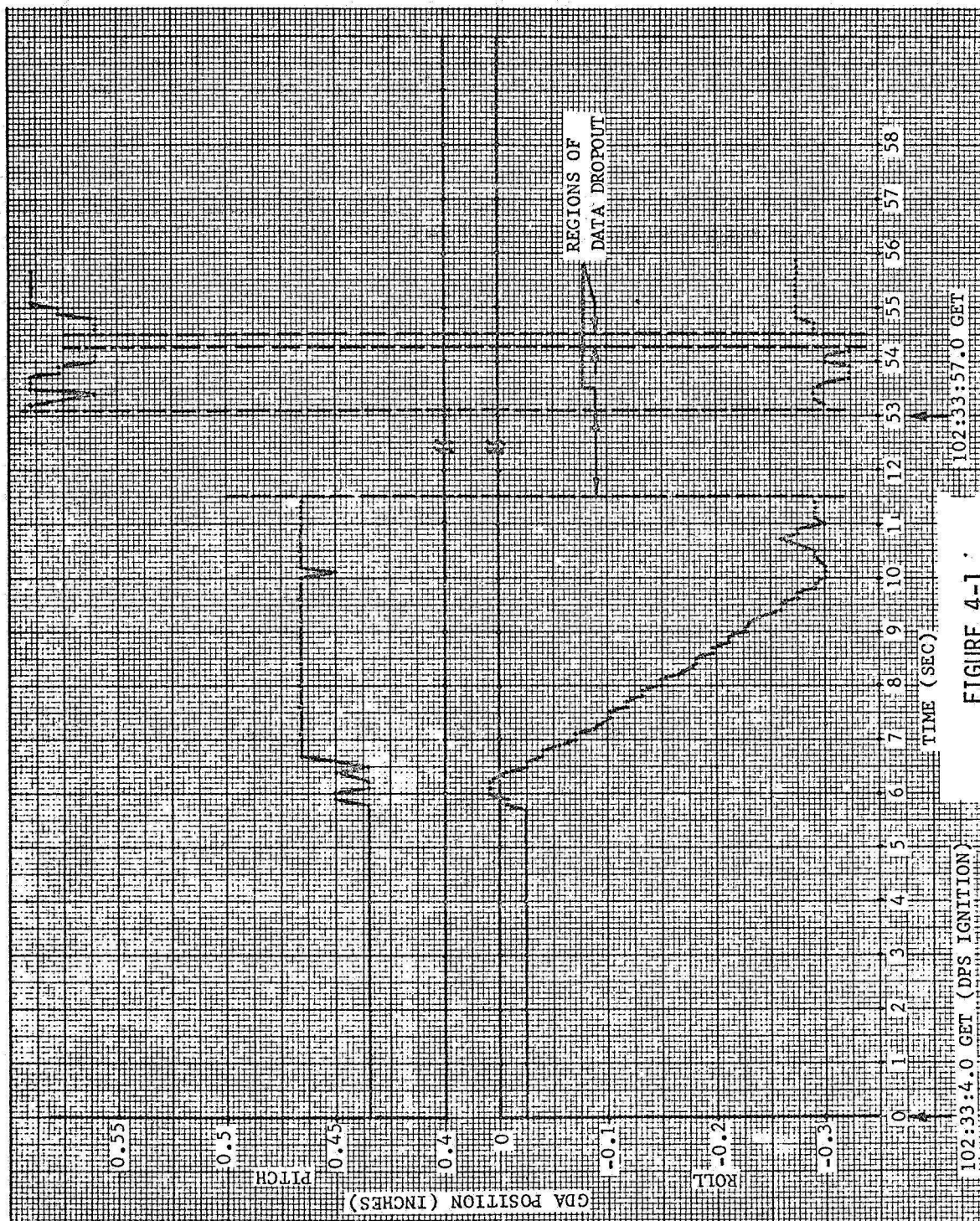
TABLE 4.6

RENDEZVOUS DATA

Event	Burn Time (sec)	$\Delta V(\text{fps})$	Residuals Before Nulling X Y Z	Residuals After Nulling X Y Z
*CSI	47.0	51.5	--- --- ---	-0.2 +0.7 -0.1
CDH	14.0	20.05	+2.1 +0.2 -0.5	+0.1 -0.1 0.0
TPI	22.7	25.02	-0.6 +0.6 +3.0	-0.2 0.0 -0.1
*TPF	28.4	31.4	--- --- ---	--- --- ---

* Downlink data not available. Data based on real time monitoring (Reference: 14)

--- No data available



102:33:4.0 GET (DPS IGNITION)

FIGURE 4-1

DPS IGNITION TRANSIENTS

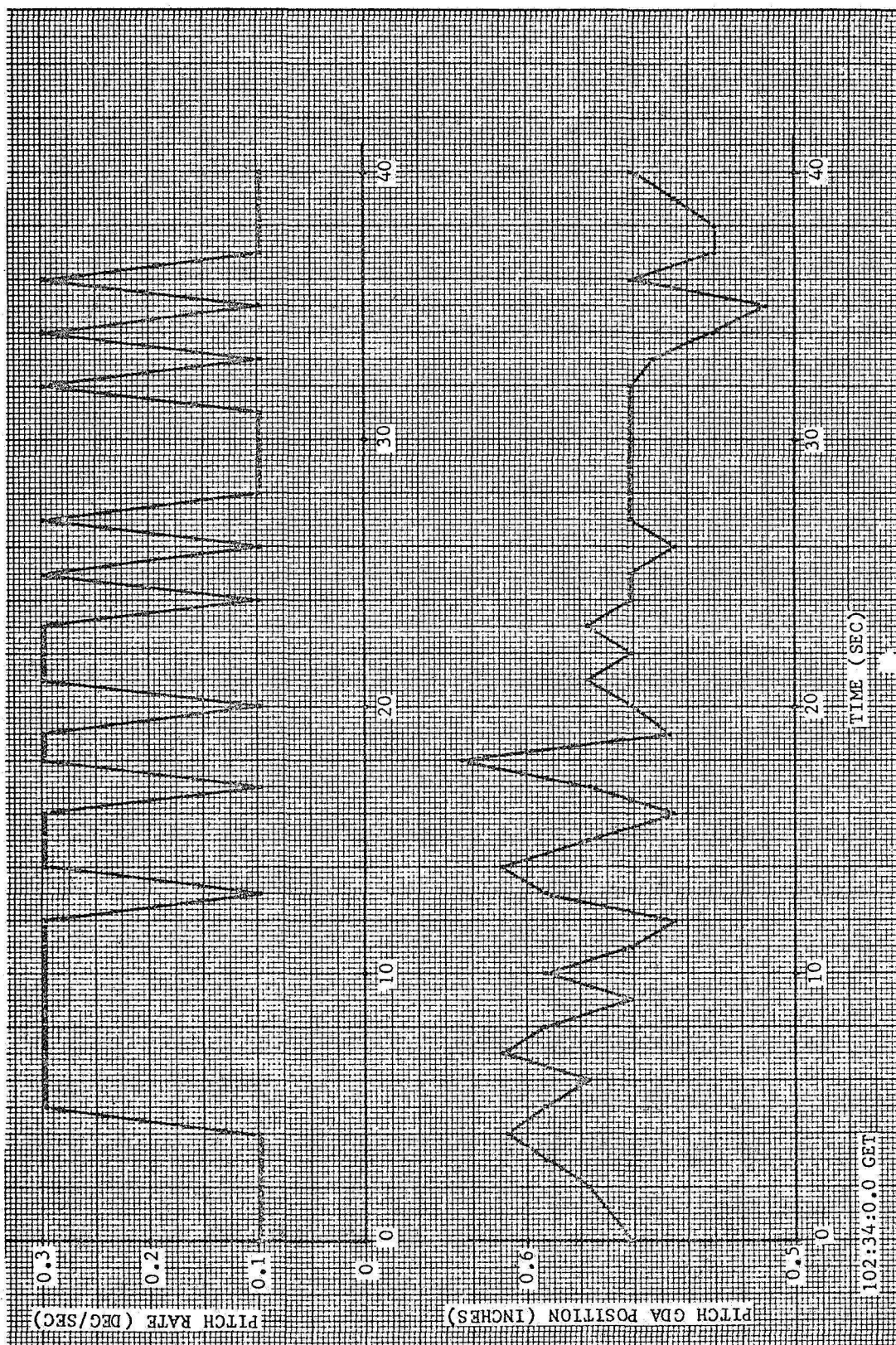


FIGURE 4-2
PITCH RATE AND GDA POSITION SHORTLY AFTER DPS IGNITION

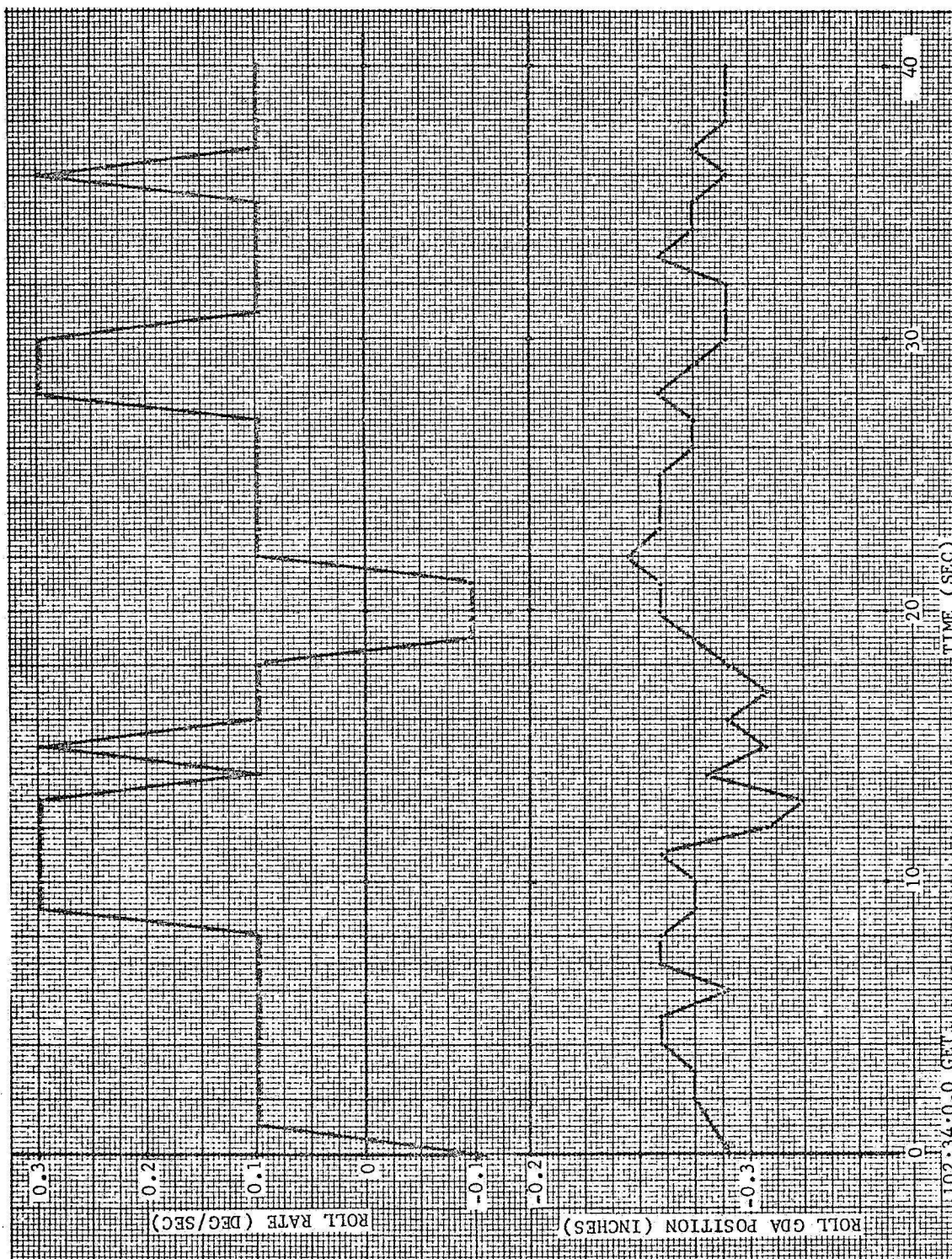


FIGURE 4-3
ROLL RATE AND GDA POSITION SHORTLY AFTER DPS IGNITION

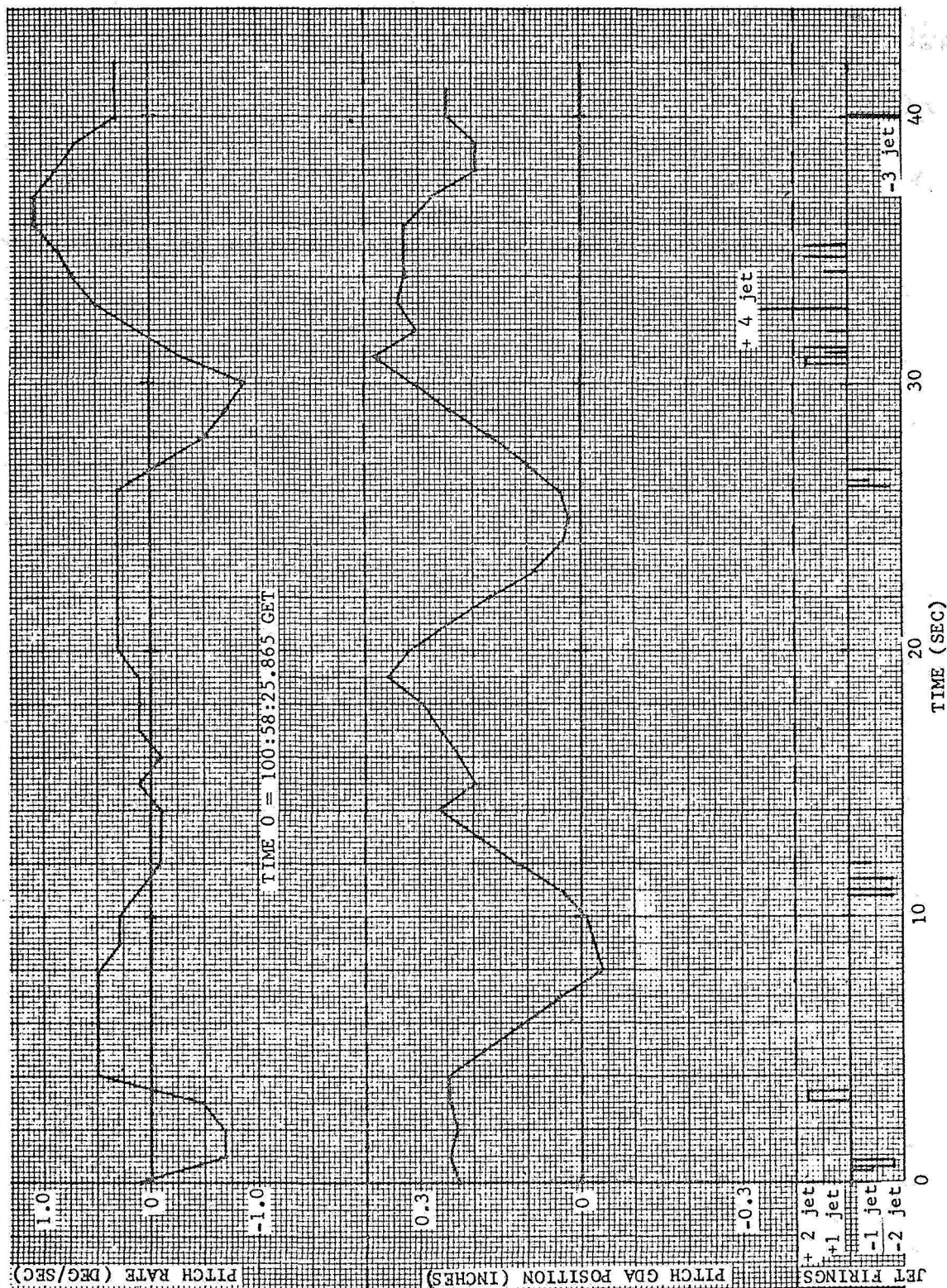


FIGURE 4-4
APOLLO 10 DPS PHASING BURN - PITCH RATE, PITCH GDA POSITION, AND PITCH JET FIRINGS

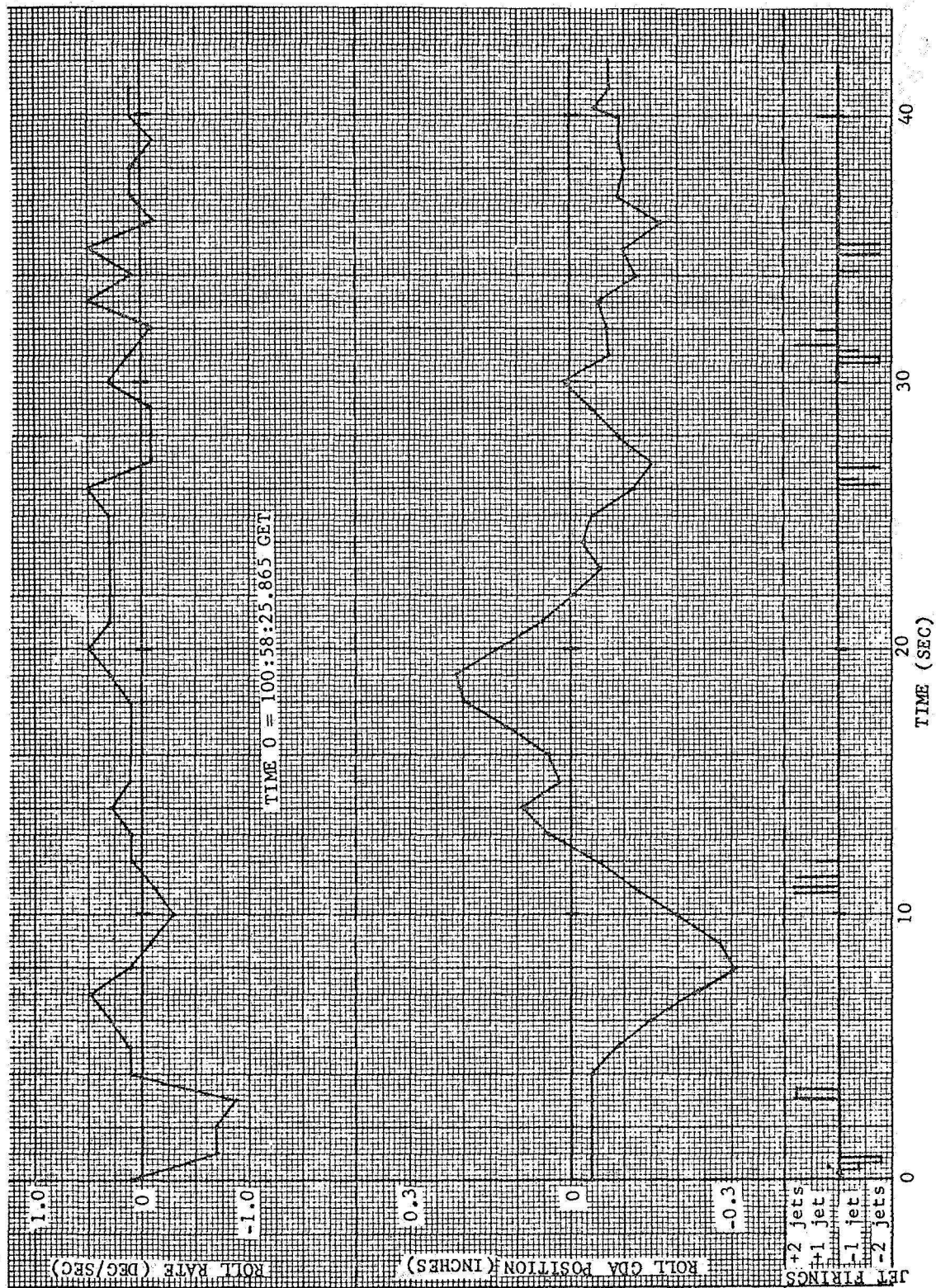


FIGURE 4-5
APOLLO 10 DPS PHASING BURN - ROLL RATE, ROLL GDA POSITION, AND ROLL JET FIRINGS

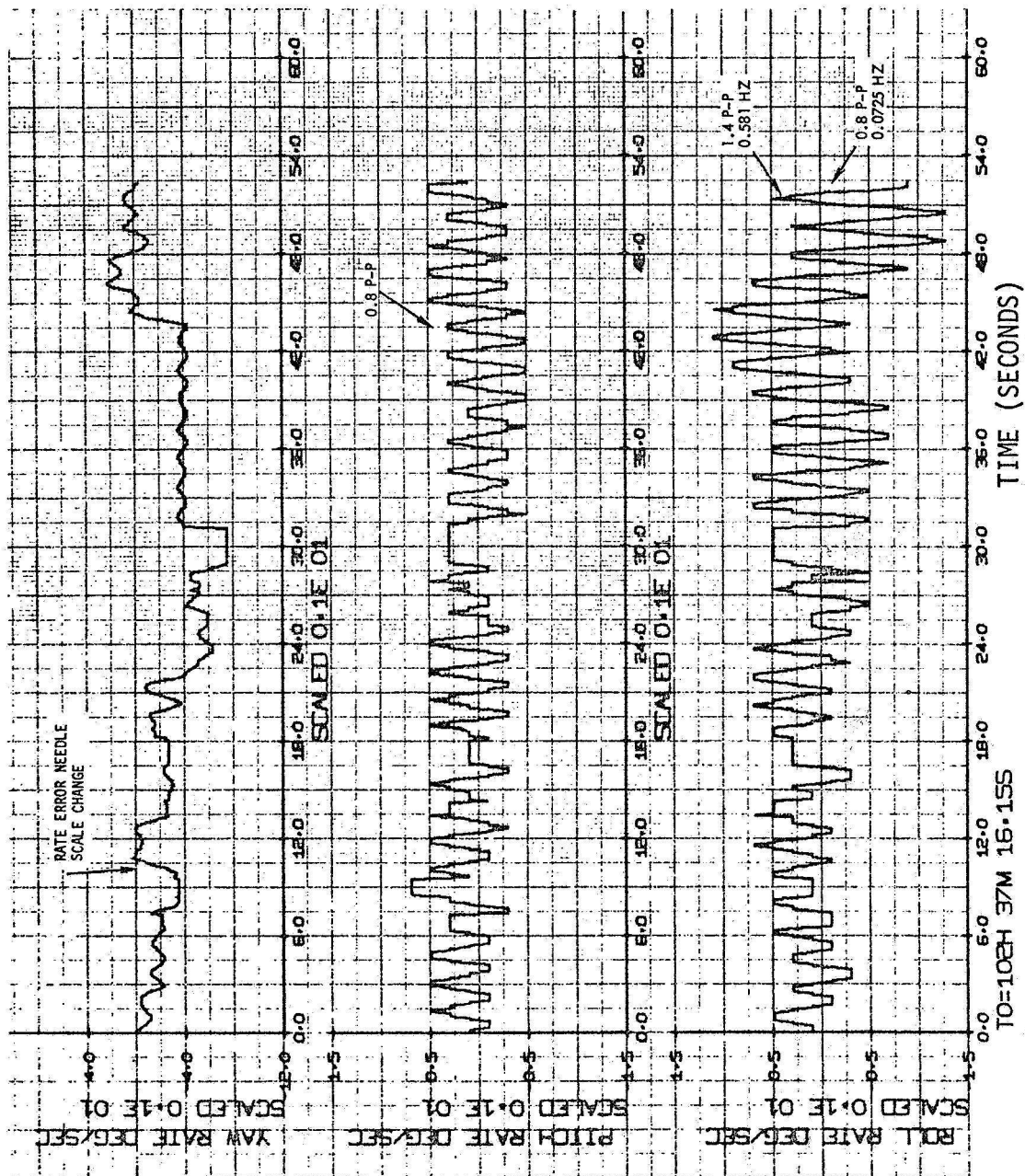


FIGURE 4-7
X-AXIS OVERRIDE IN P63

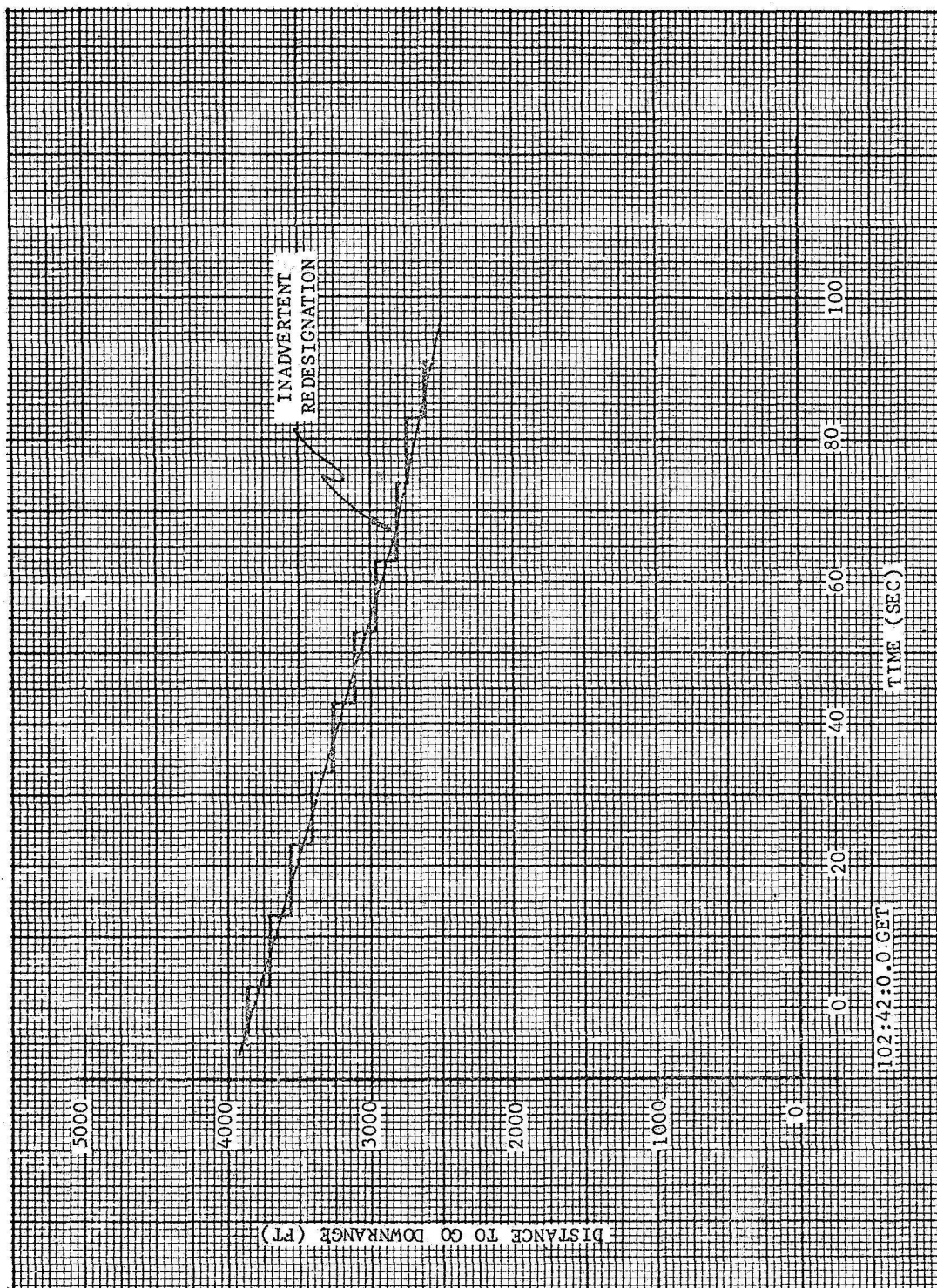


FIGURE 4-8
DISTANCE-TO-GO DOWNRANGE VS TIME

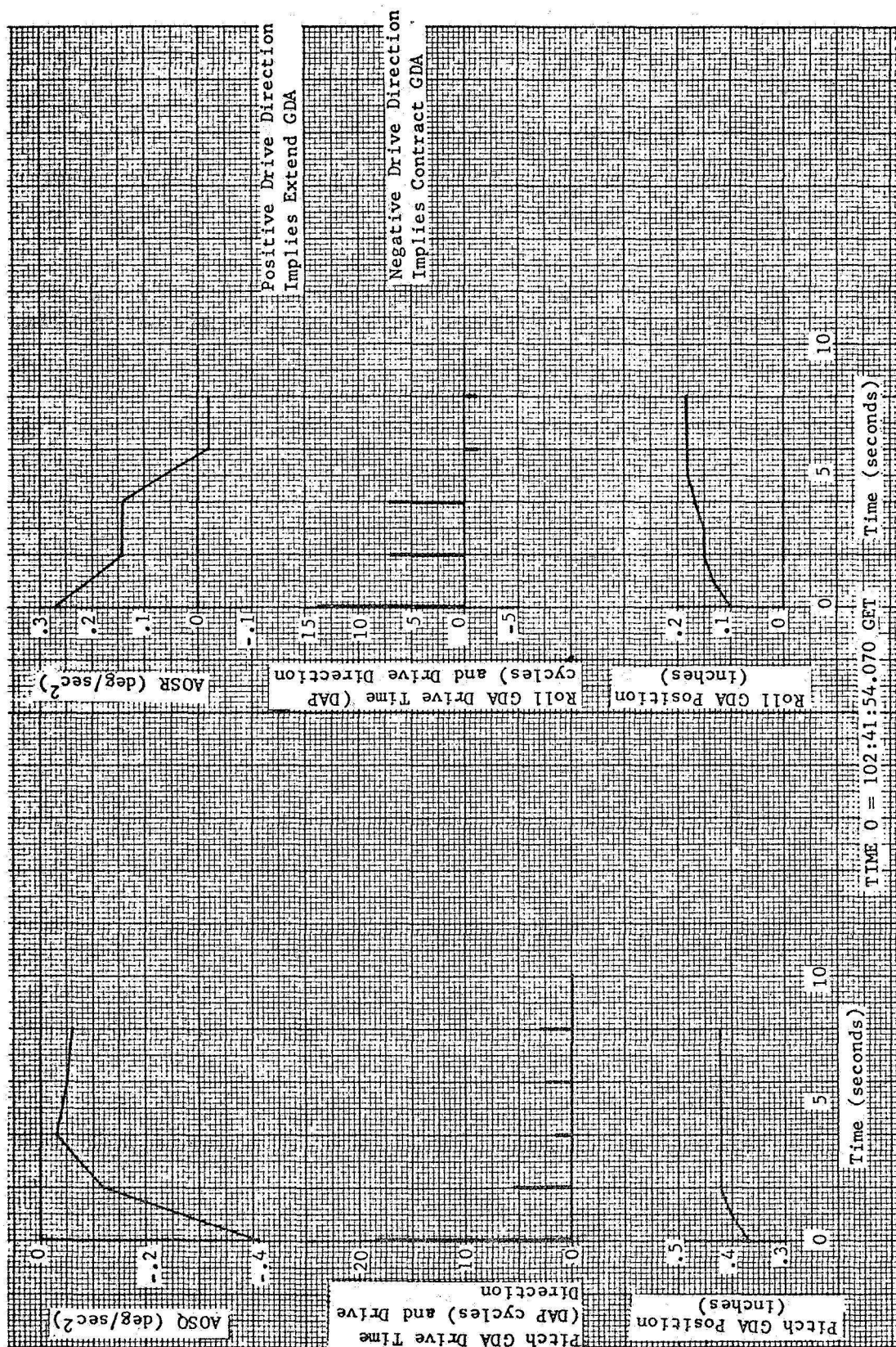


FIGURE 4-9A
AOSQ, PITCH GDA DRIVE TIME AND DRIVE
DIRECTION, PITCH GDA POSITION

FIGURE 4-9B
AOSR, ROLL GDA DRIVE TIME AND DRIVE
DIRECTION, ROLL GDA POSITION

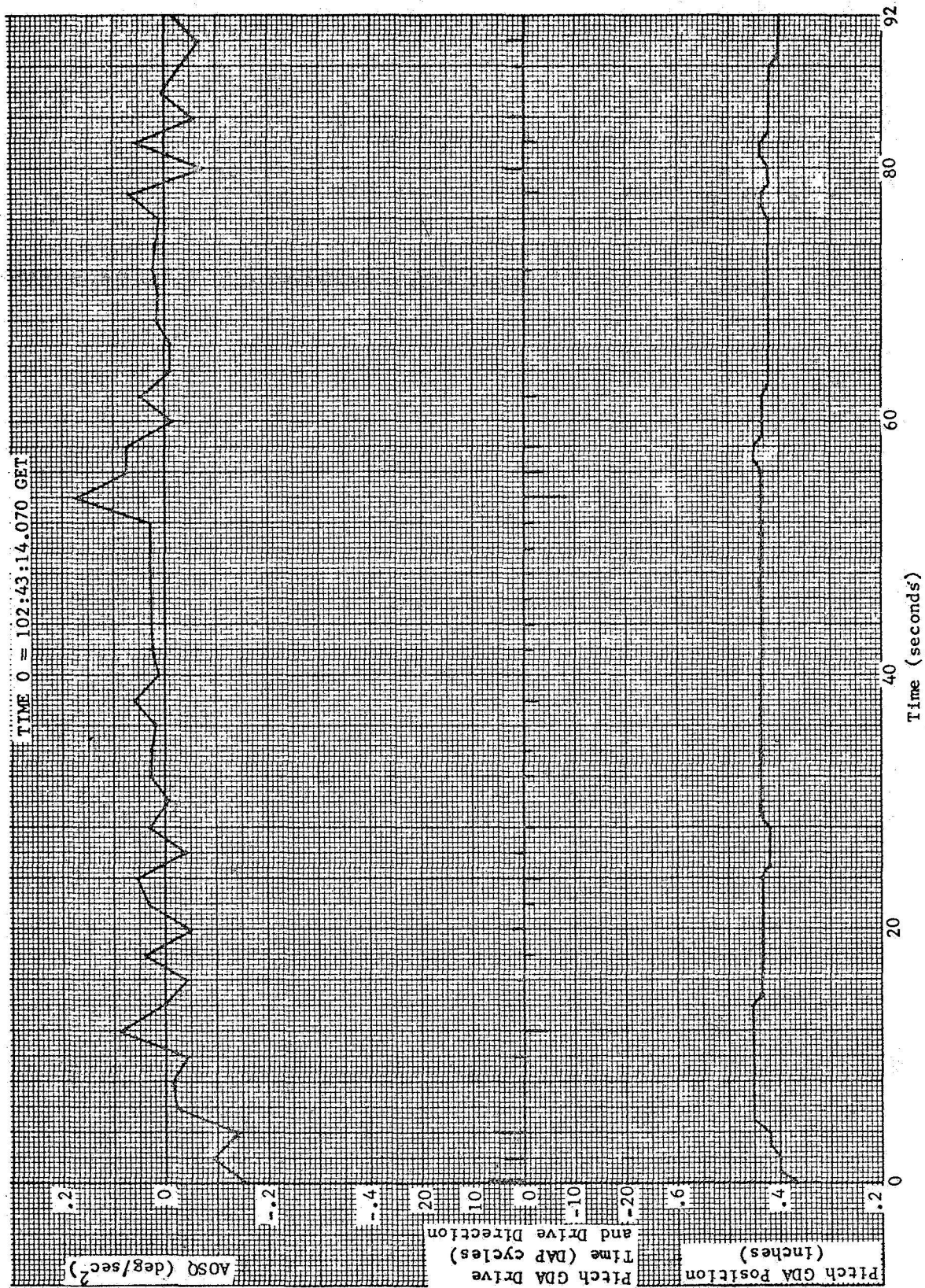


FIGURE 4-10
OFFSET ACCELERATION, PITCH GDA DRIVE TIME AND DRIVE DIRECTION, PITCH GDA POSITION

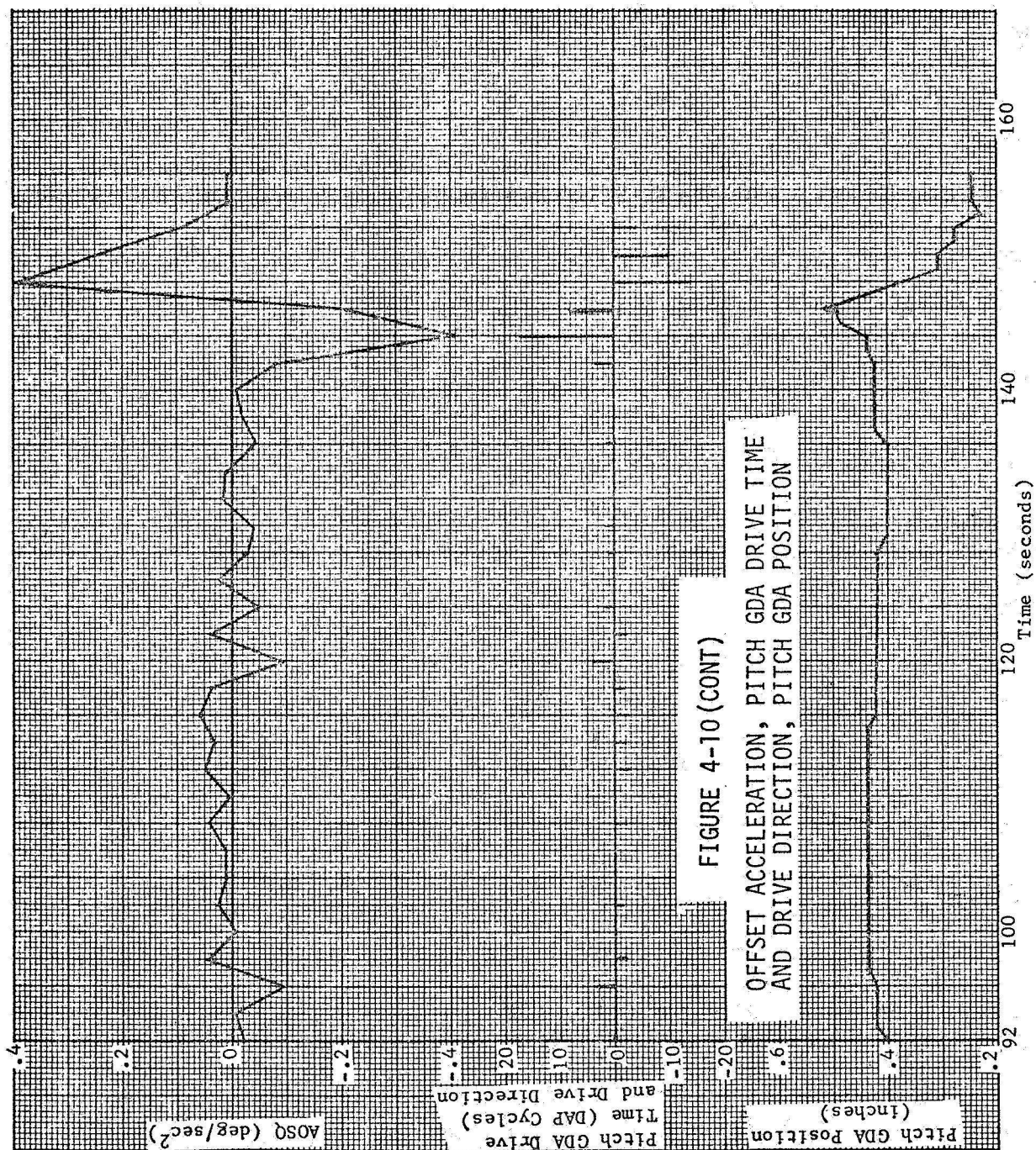


FIGURE 4-10 (CONT)

OFFSET ACCELERATION, PITCH GDA DRIVE TIME
AND DRIVE DIRECTION, PITCH GDA POSITION

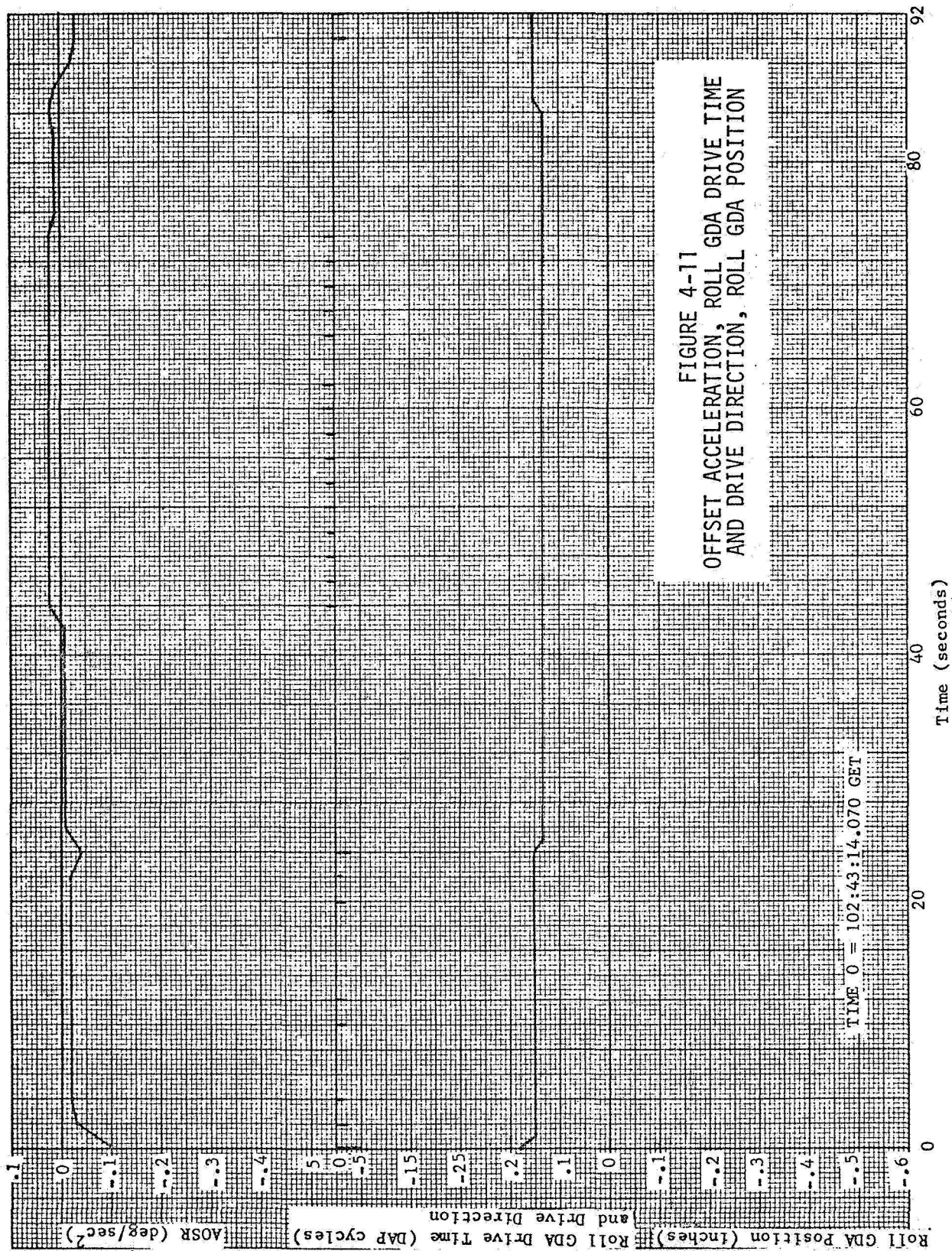


FIGURE 4-11
 OFFSET ACCELERATION, ROLL GDA DRIVE TIME
 AND DRIVE DIRECTION, ROLL GDA POSITION

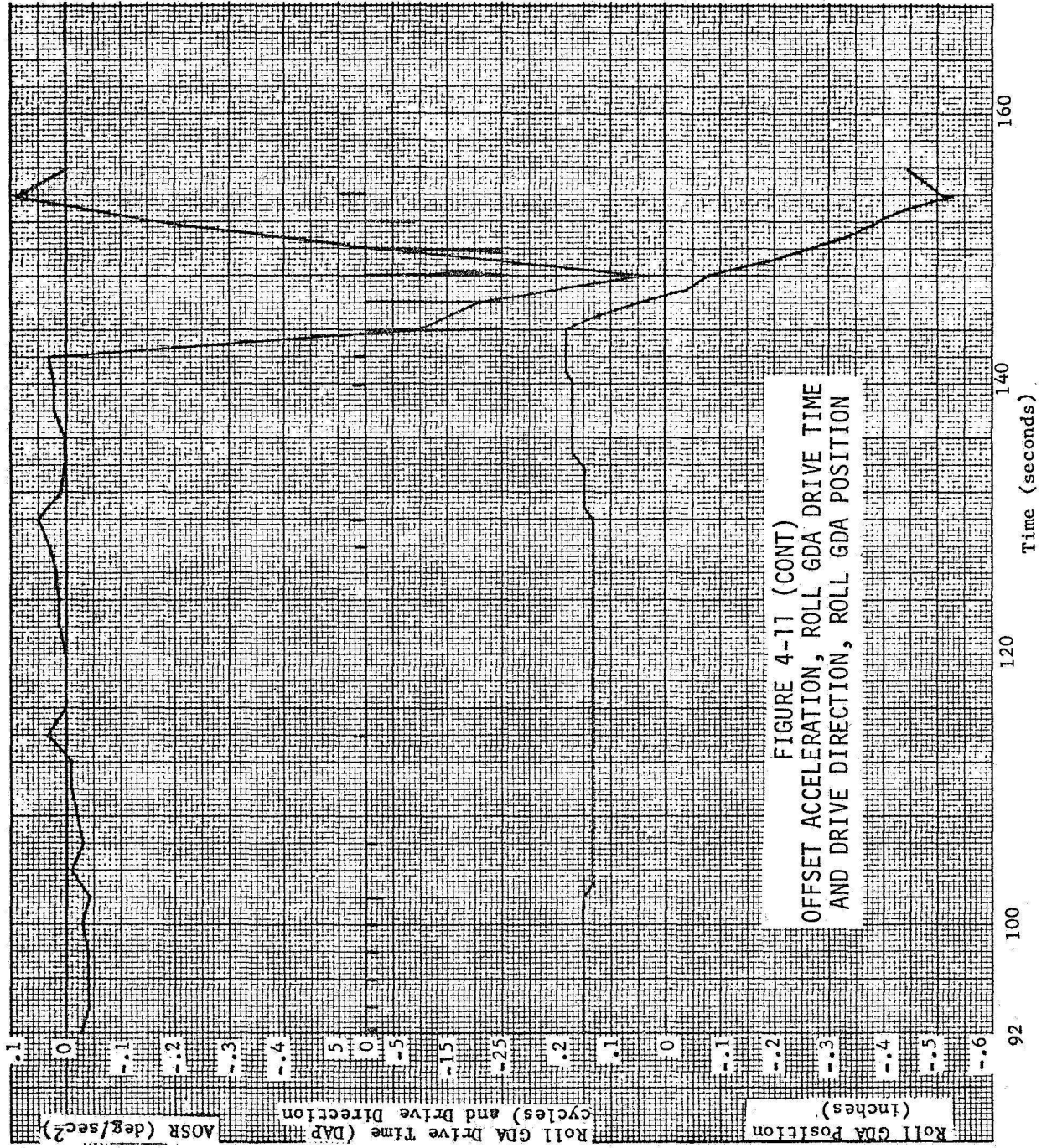


FIGURE 4-11 (CONT)
 OFFSET ACCELERATION, ROLL GDA DRIVE TIME
 AND DRIVE DIRECTION, ROLL GDA POSITION

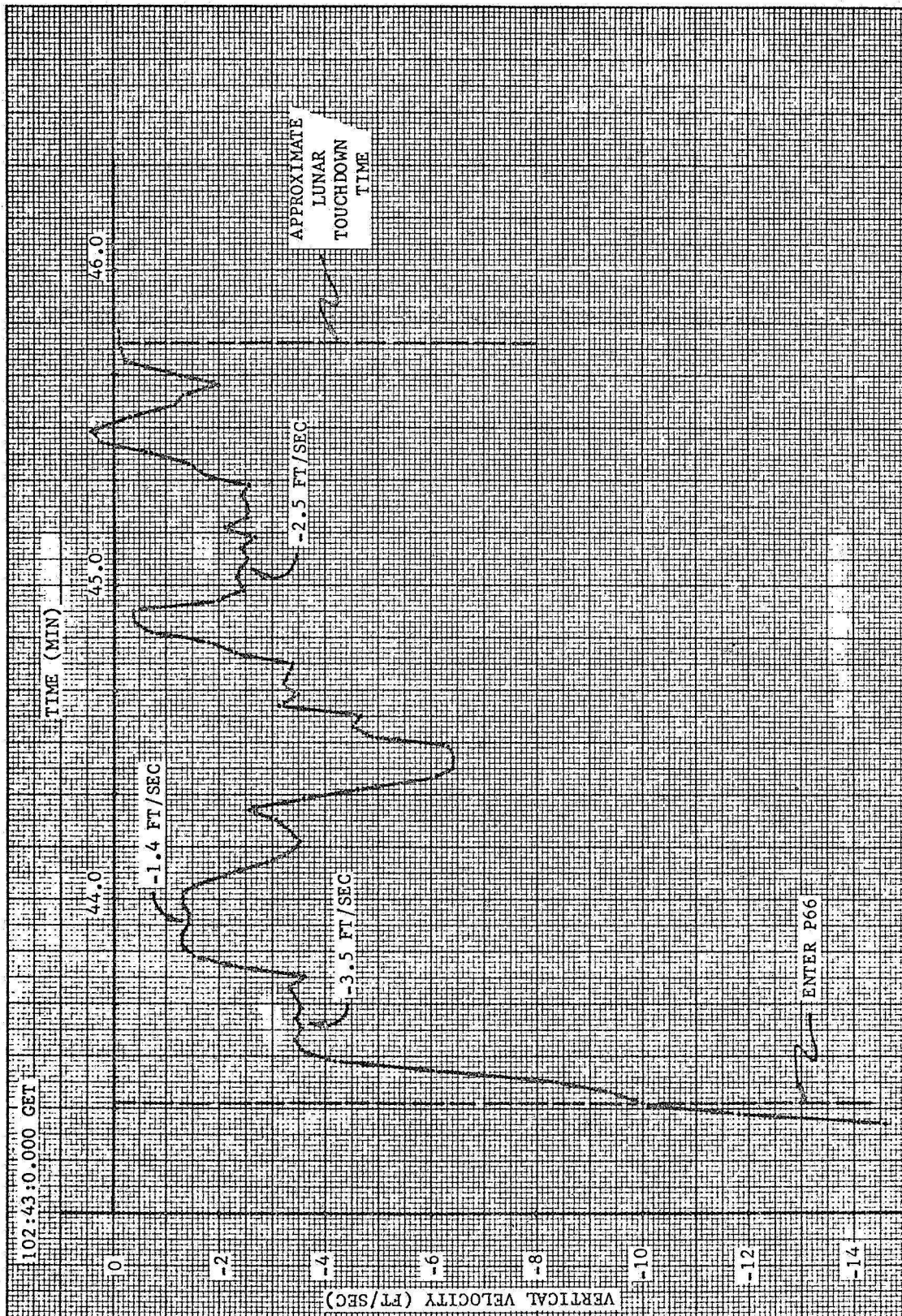


FIGURE 4-12
VERTICAL VELOCITY (HDOT) VS TIME

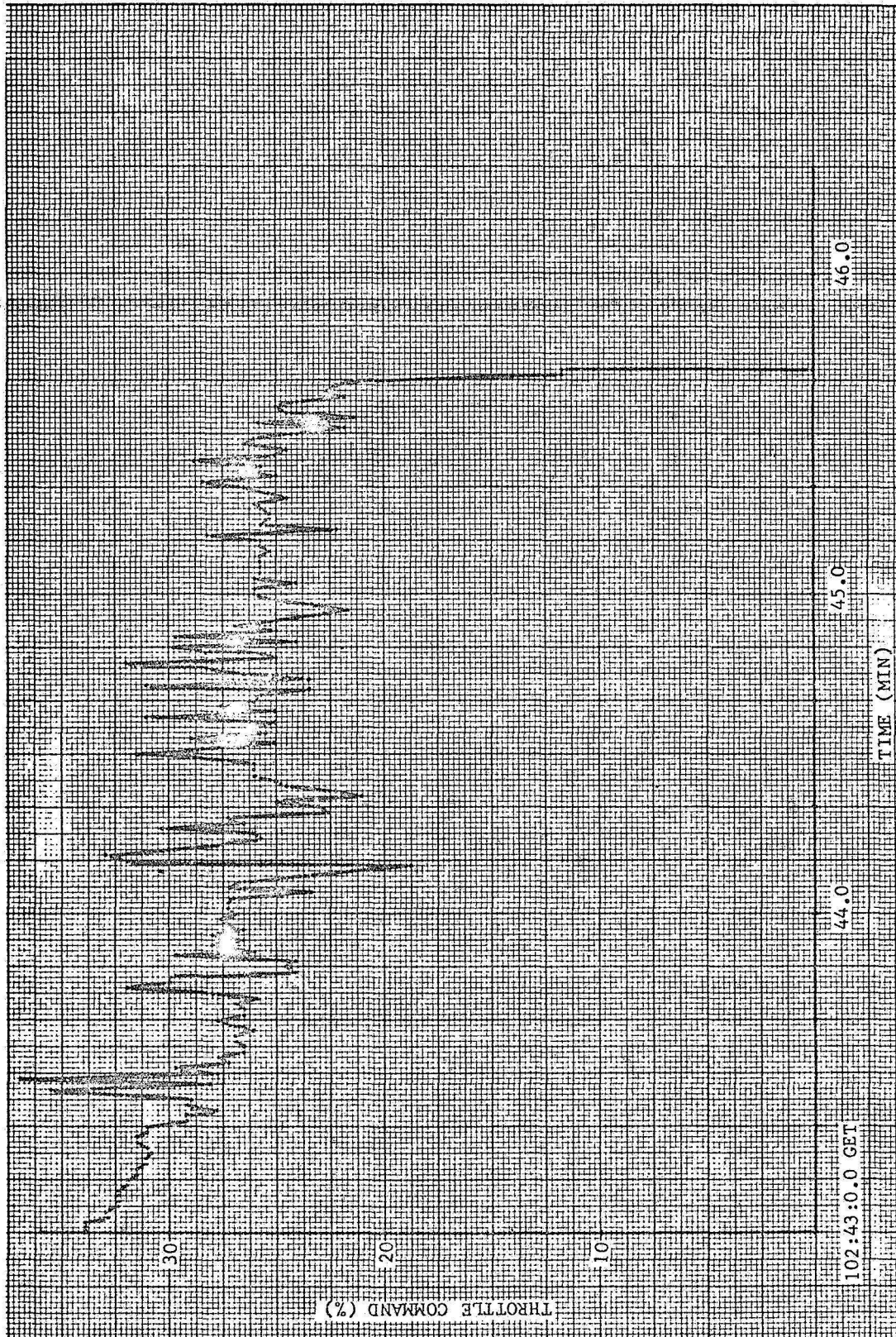


FIGURE 4-13
DPS THROTTLE COMMAND VS TIME

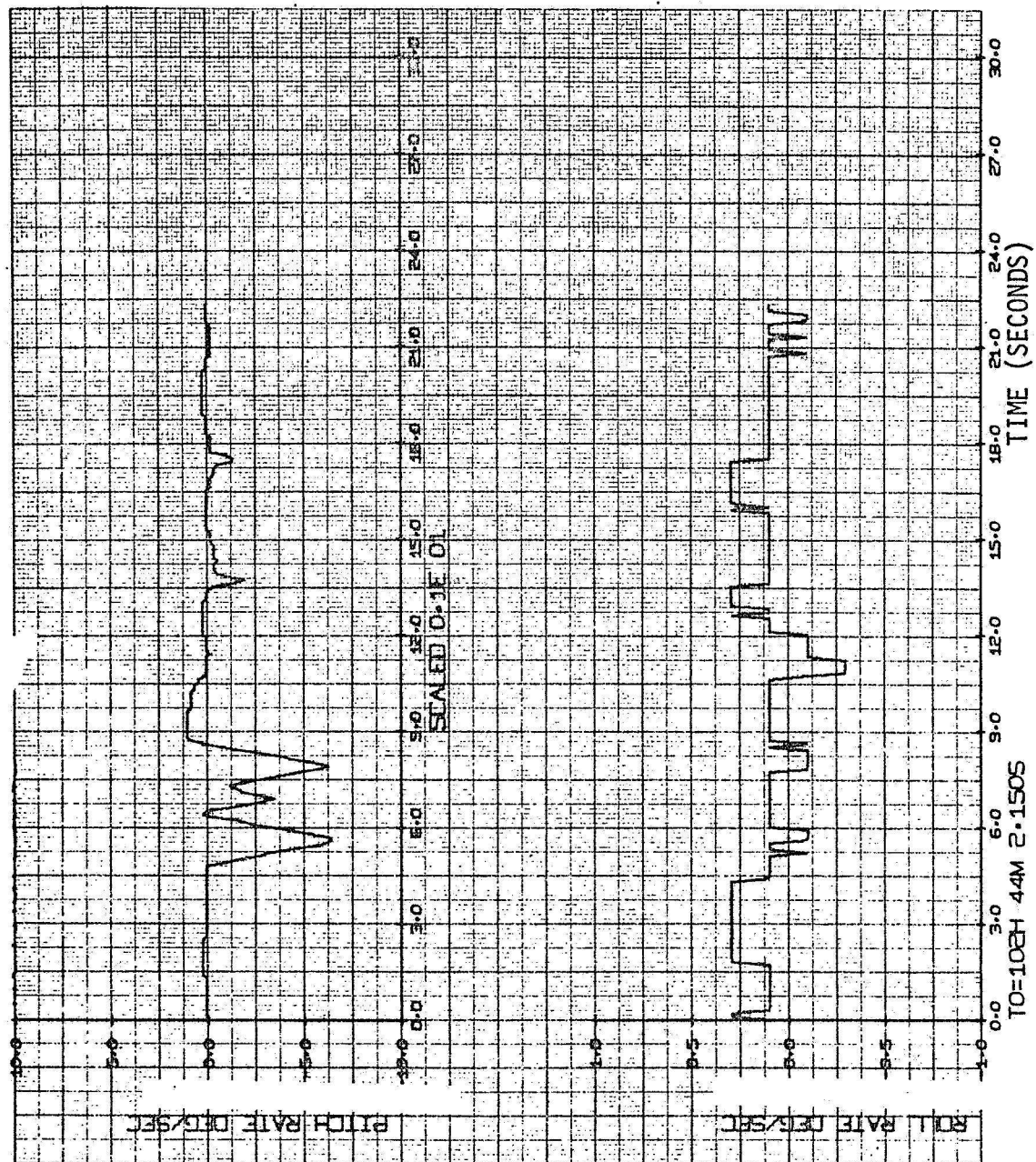


FIGURE 4-14
RHC PITCH COMMAND

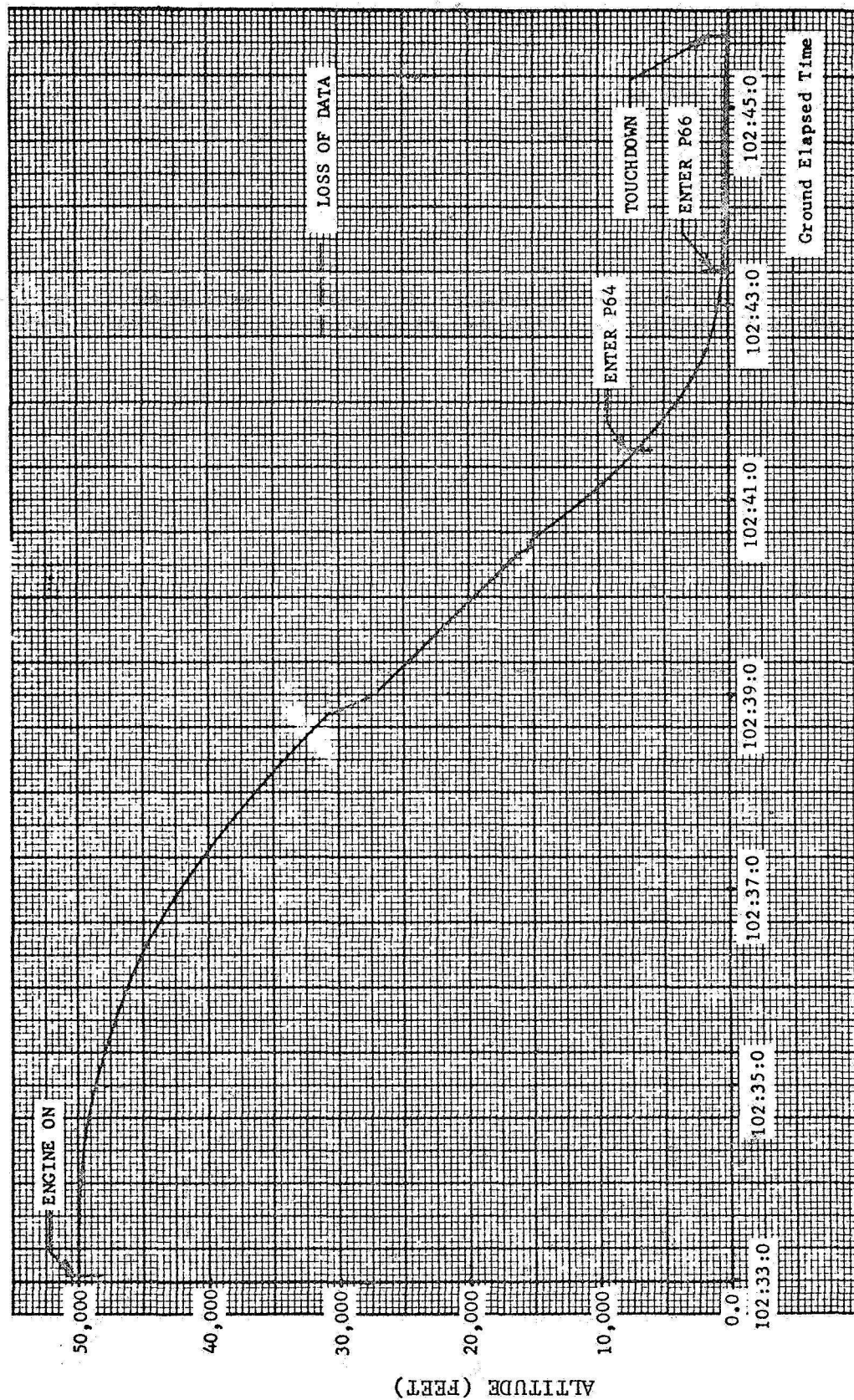


Figure 4-15
ALTITUDE VS TIME

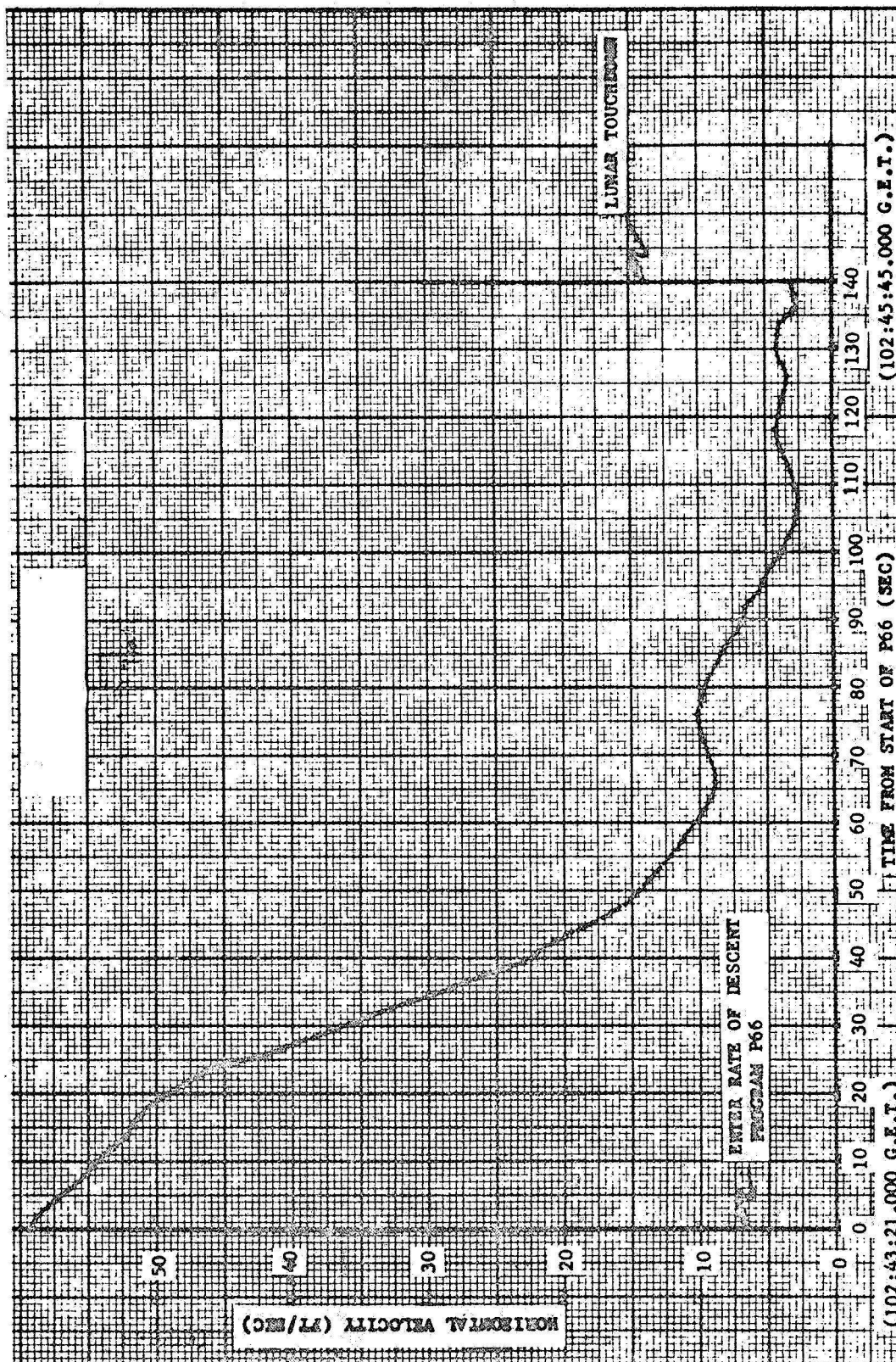


Figure 4-16
HORIZONTAL VELOCITY VS TIME

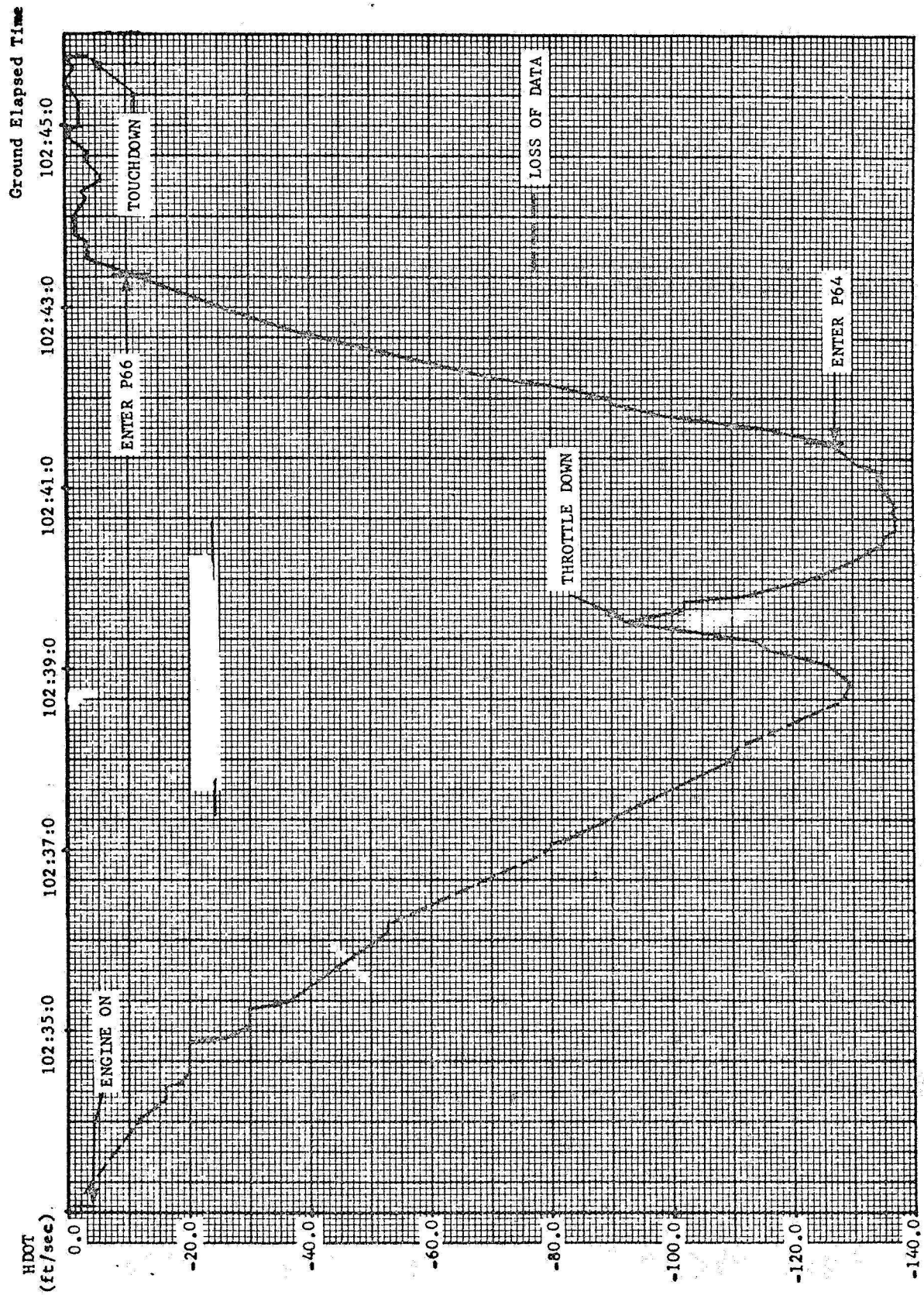


Figure 4-17
ALTITUDE RATE VS TIME

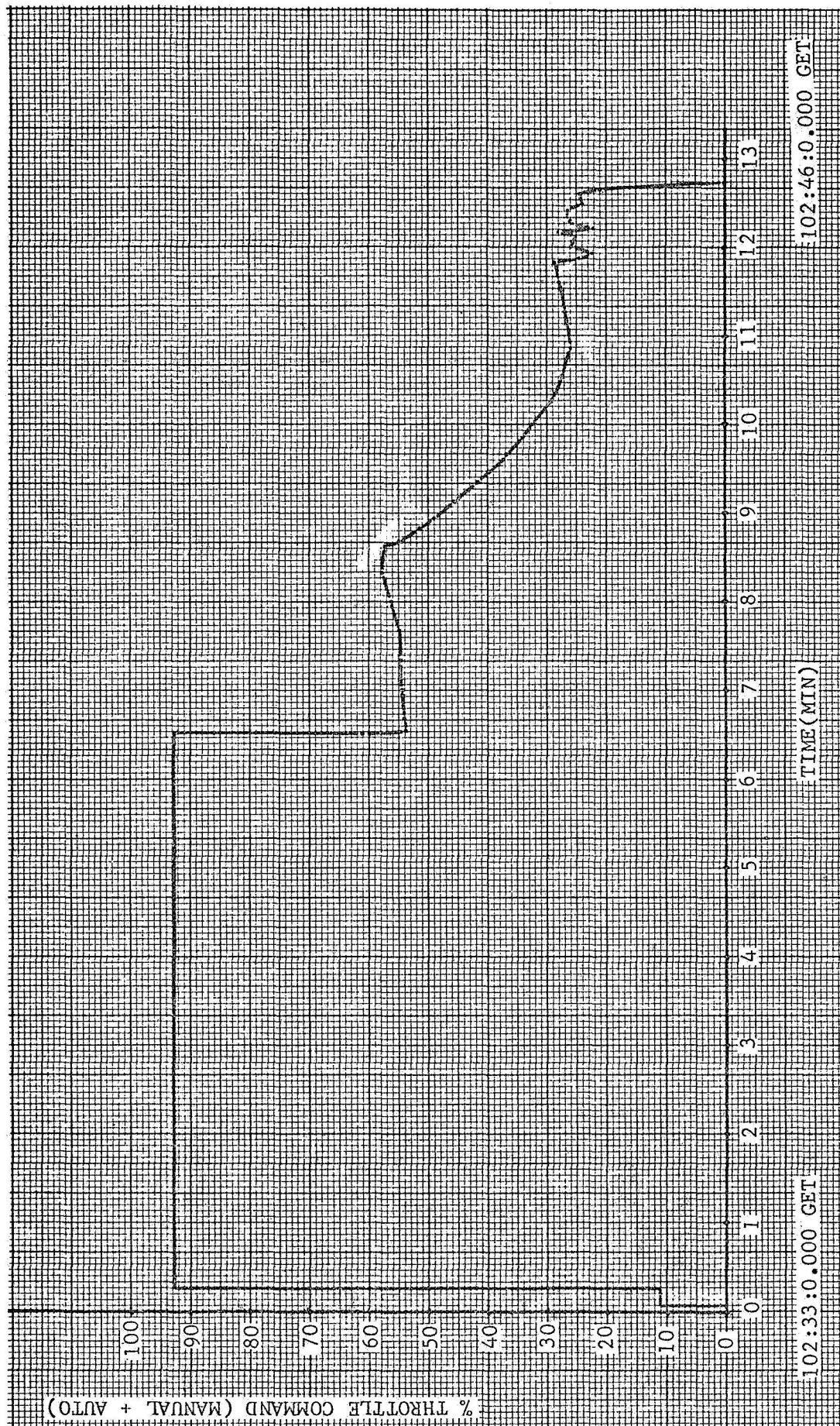


Figure 4-18
DPS THROTTLE COMMAND VS TIME

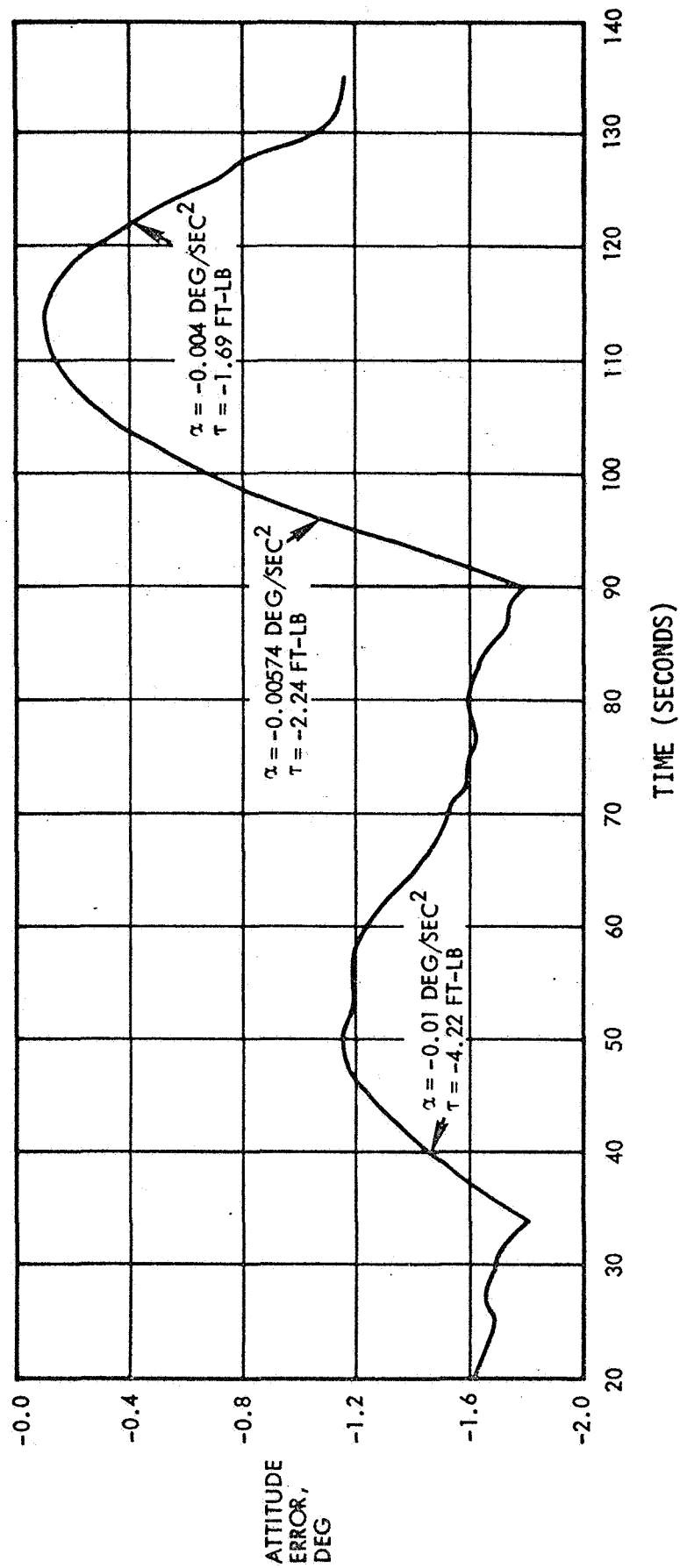


Figure 4-19
P-AXIS ATTITUDE ERROR - P63

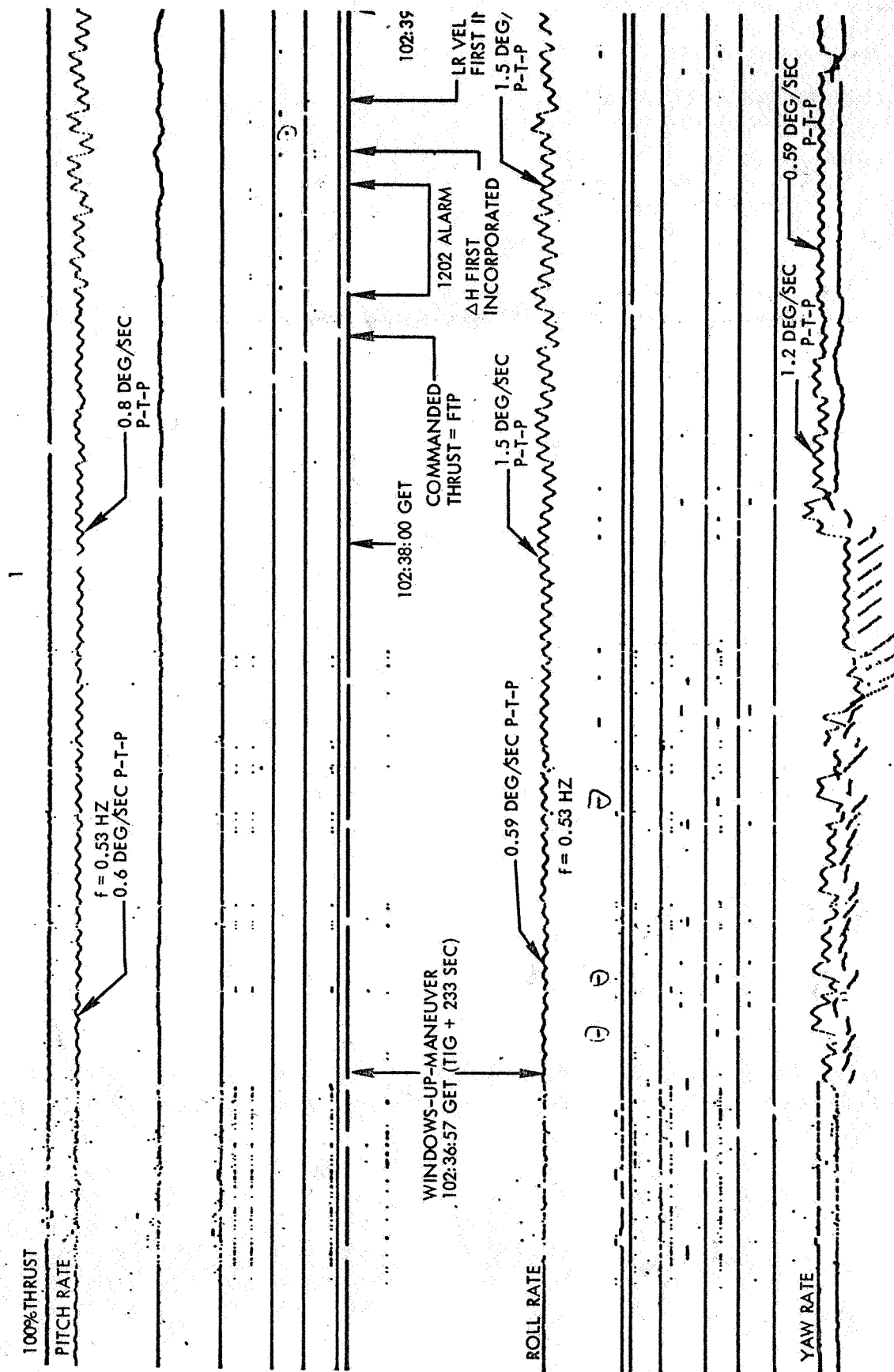


FIGURE 4-20
SPACECRAFT ANGULAR RESPONSE - P63/P64

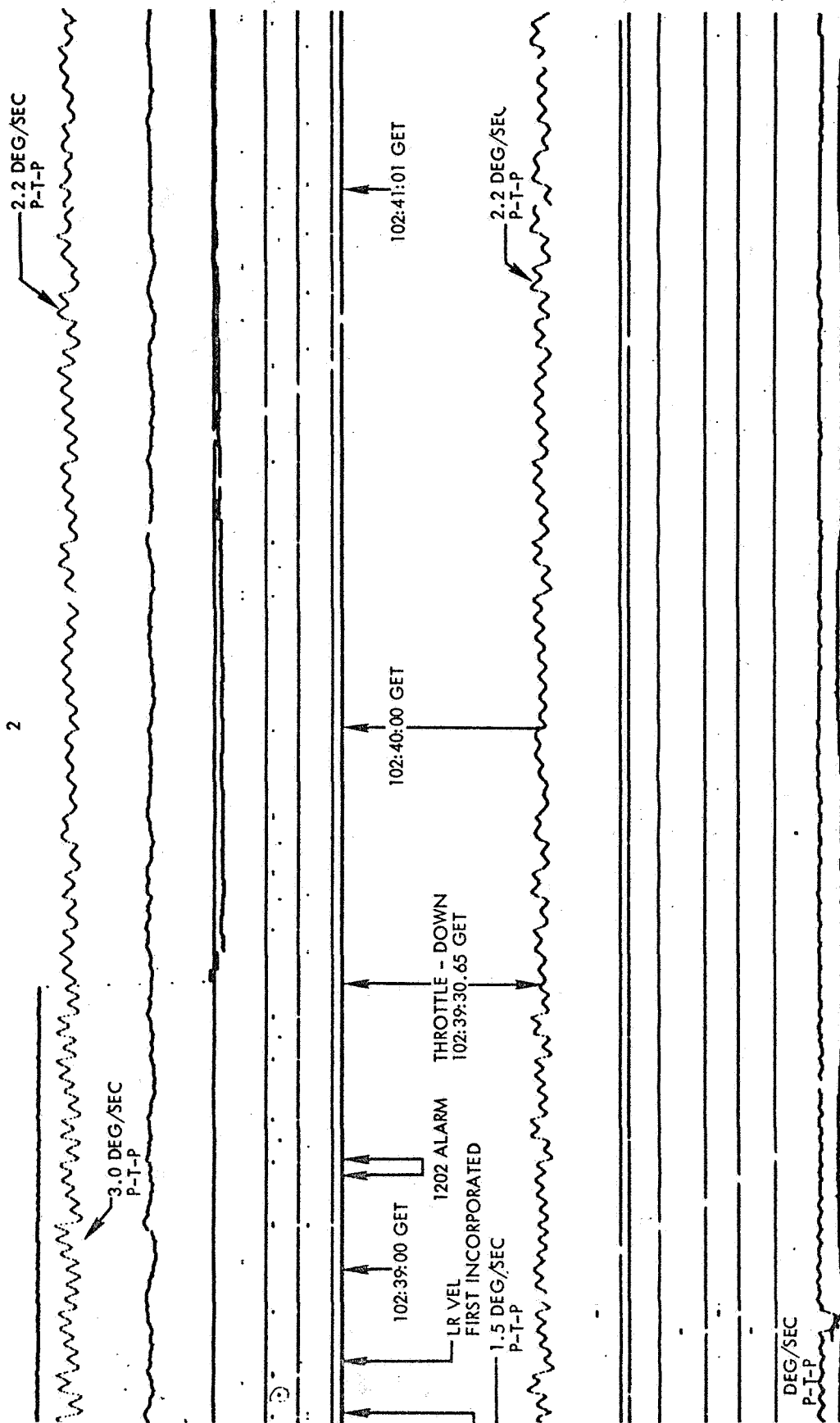
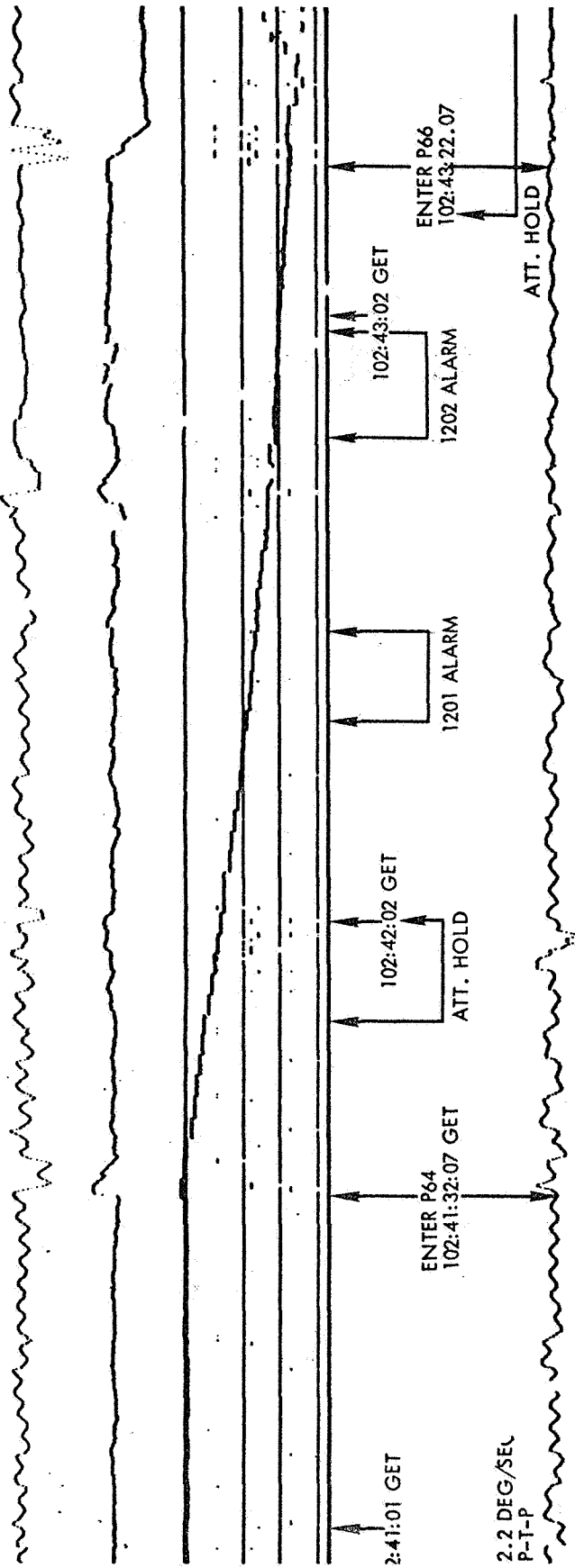


FIGURE 4-20 (CONT)
SPACECRAFT ANGULAR RESPONSE - P63/P64

-2.2 DEG/SEC
P-T-P

3



2.2 DEG/SEC
P-T-P

FIGURE 4-20 (CONT)
SPACECRAFT ANGULAR RESPONSE - P63/P64

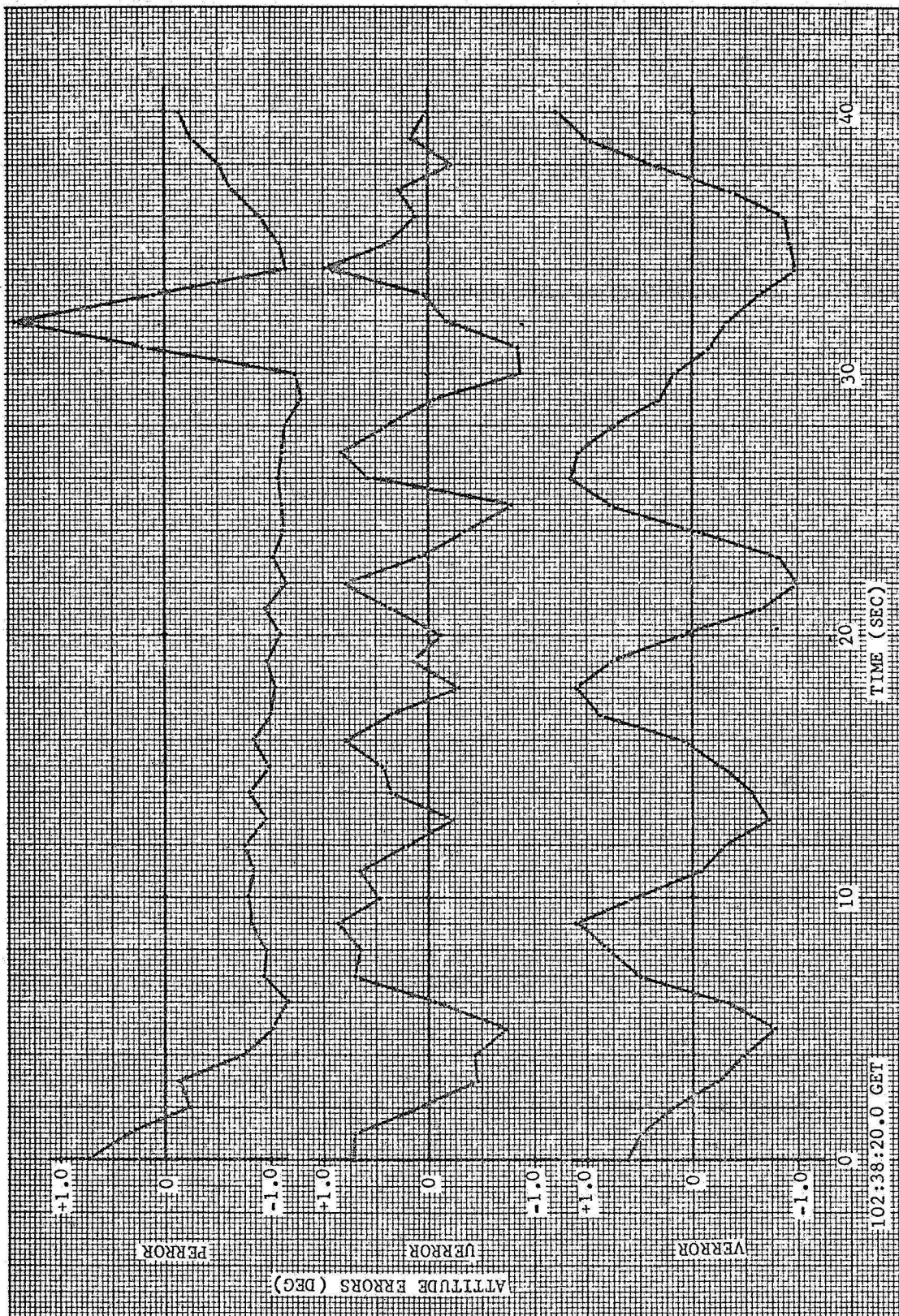


FIGURE 4-21
ATTITUDE ERRORS VS TIME

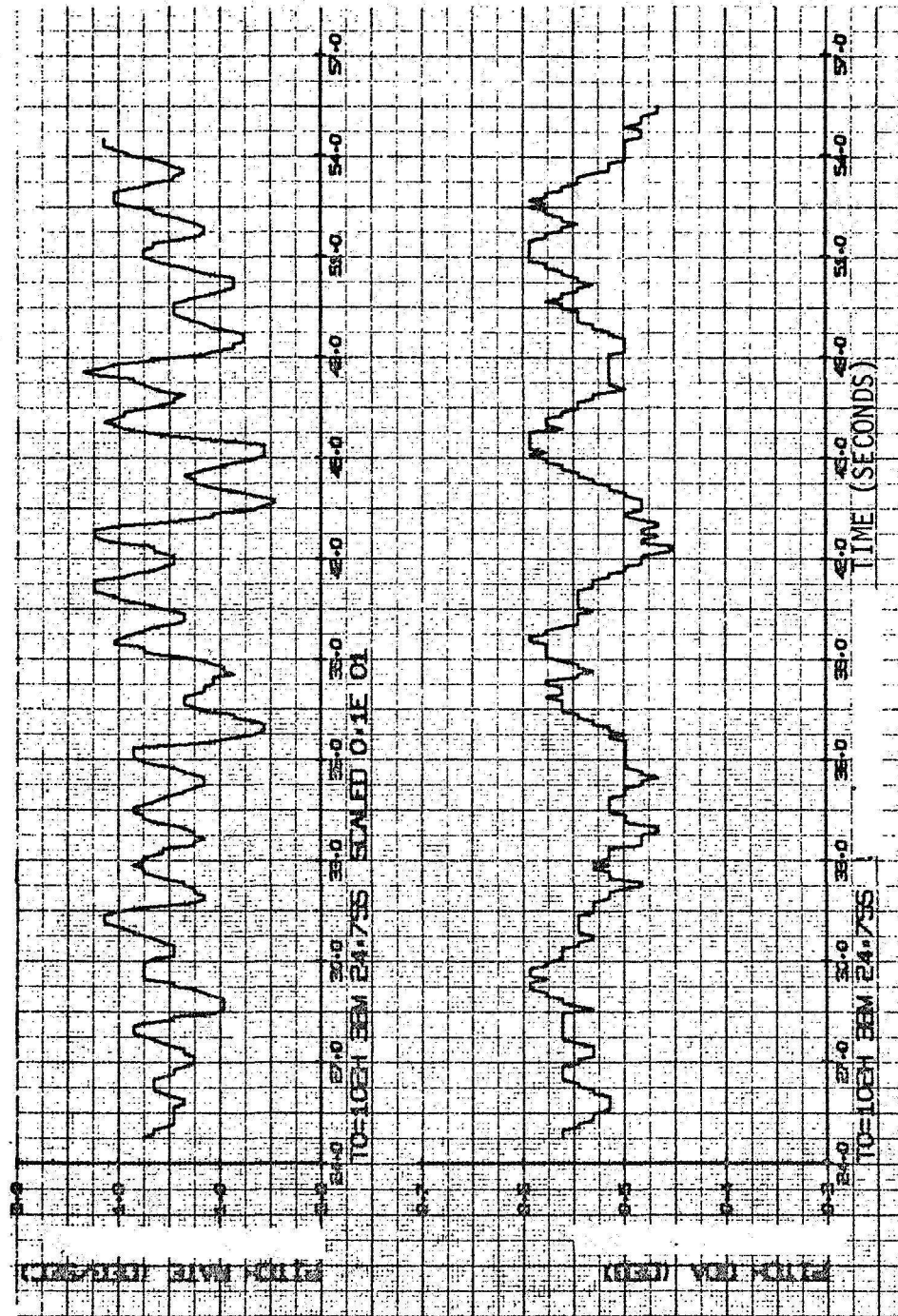


FIGURE 4-22
PITCH AXIS VARIABLES

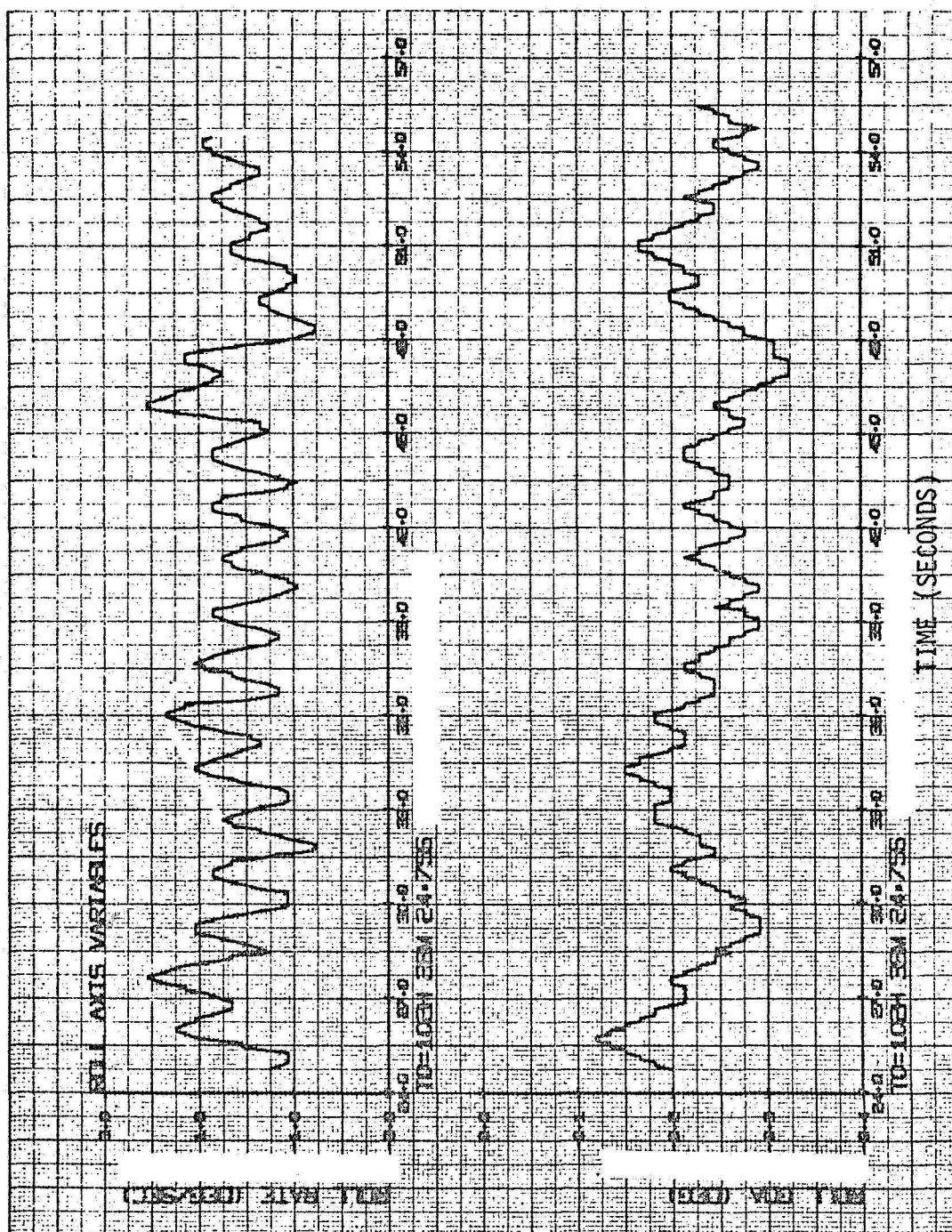


FIGURE 4-23
ROLL AXIS VARIABLES

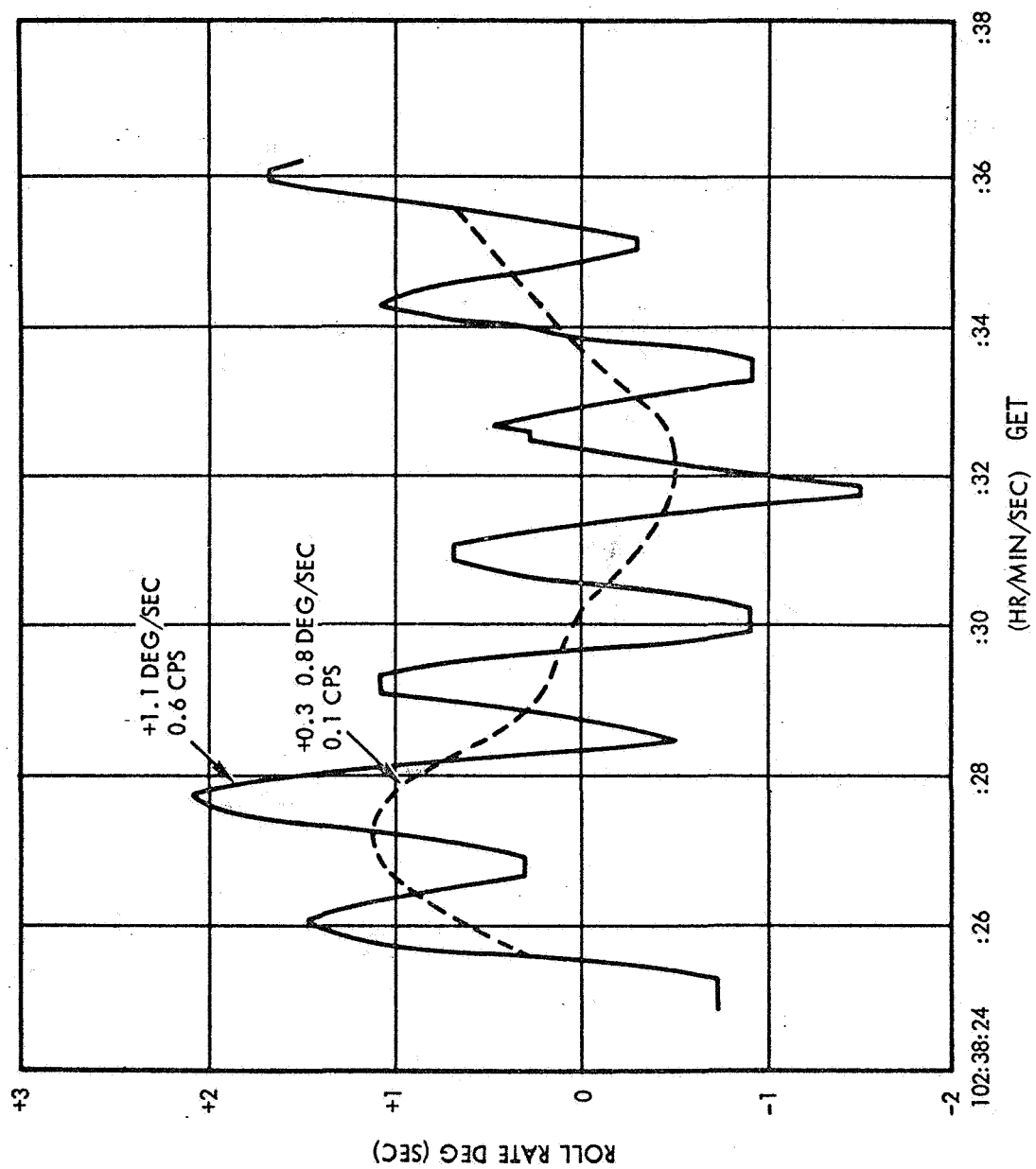


FIGURE 4-24
ROLL RATE VS TIME

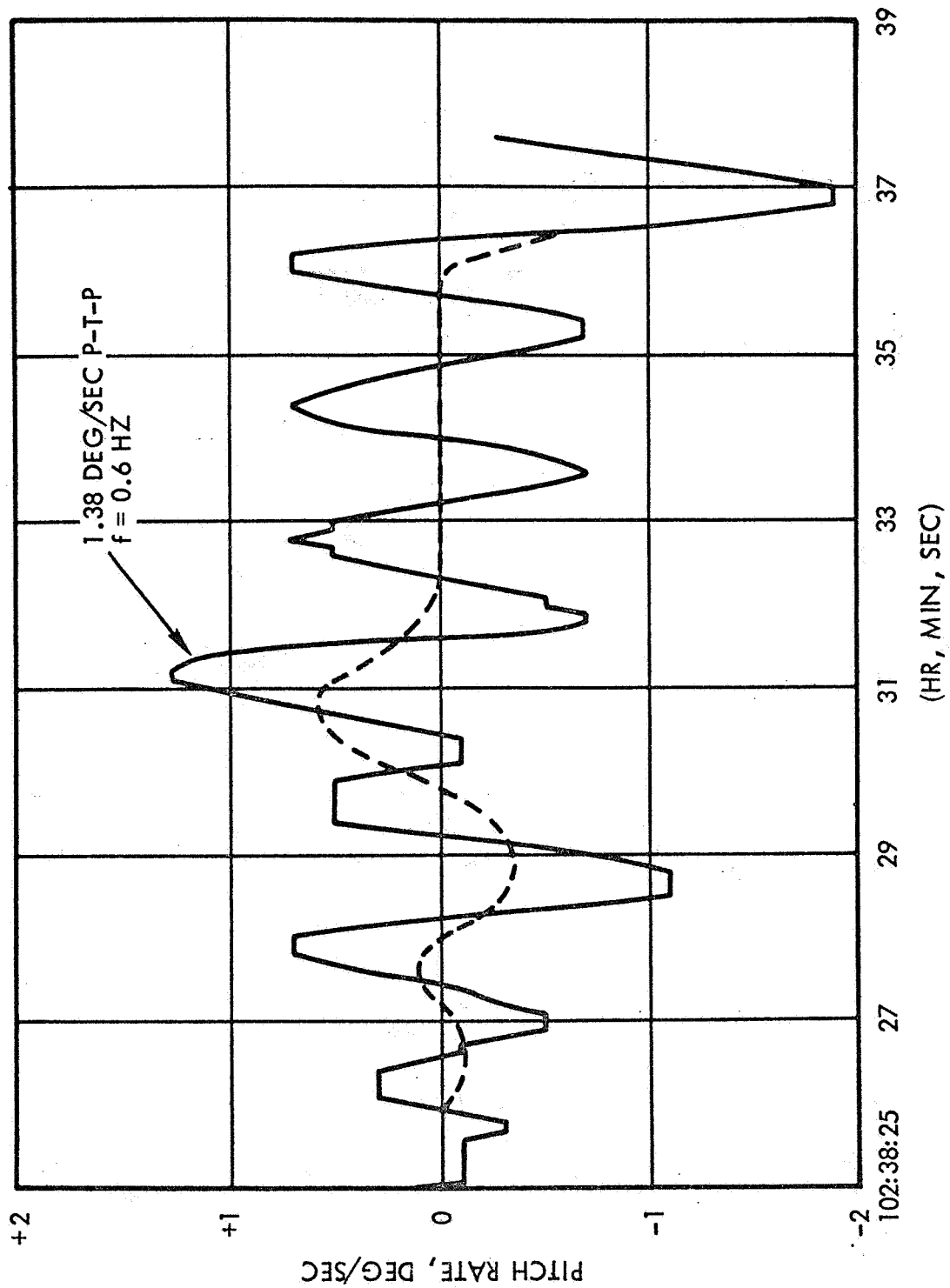


FIGURE 4-25
PITCH RATE VS TIME

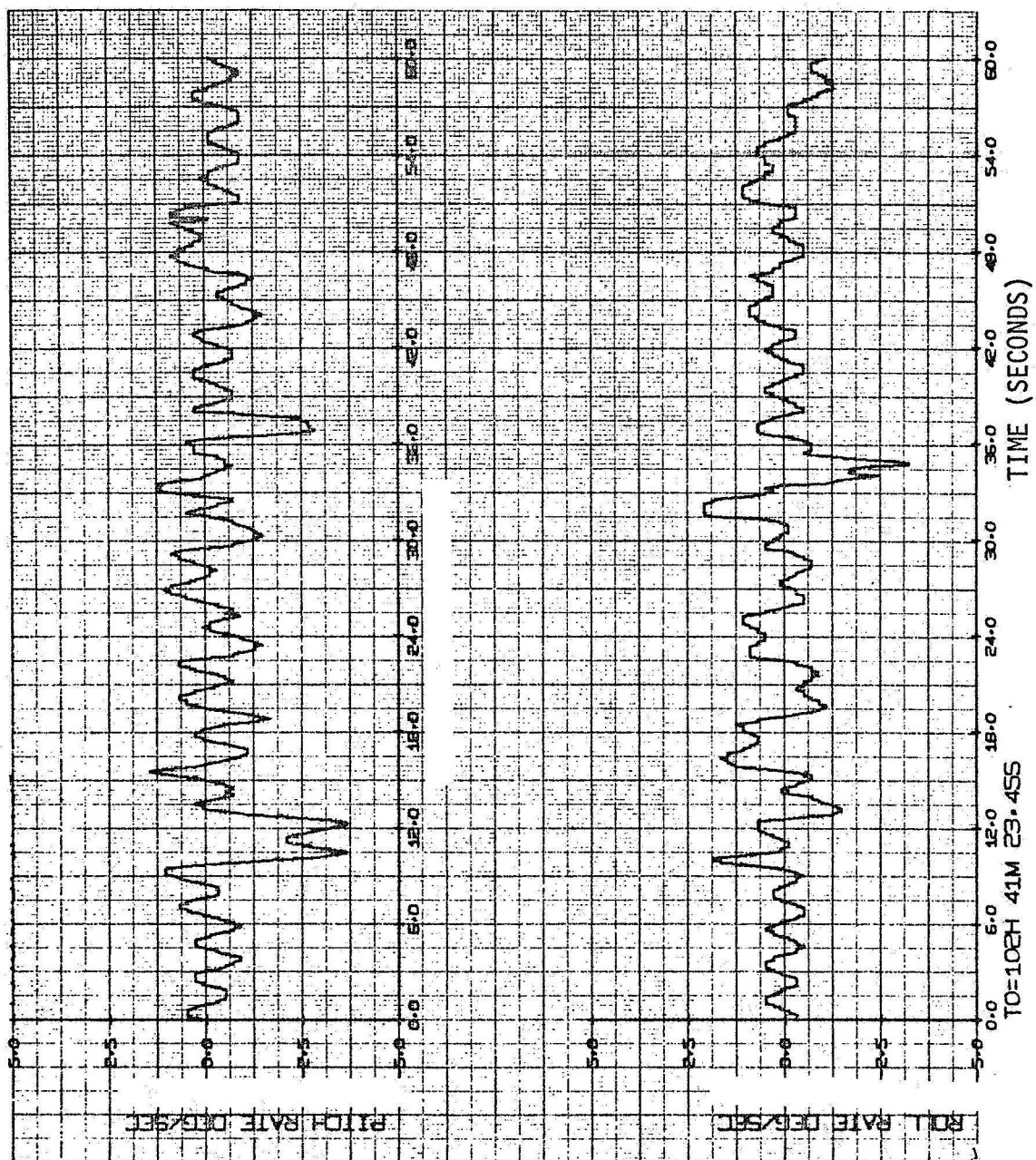


FIGURE 4-26
PITCHOVER IN P64

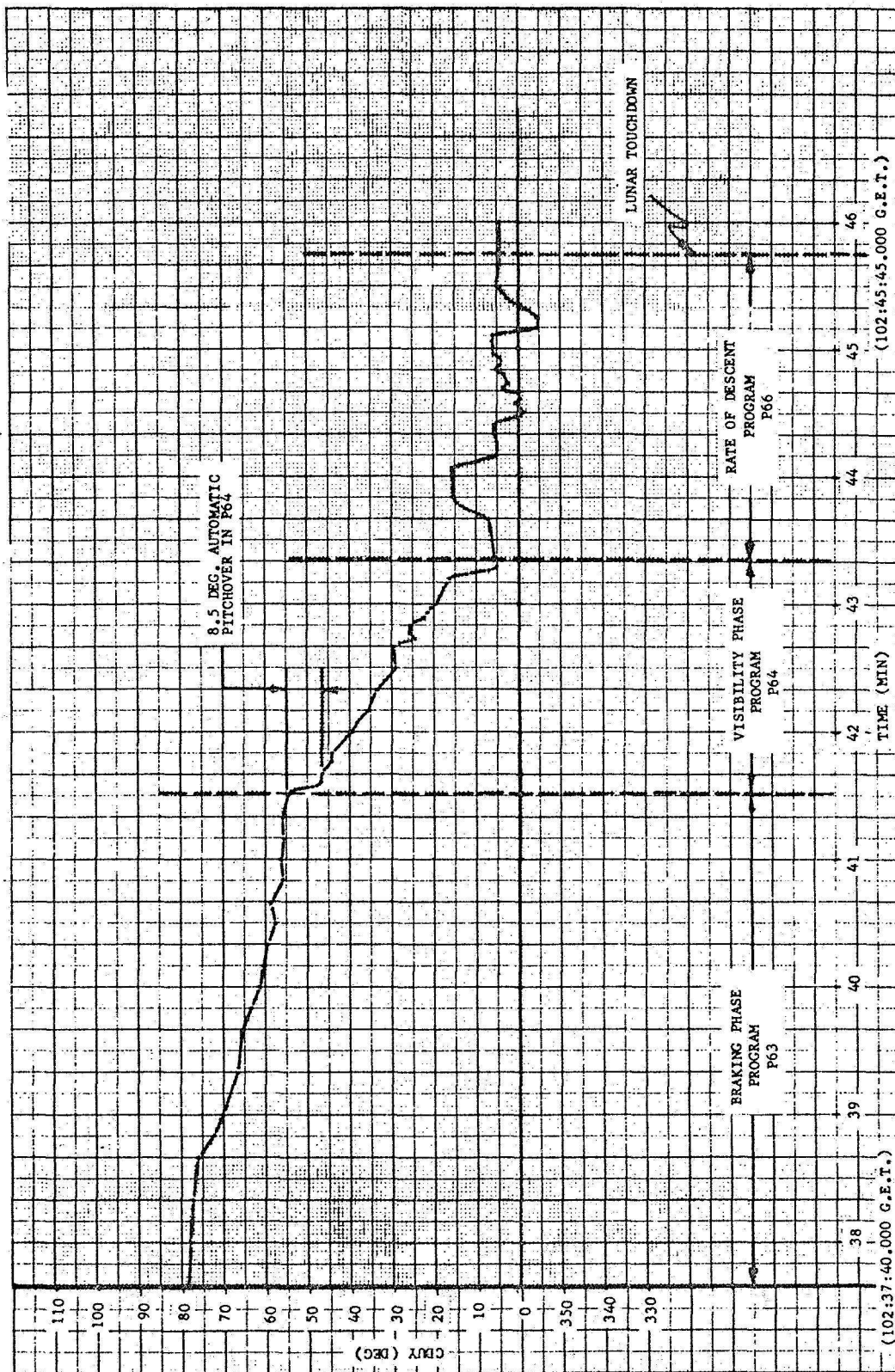


FIGURE 4-27
CDUY (INNER GIMBAL ANGLE) VS TIME

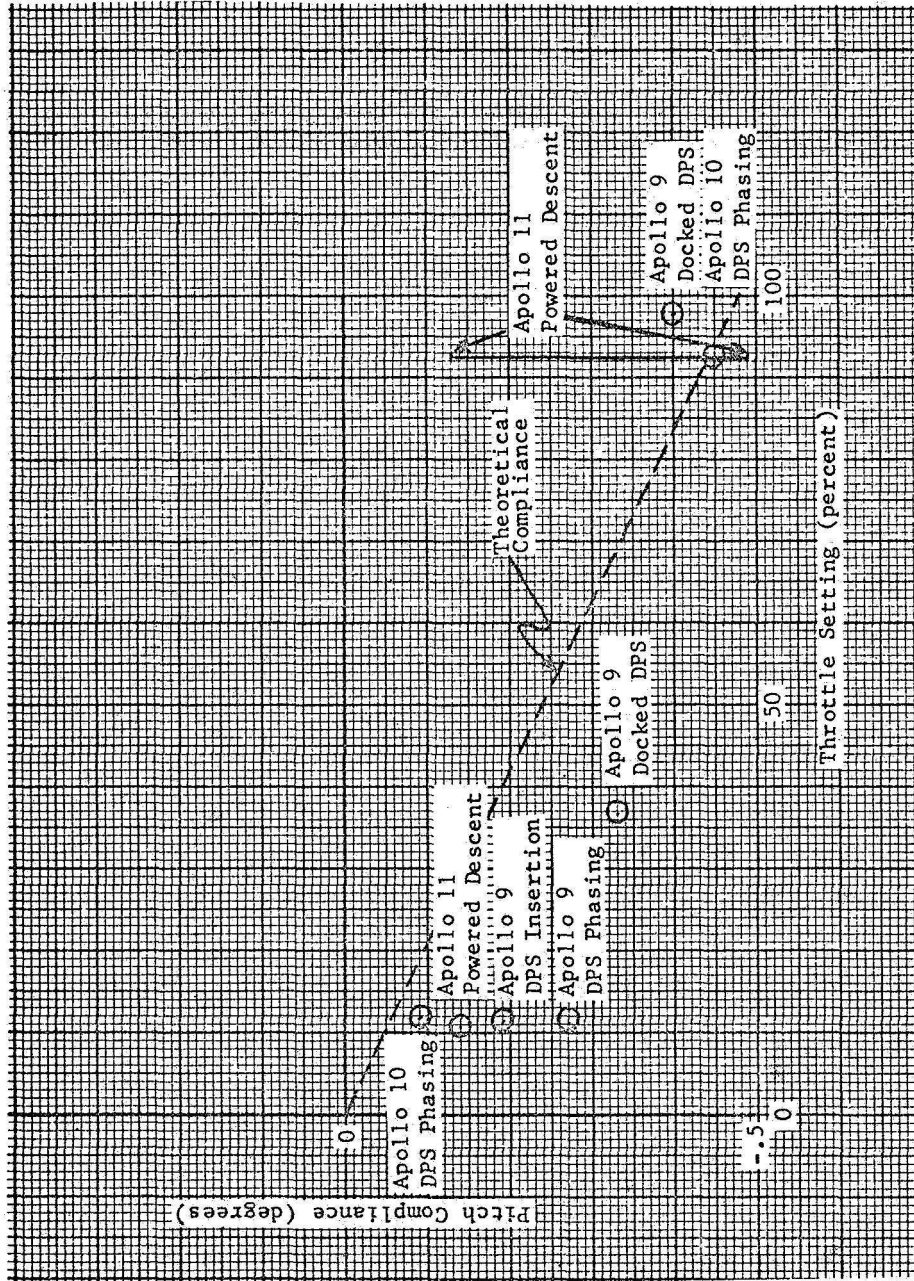


FIGURE 4-28
PITCH COMPLIANCE VS THROTTLE SETTING

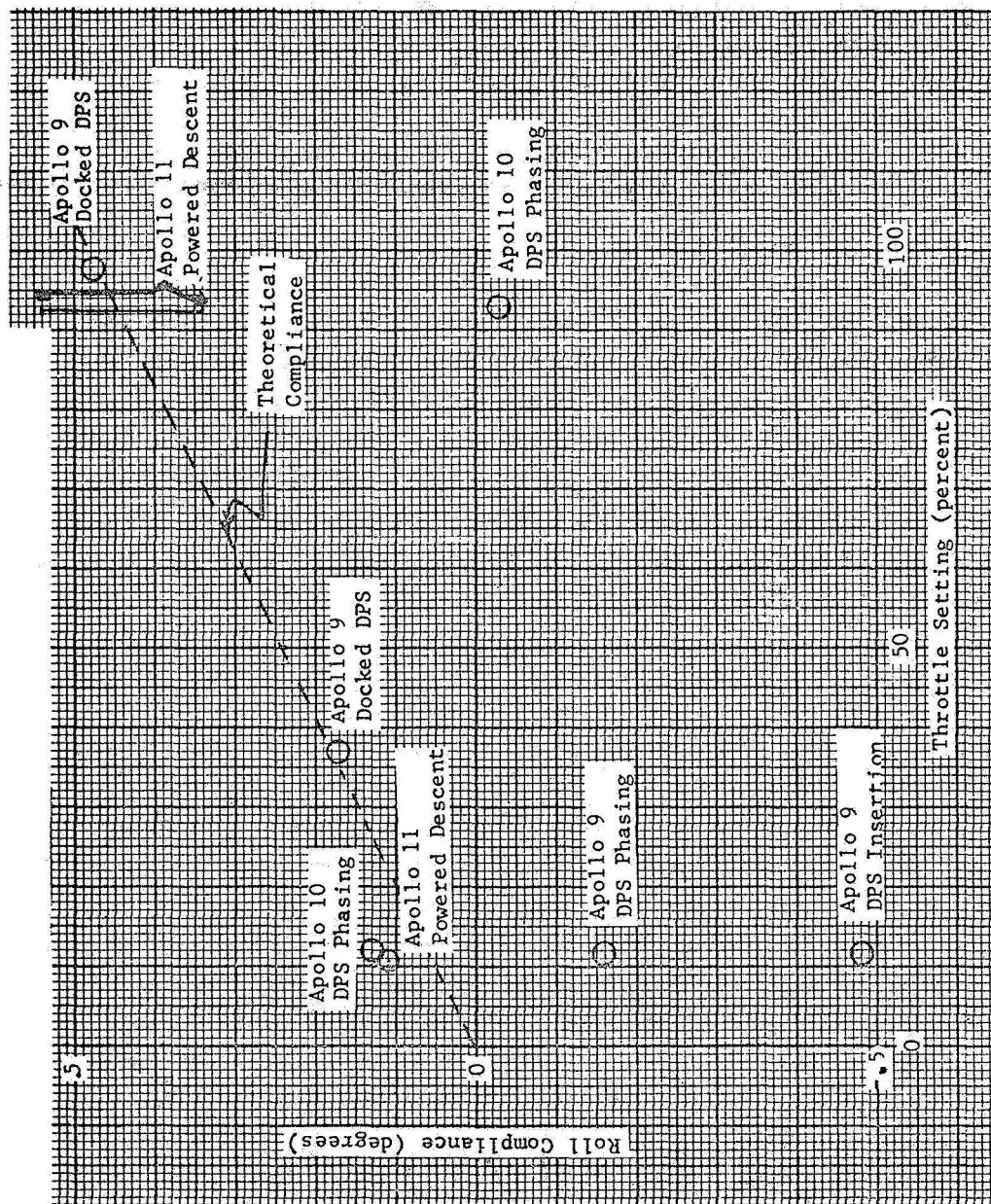


FIGURE 4-29
ROLL COMPLIANCE VS THROTTLE SETTING

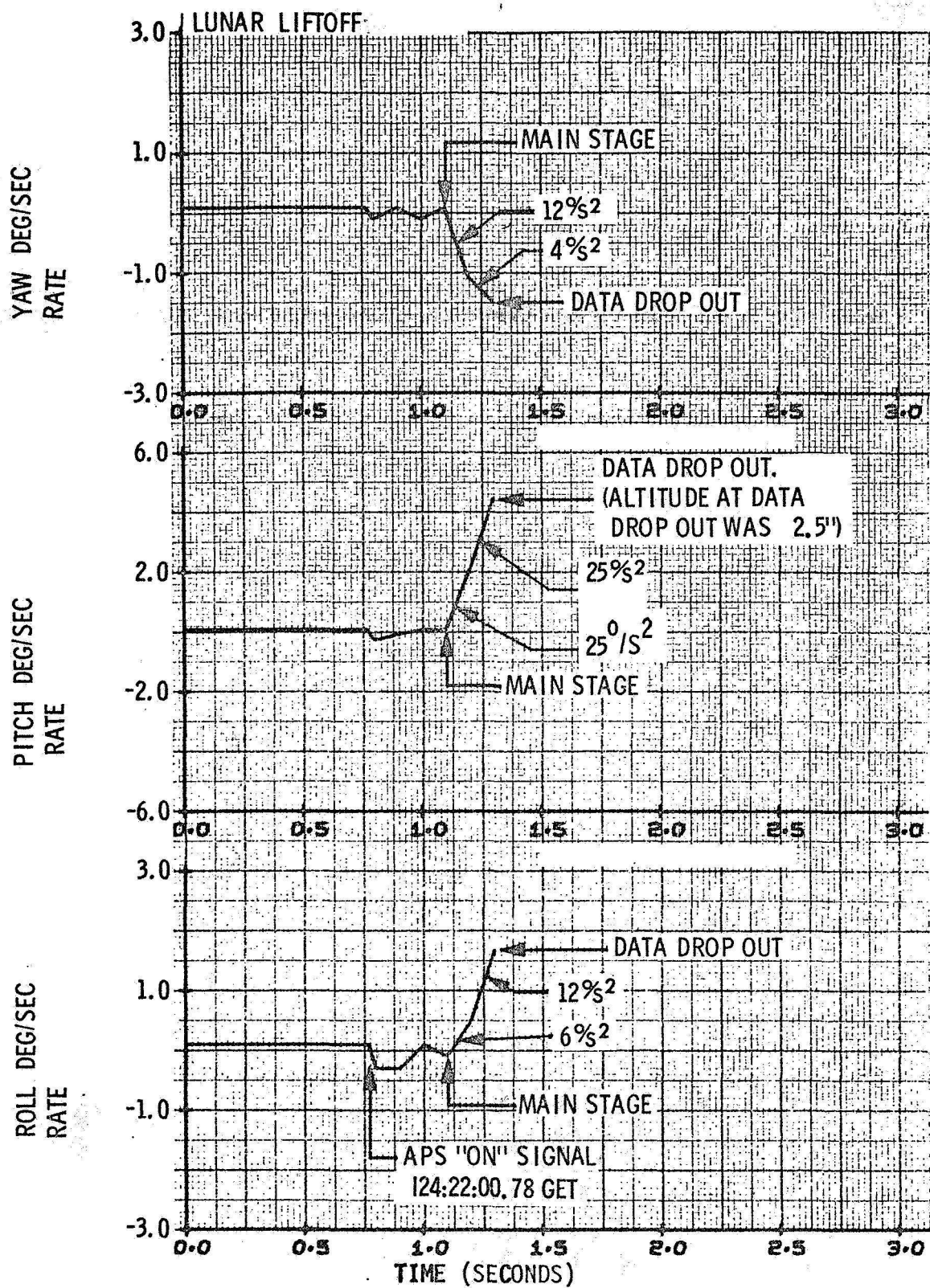
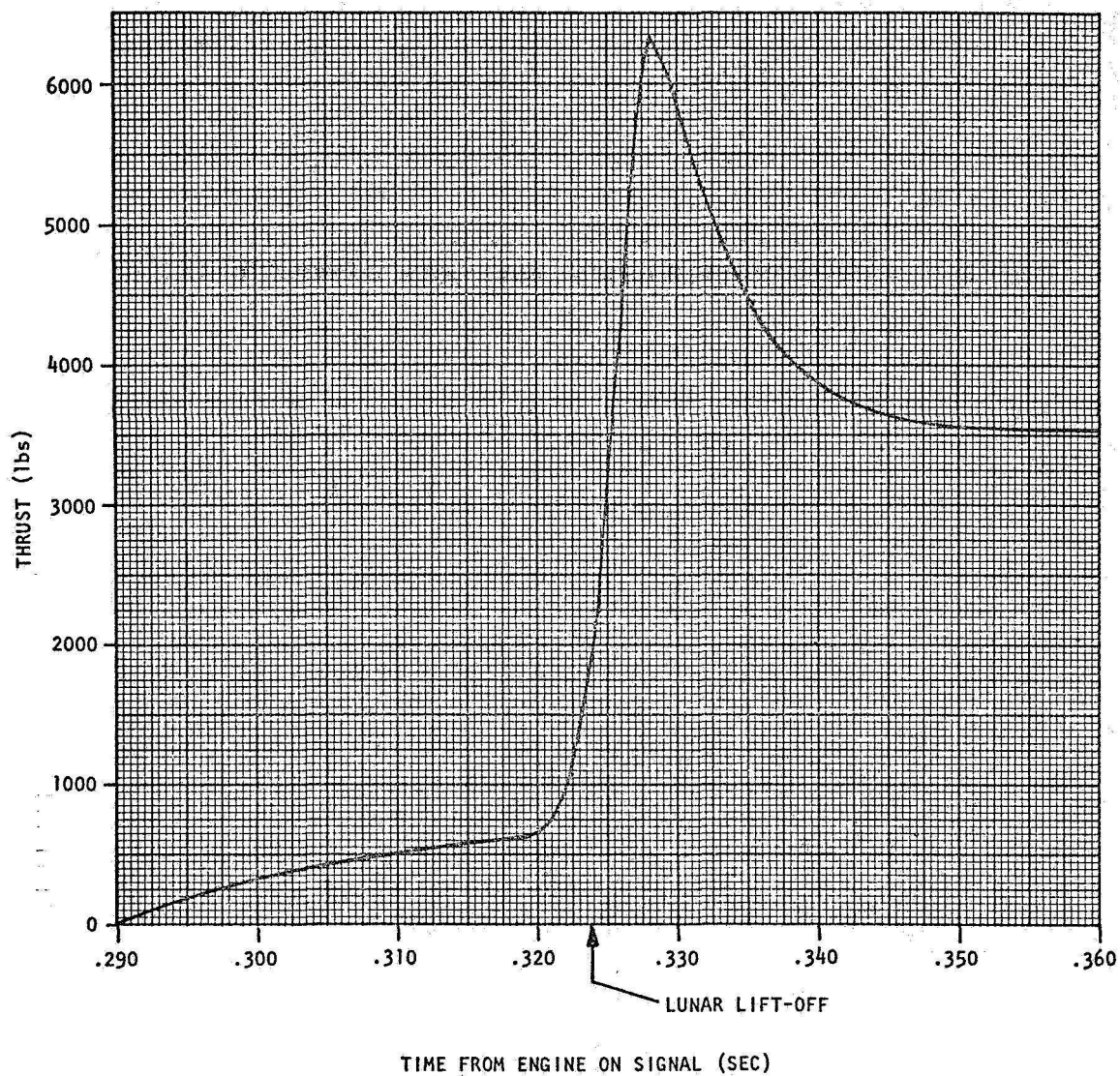


FIGURE 4-30
LUNAR LIFTOFF

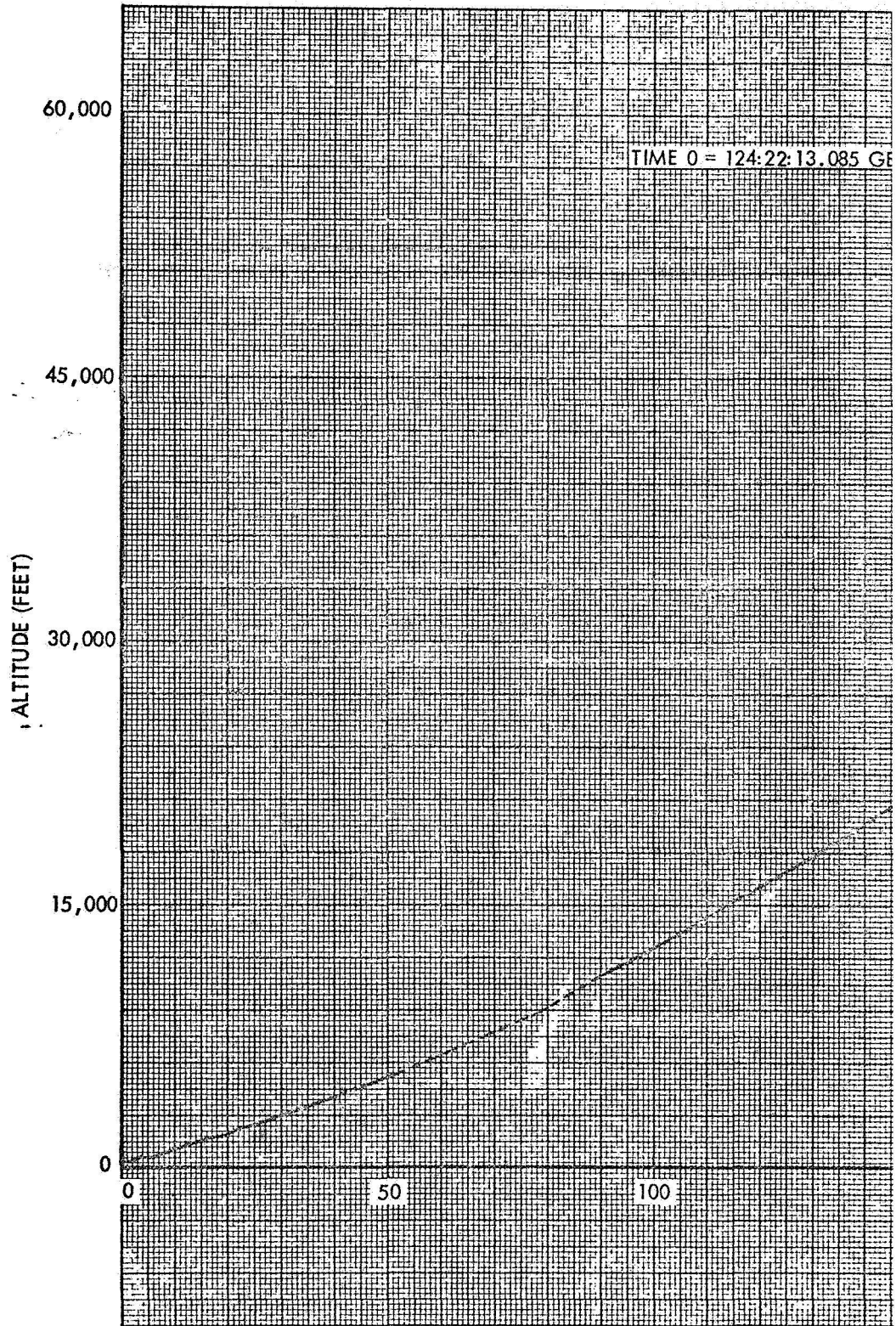


LM-5 APS ENGINE DATA FOR A PRESSURIZED FIRST START
.017 SEC FROM ENGINE ON SIGNAL TO BLOWING OF THE BOLTS

FIGURE 4-31
THEORETICAL APS THRUST BUILDUP

FOLDOUT FRAME

A.



FOLDOUT FRAME

B.

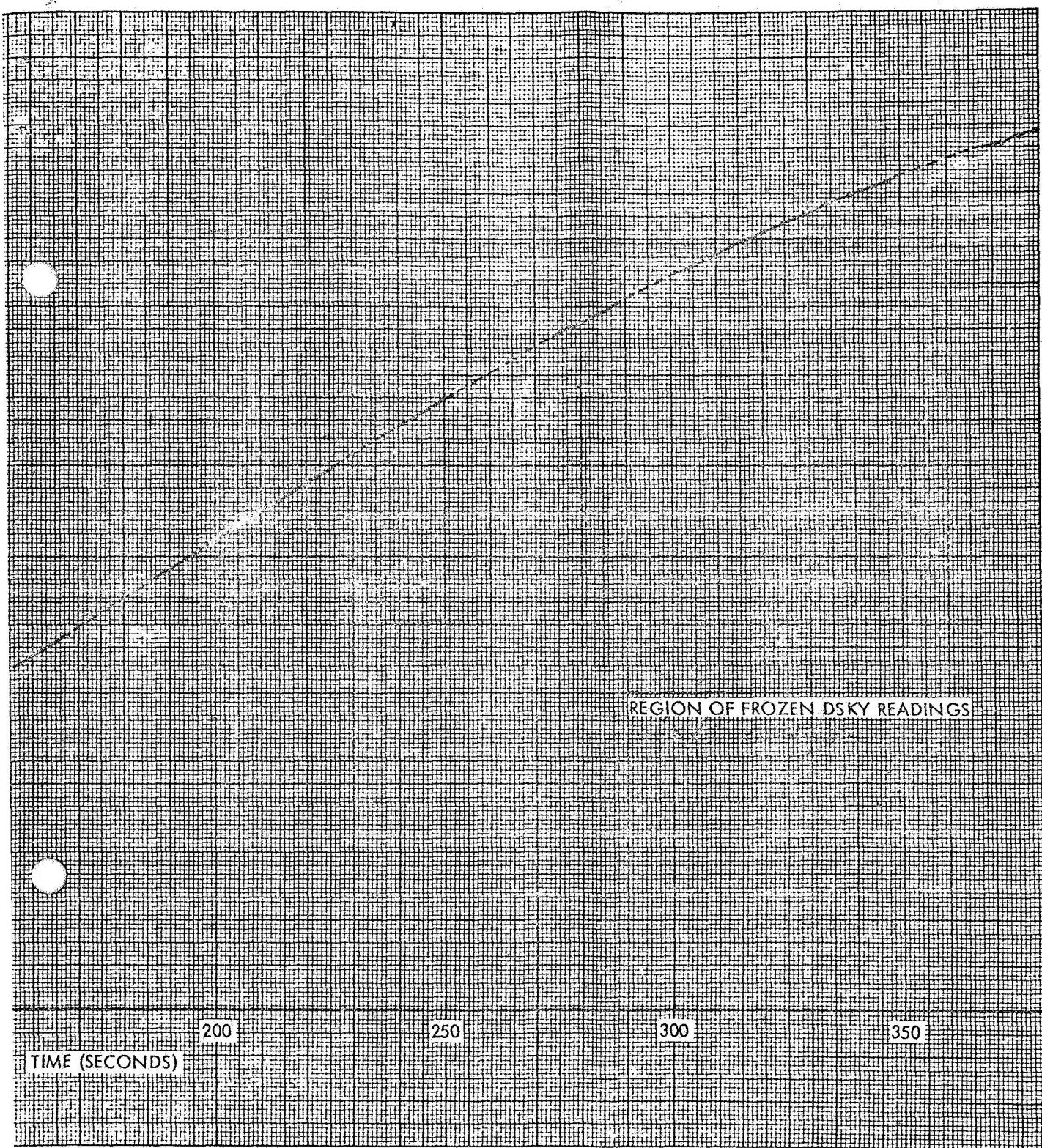
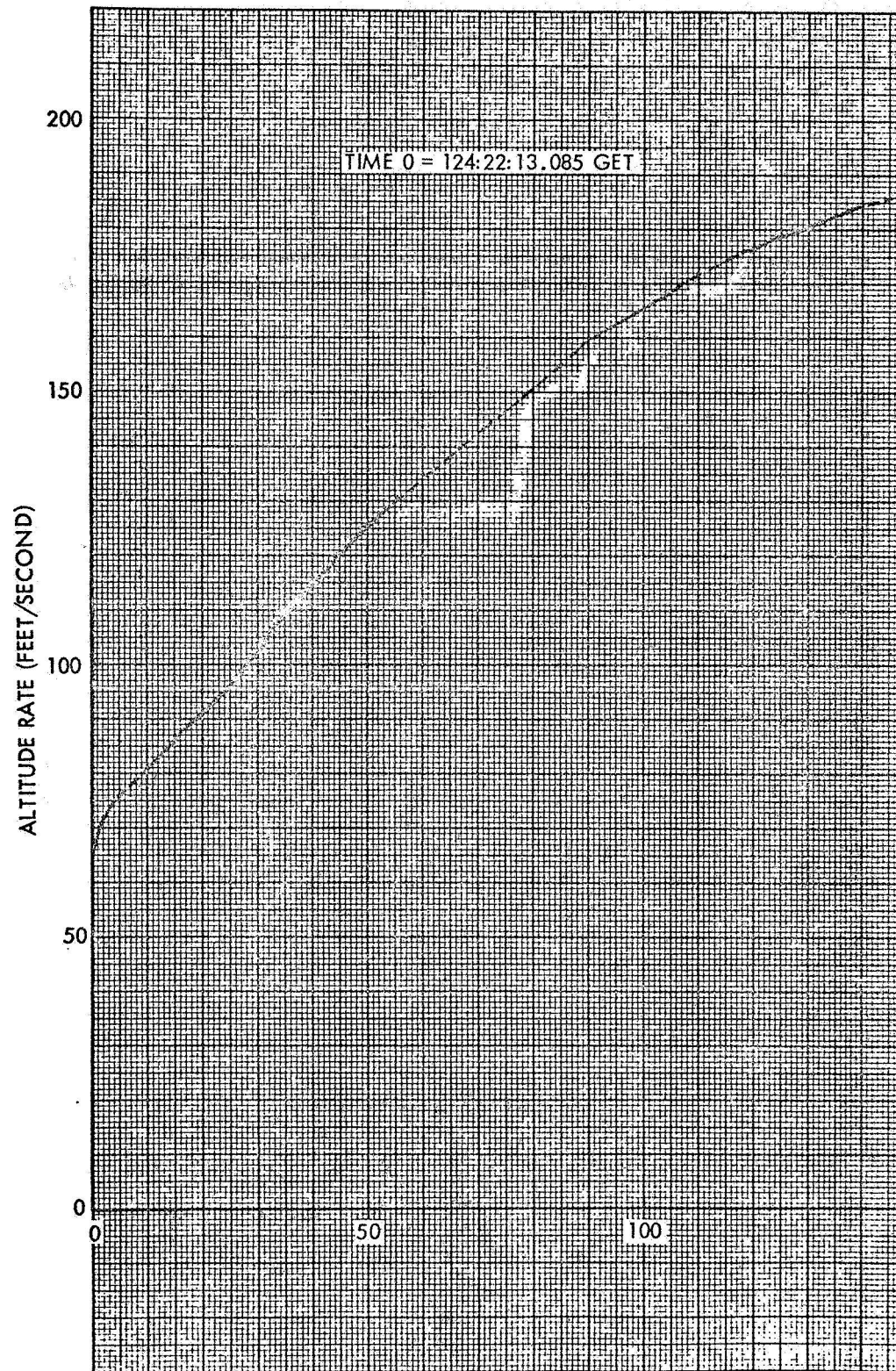


FIGURE 4-32
ALTITUDE VS TIME DURING POWERED ASCENT

FOLDOUT FRAME

A.



FOLDOUT FRAME

B.

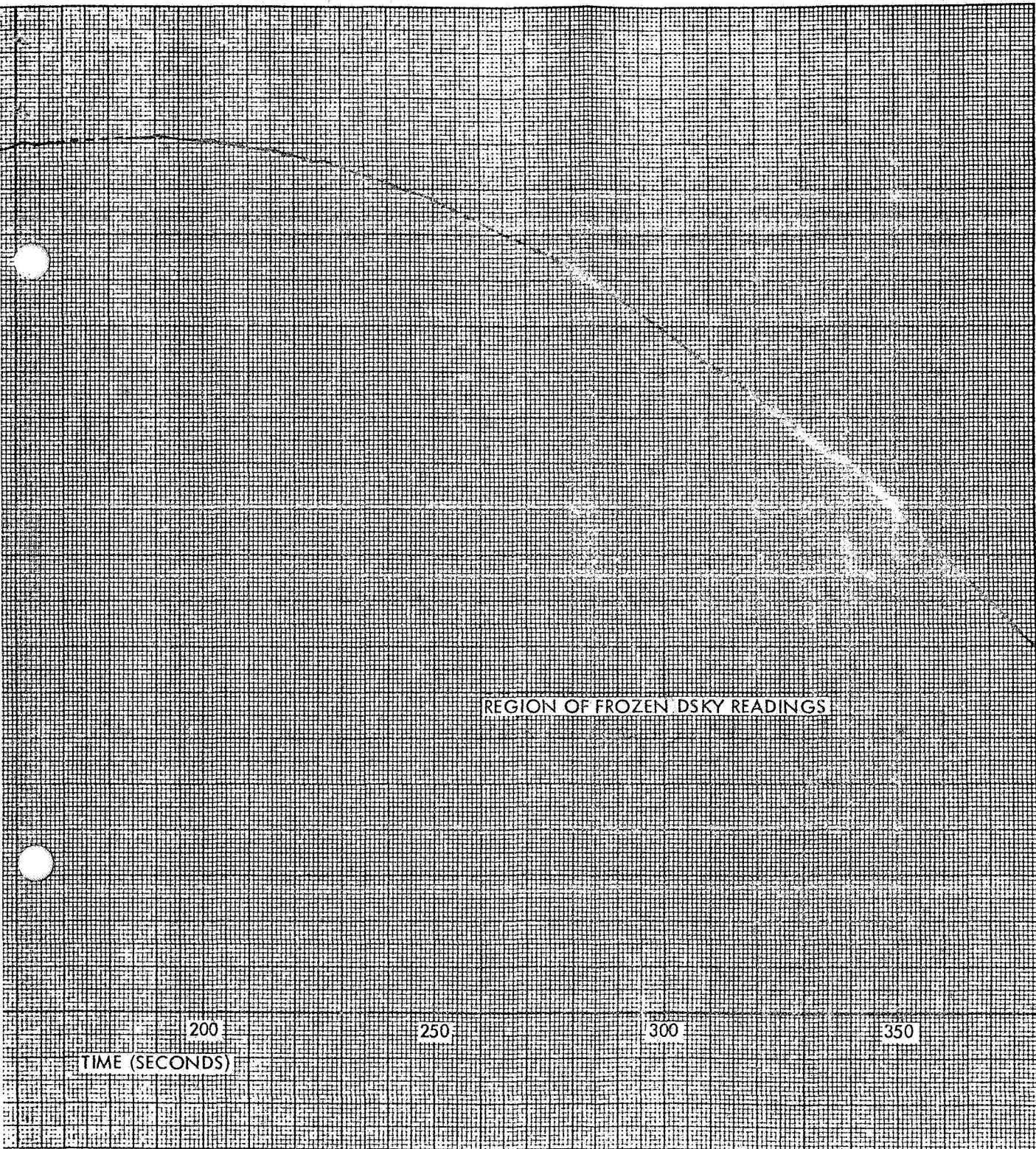


FIGURE 4-33
ALTITUDE RATE VS TIME DURING POWERED ASCENT

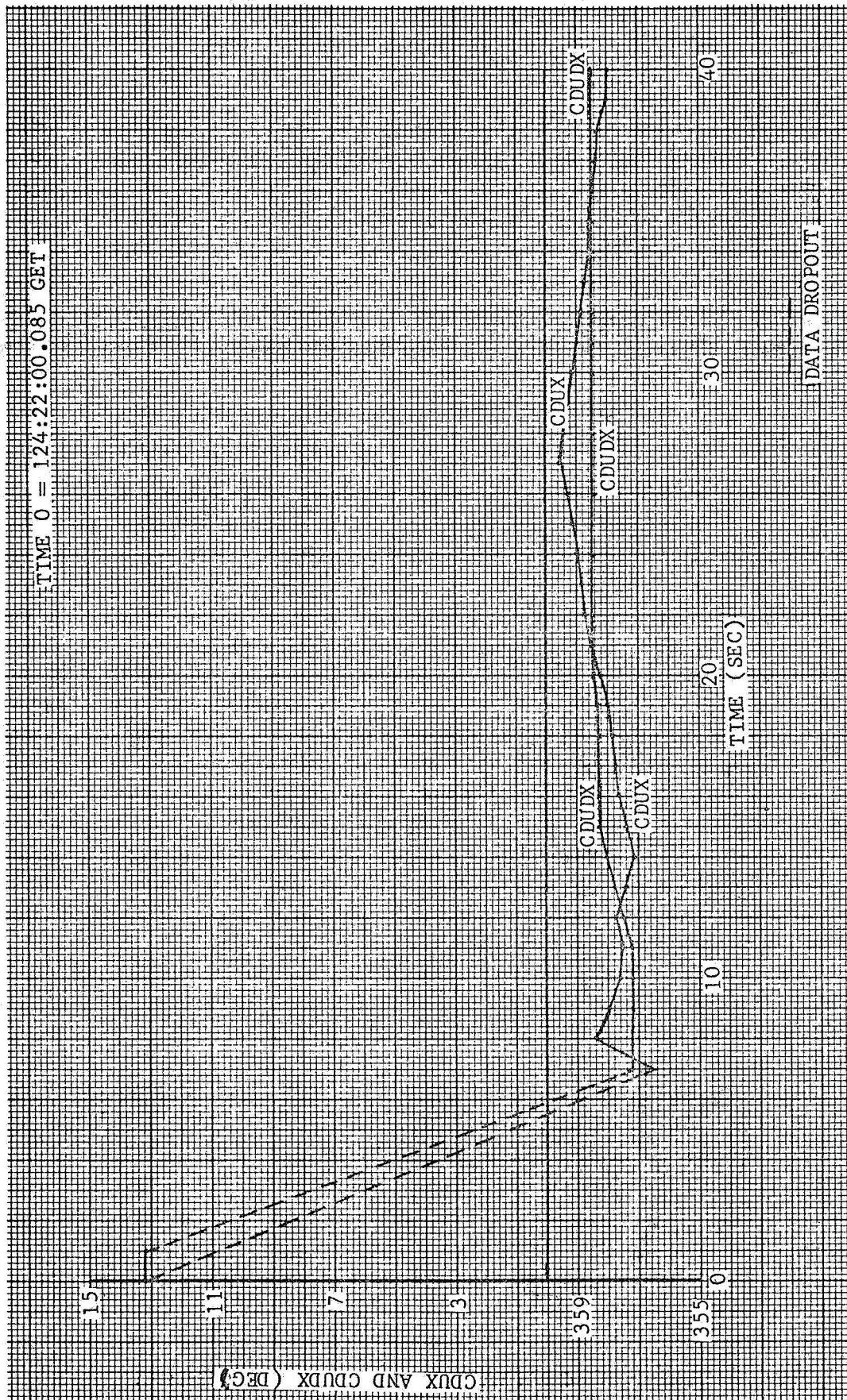


FIGURE 4-34

YAW GUIDANCE COMMANDS AND RESPONSE - INITIAL PHASE OF POWERED ASCENT

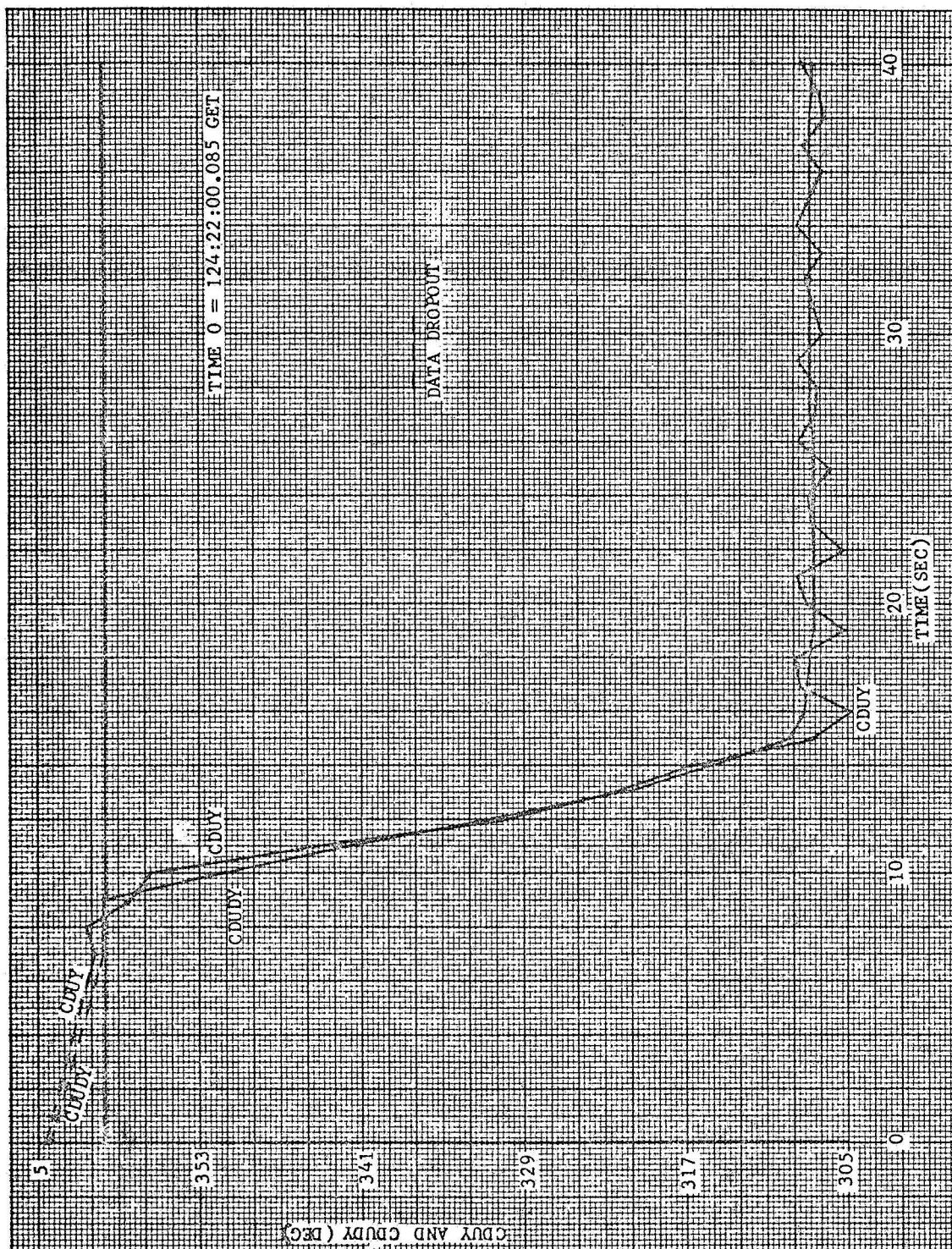


FIGURE 4-35
PITCH GUIDANCE COMMANDS AND RESPONSE - INITIAL PHASE OF POWERED ASCENT

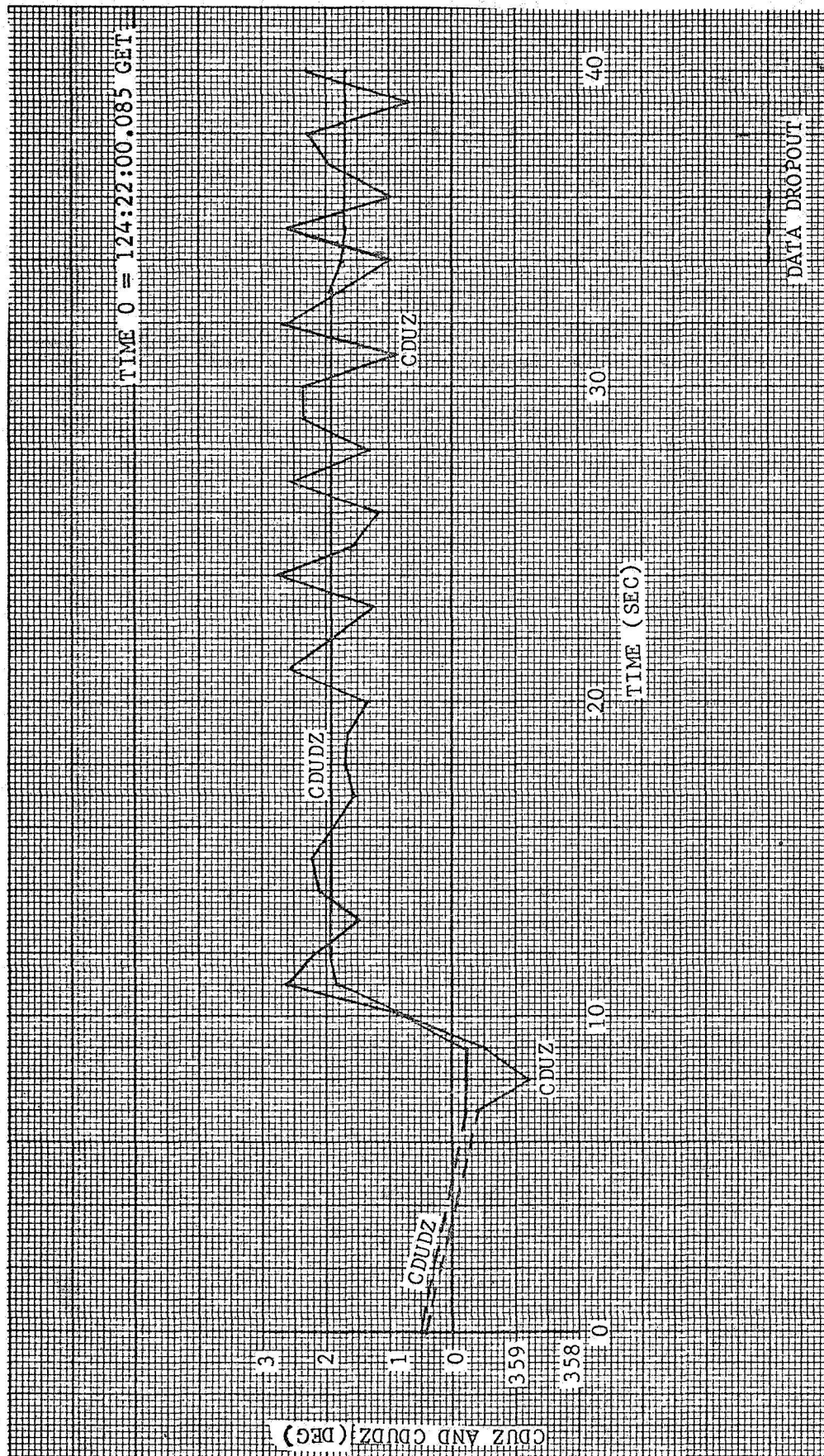
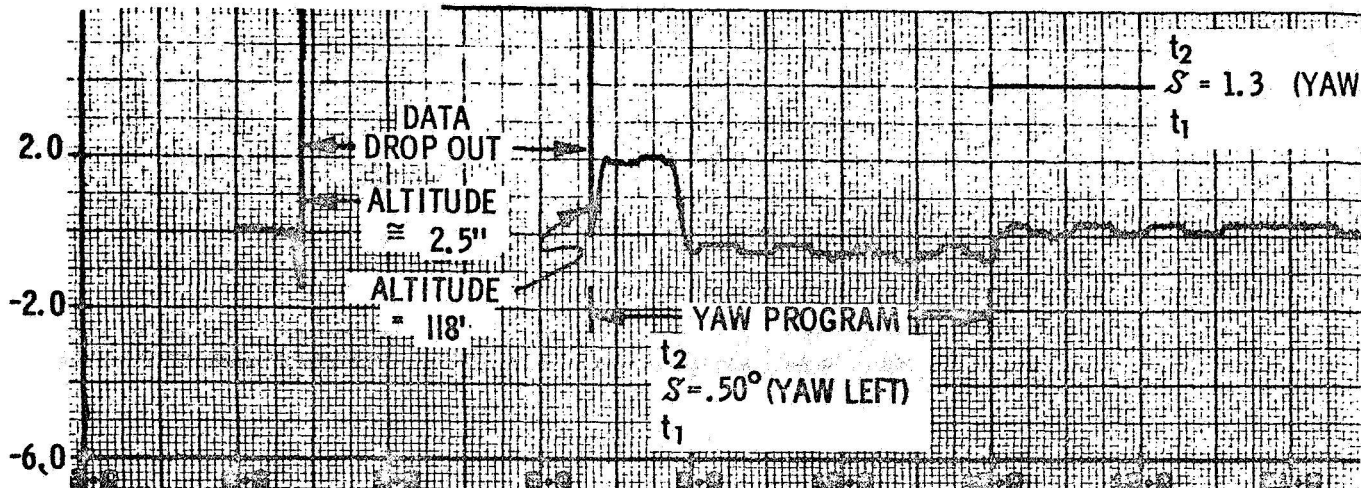


FIGURE 4-36
ROLL GUIDANCE COMMANDS AND RESPONSE - INITIAL PHASE OF POWERED ASCENT

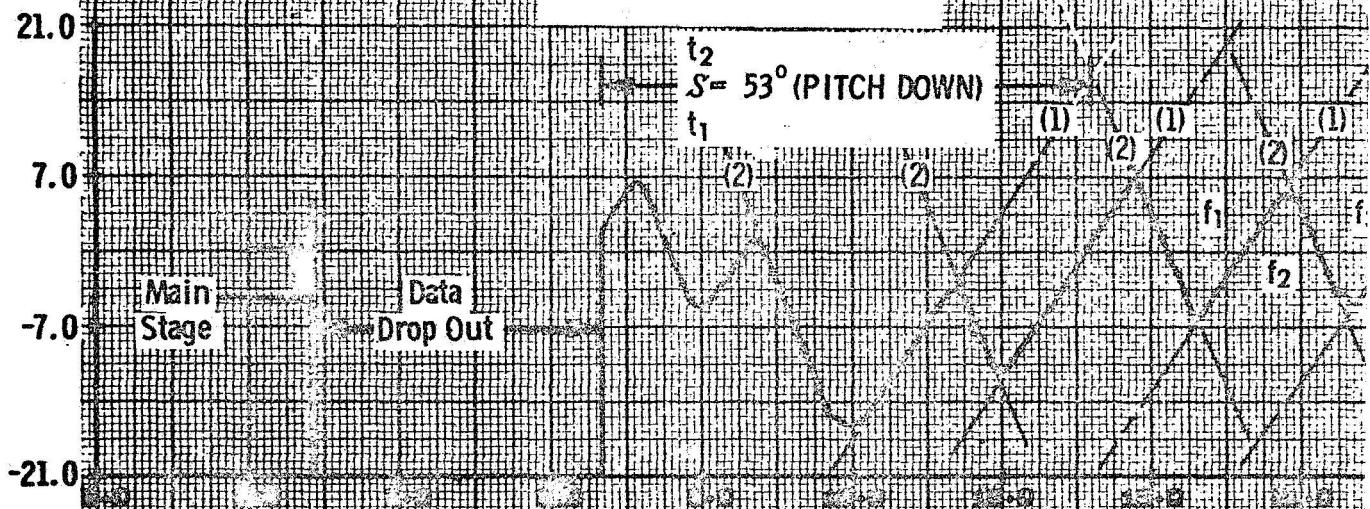
FOLDOUT FRAME

A

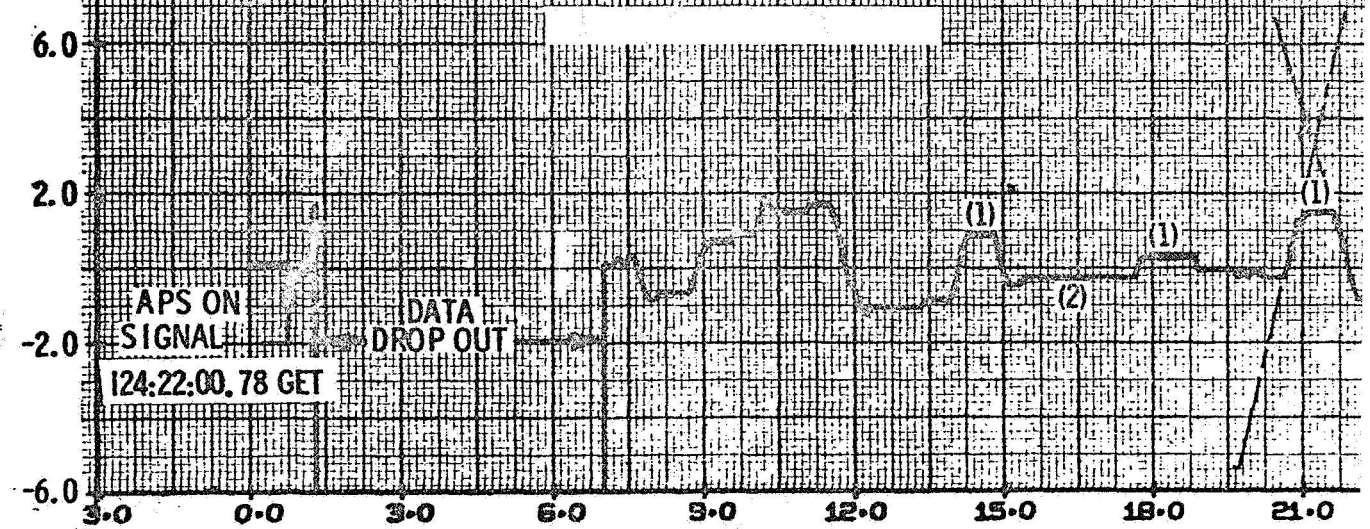
YAW DEG/SEC
RATE



PITCH DEG/SEC
RATE



ROLL DEG/SEC
RATE



B.

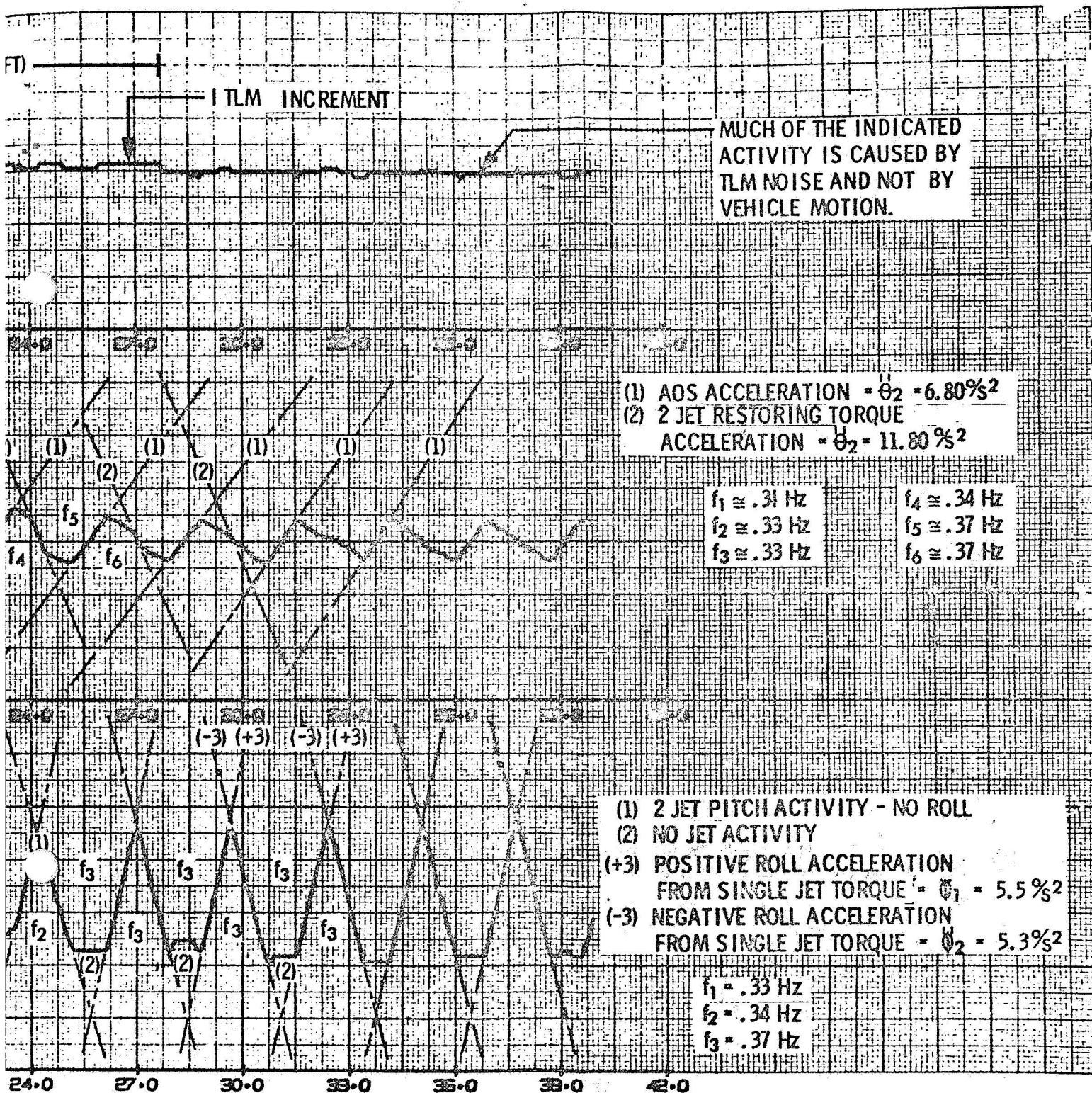
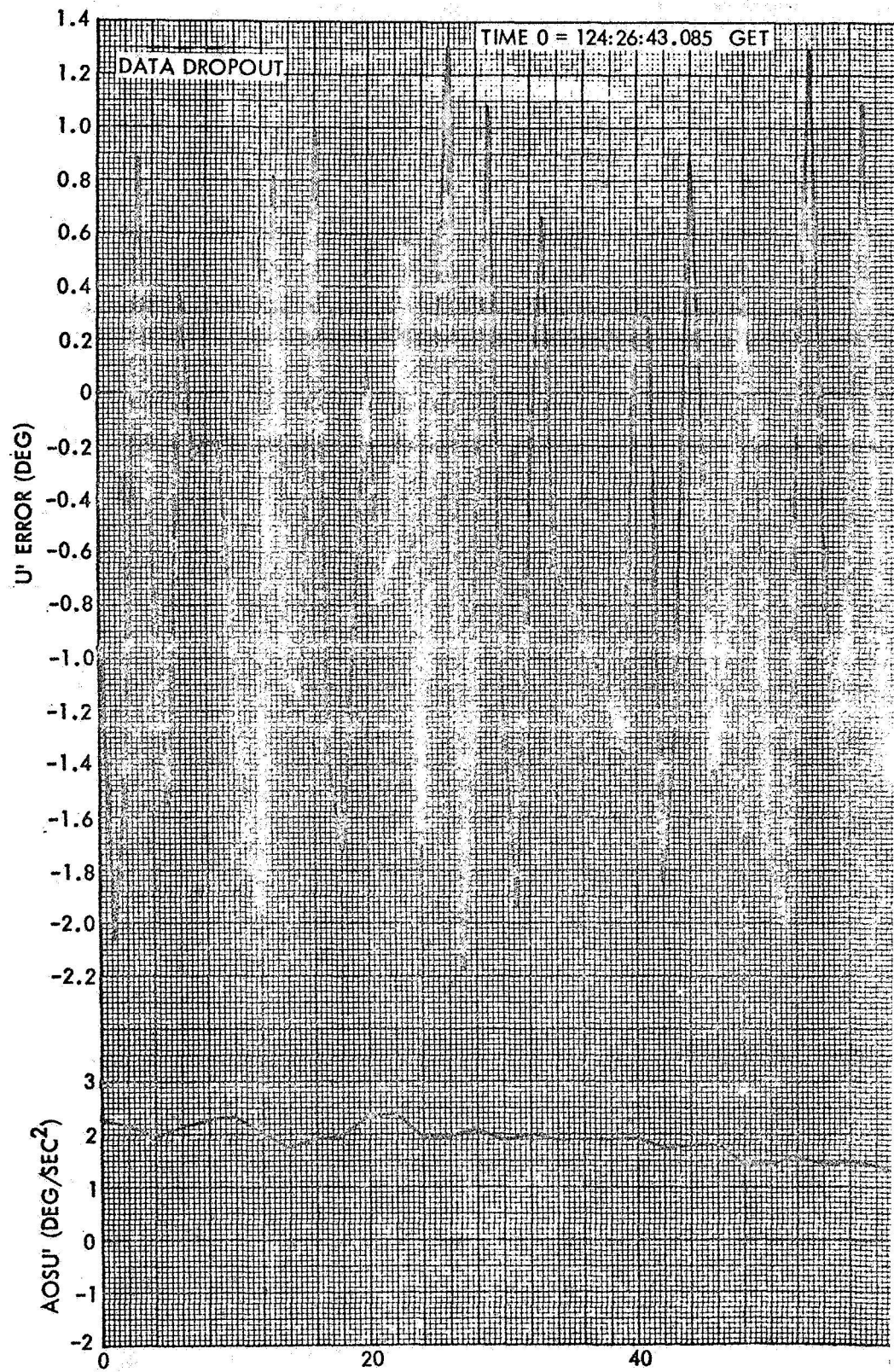


FIGURE 4-37
LUNAR ORBIT INSERTION RESPONSE

FOLDOUT FRAME

A



FOLDOUT FRAME

B,

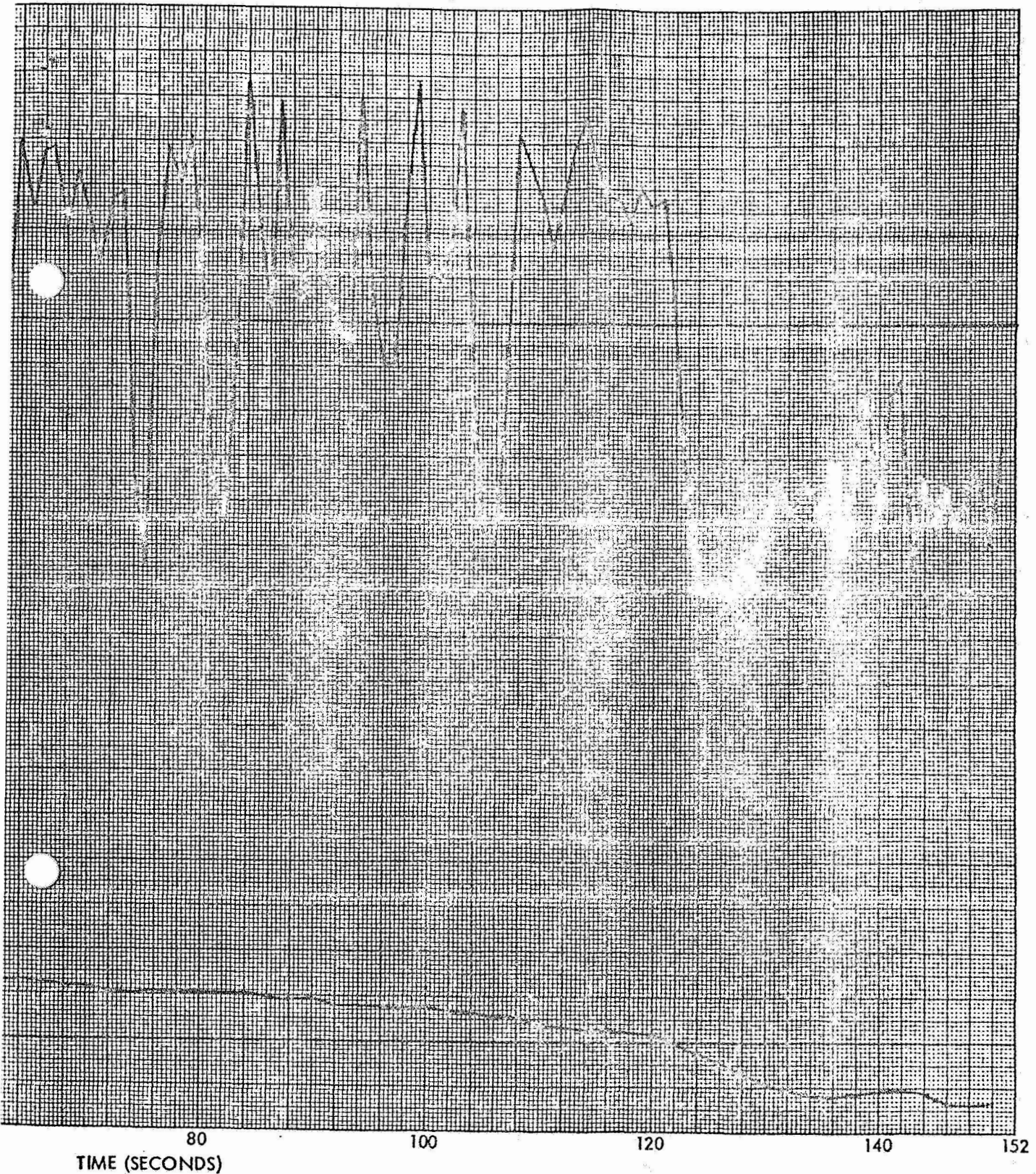
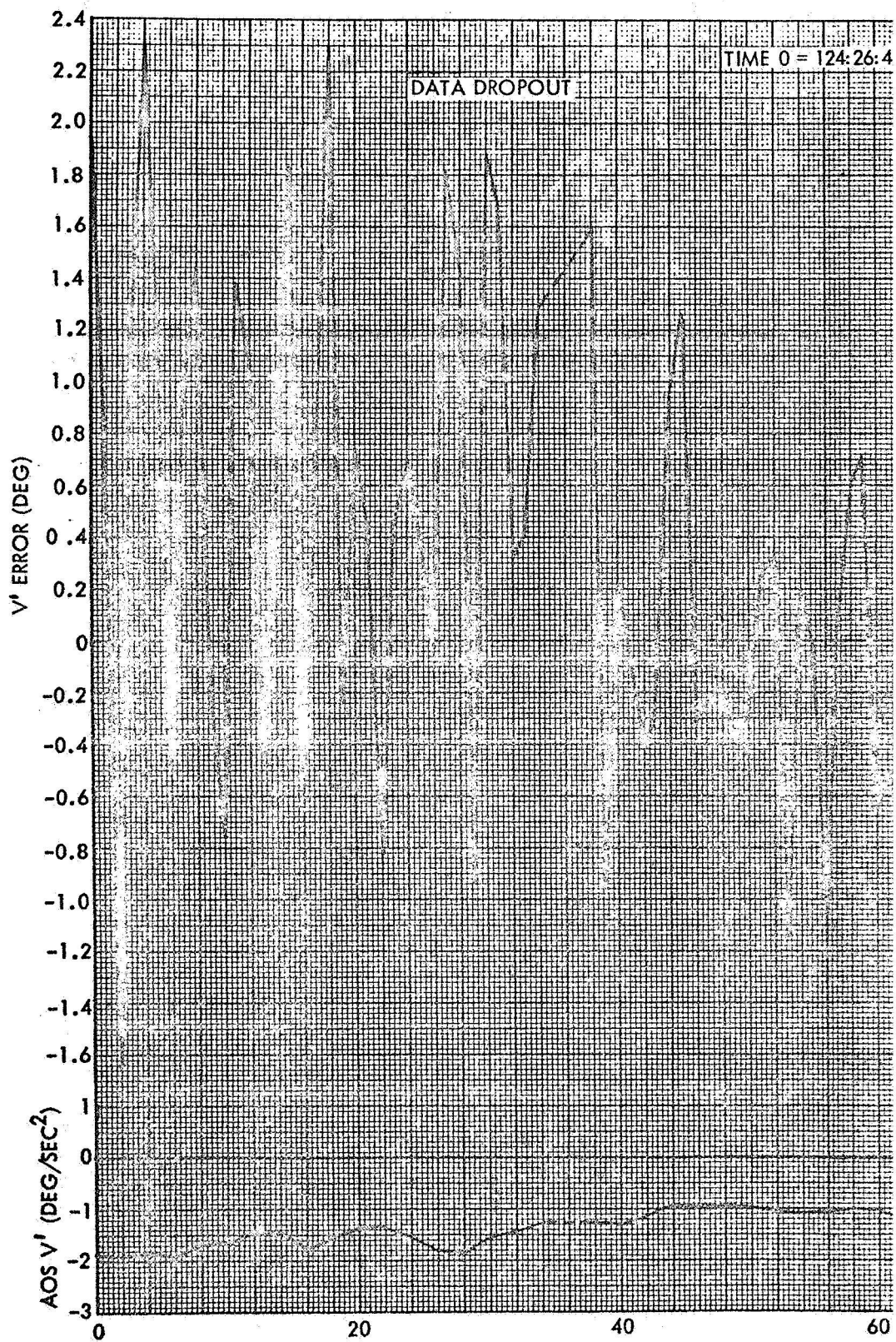


FIGURE 4-38
U' AXIS ATTITUDE ERROR AND OFFSET ACCELERATION
FOR FINAL PHASE OF POWERED ASCENT

FOLDOUT FRAME

A



FOLDOUT FRAME

B

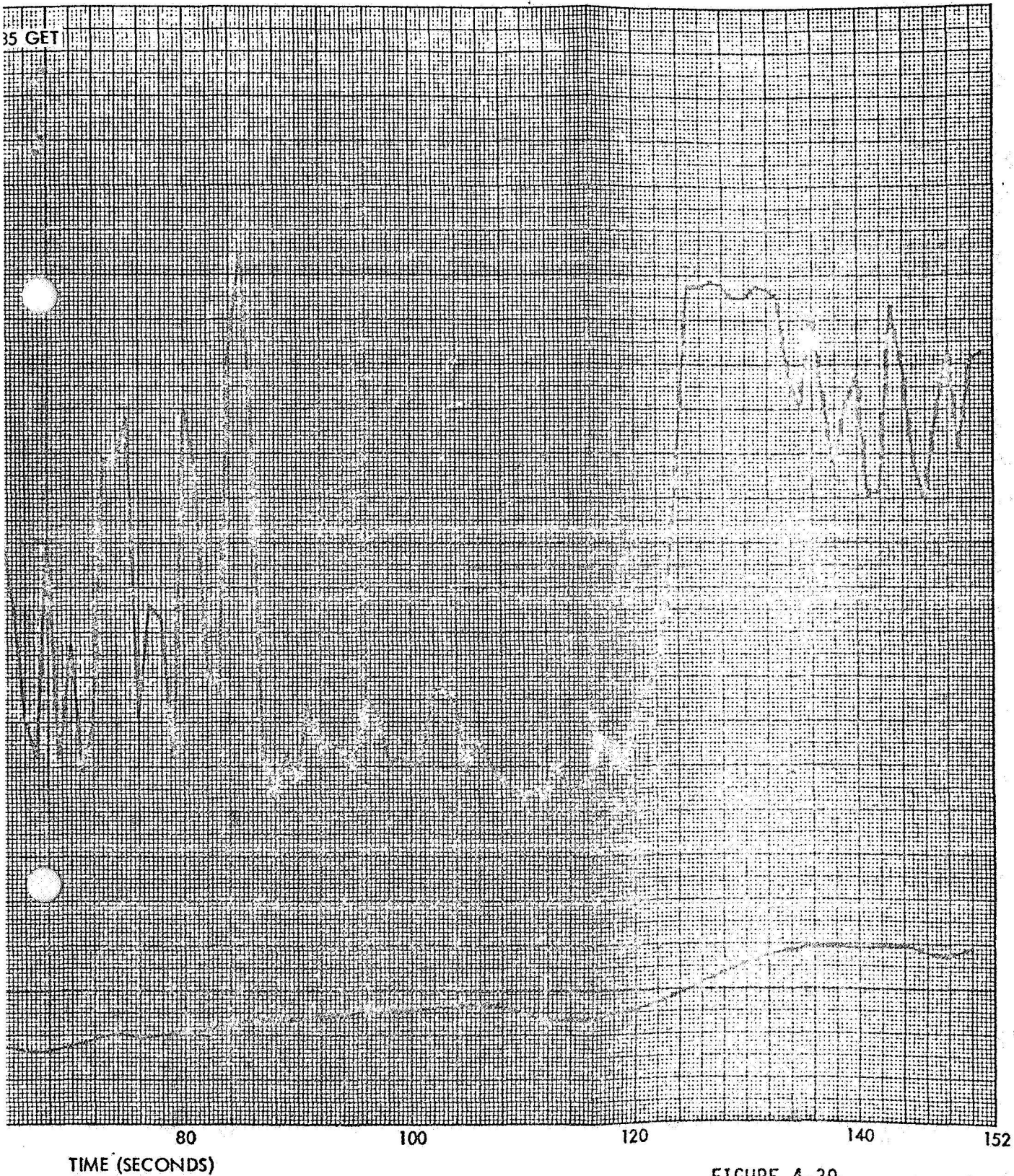
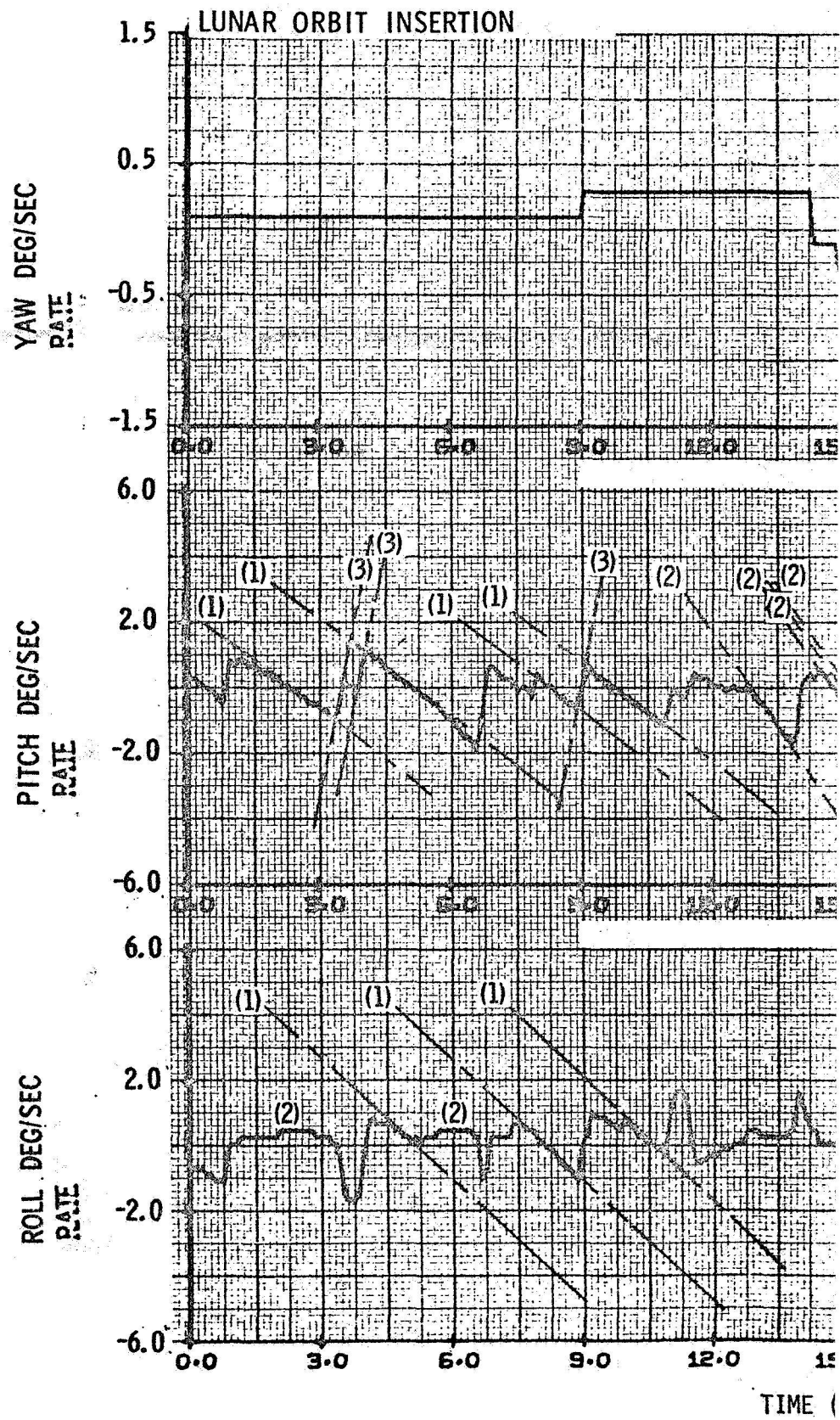


FIGURE 4-39
V'AXIS ATTITUDE ERROR AND OFFSET ACCELERATION
FOR FINAL PHASE OF POWERED ASCENT

FOLDOUT FRAME

A



B.

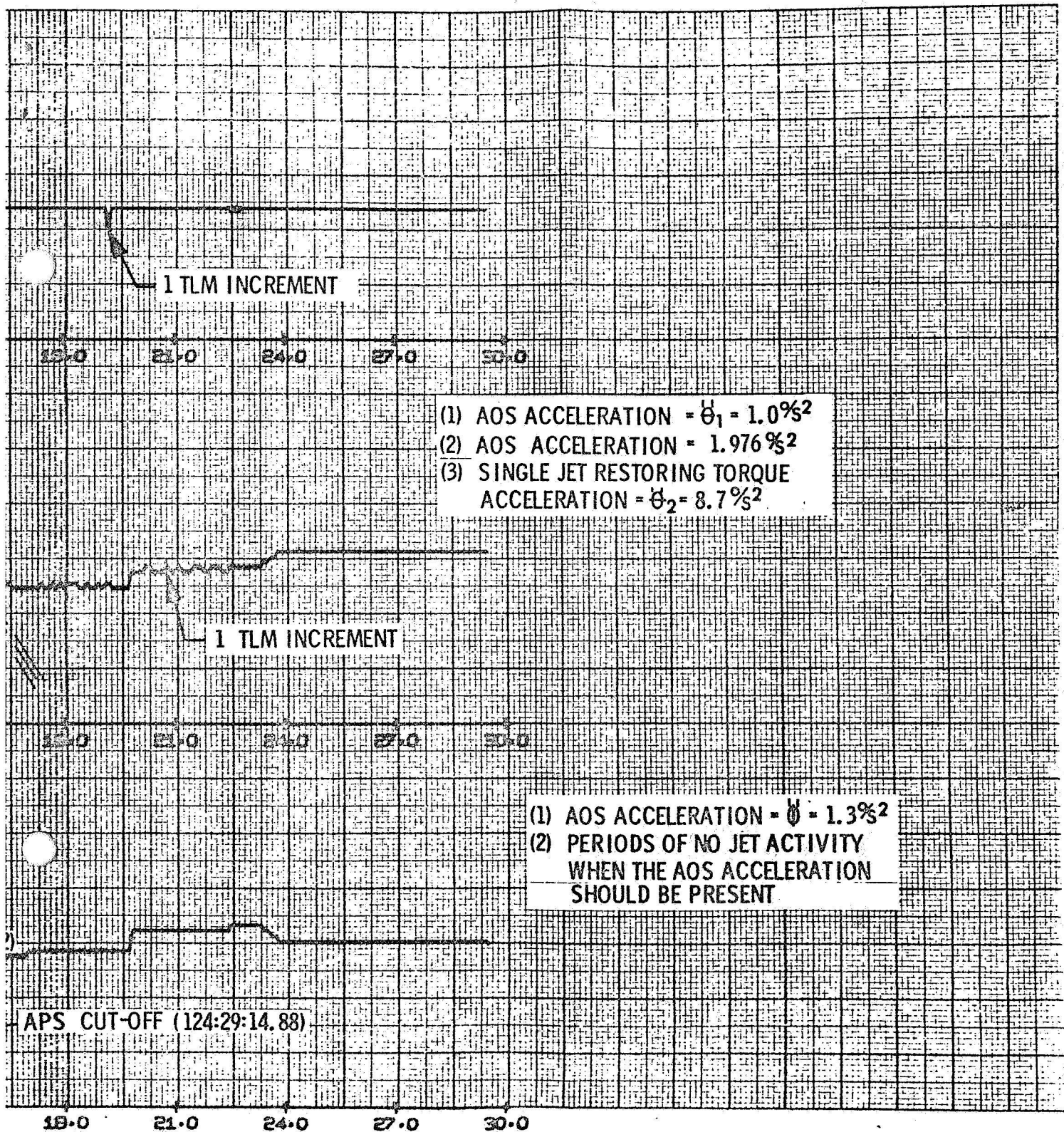
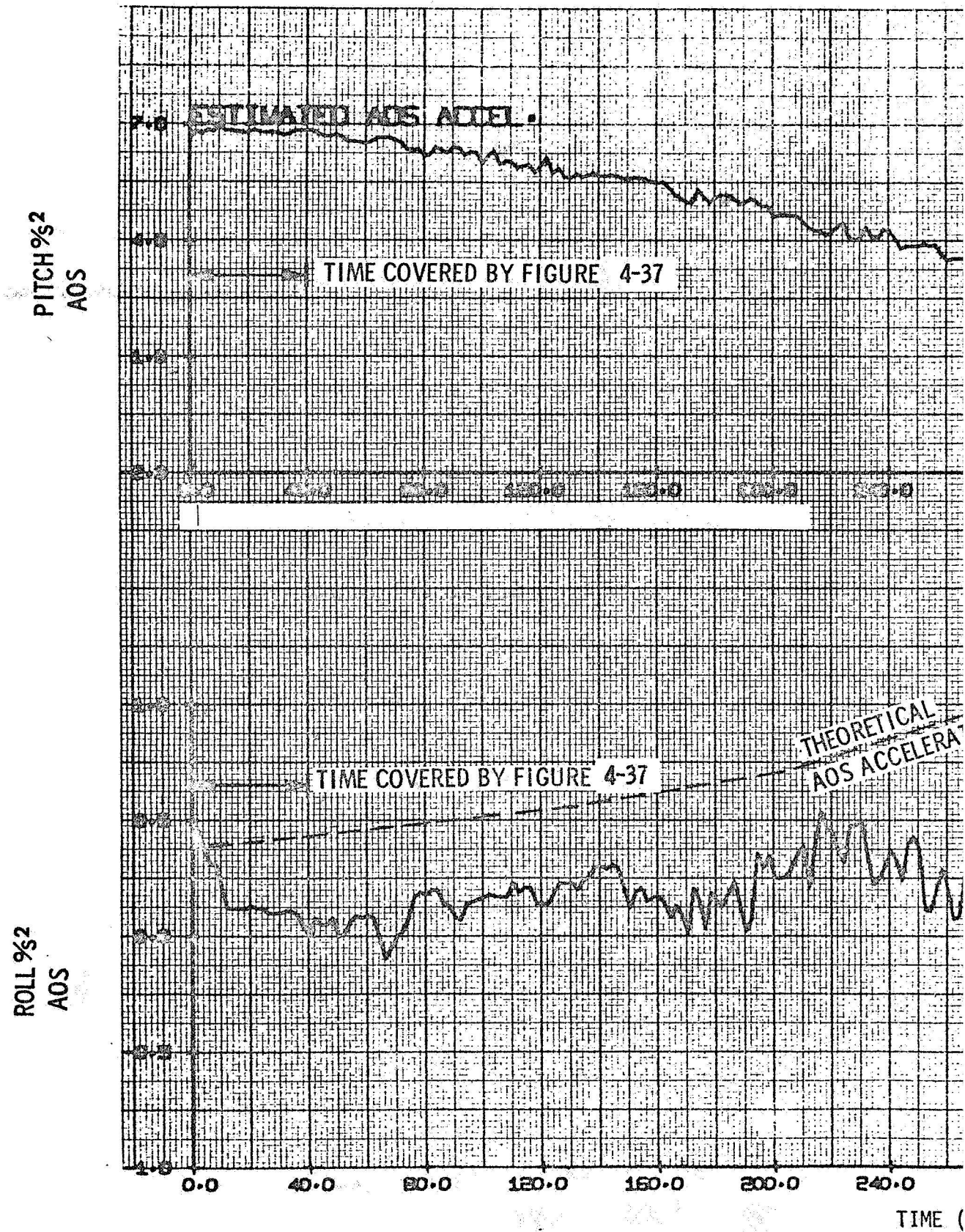


FIGURE 4-40
SPACECRAFT RESPONSE AT APS CUTOFF

FOLDOUT FRAME

A



FOLDOUT FRAME

B.

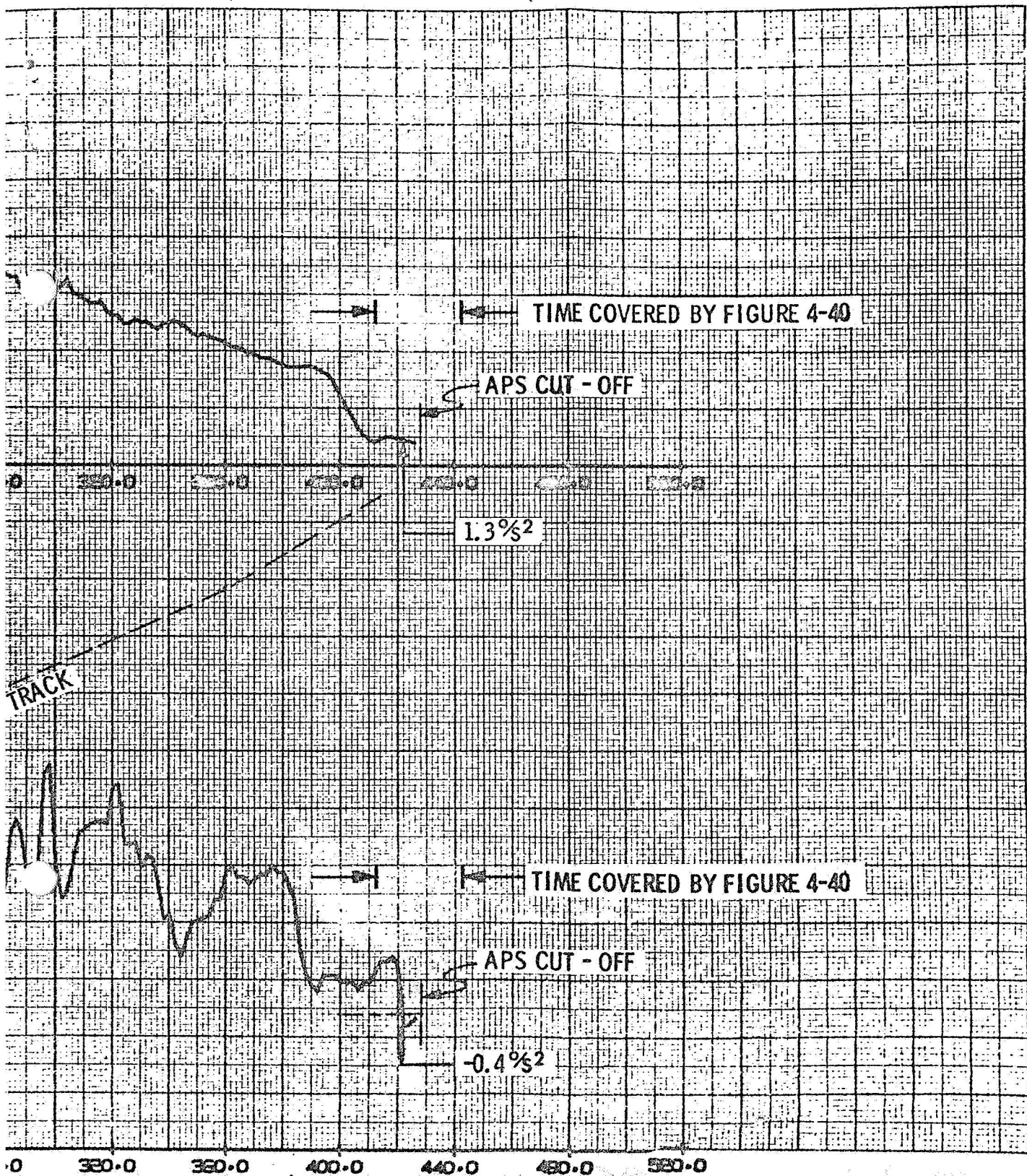


FIGURE 4-41
ESTIMATED AOS ACCELERATION

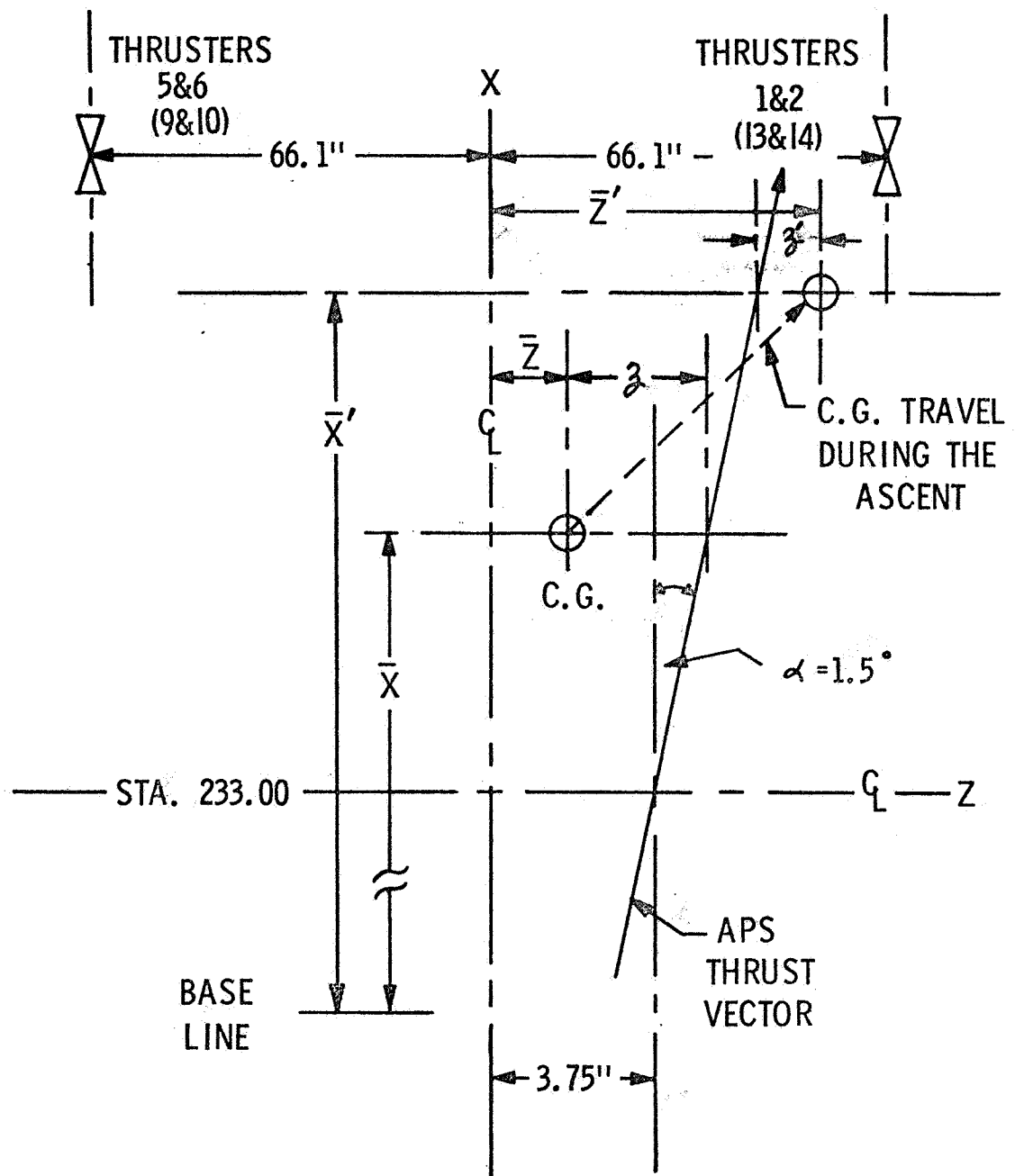


FIGURE 4-42
RELATIONSHIP OF THRUST VECTORS, BODY CENTERLINES
AND CENTER OF GRAVITY ON THE LM IN THE X-Z PLANE

REFERENCES

1. MIT R-577, "Guidance System Operations Plan for Manned CM Earth Orbital and Lunar Missions Using Program COLOSSUS 2A (COMANCHE, Rev. 55), Section 3 Digital Autopilots (Rev. 6)," April 1969.
2. MIT R-577, "Guidance System Operations Plan for Manned CM Earth Orbital and Lunar Missions Using Program COLOSSUS 2A (COMANCHE, Rev 55), Section 2 Data Links (Rev. 5)", June 1969.
3. MSC Internal Note MSC-00120, "Data Processing Plan for Apollo 11," 27 June 1969.
4. MIT E-2409, "COLOSSUS 2, TVC DAP Simulation Results," April 1969.
5. TRW Project Technical Report, "Apollo X Guidance, Navigation, and Control Systems Performance Analysis Report," to be published.
6. MIT/IL R-567, "Guidance System Operations Plan for Manned LM Earth Orbital and Lunar Missions Using Program LUMINARY IA (Rev. 099), Section 3 Digital Autopilot (Rev. 1)," June 1969.
7. MIT/IL R-567, "Guidance System Operations Plan for Manned LM Earth Orbital and Lunar Missions Using Program LUMINARY IA (Rev. 099), Section 2 Data Links (Rev. 4)," June 1969.
8. MIT/IL R-567, "Guidance System Operations Plan for Manned LM Earth Orbital and Lunar Missions Using Program LUMINARY IA (Rev. 099), Section 4 PGNCs Operational Modes (Rev. 4), Supplement to LUMINARY I (Rev. 069) ," June 1969.
9. TRW Project Technical Report 11176-H287-R0-00, "Digital Autopilot Software Verification Test Results for the Apollo 11 Mission - LUMINARY IA," 14 July 1969.
10. MSC Internal Note, "Apollo 11 Mission Report", to be published.
11. TRW Transmittal No. 69:7254.5-132, "LM RCS Propellant Consumption Mission G (Apollo 11) Final Postflight Analysis," dated 16 September 1969.
12. NASA SNA-8-D-027 (III) Rev. 2, "CSM/LM Spacecraft Operational Data Book, Volume III - Mass Properties," dated 20 August 1969.

RELATIONSHIP OF THESE DOCUMENTS TO THE CENTER TASK

13. MIT/IL R-567, "Guidance System Operations Plan for Manned LM Earth Orbital and Lunar Missions Using Program LUMINARY, Section 6 Control Data," November 1968.
14. MIT/IL Spacecraft Autopilot Development Memo #25-69, "DAP Performance in the Presence of a Small Disturbing Acceleration About the U' or V' Control Axes During Powered Descent," 26 June 1969.